Nucleic Acid Modifications in Bacterial Pathogens – Impact on Pathogenesis, Diagnosis, and Therapy

by

Brandon S. Russell

B.S. Chemistry (2008)
University of Mississippi
Sally McDonnell Barksdale Honors College

Submitted to the Department of Biological Engineering
in Partial Fulfillment of the Requirements for the Degree of

Doctor of Philosophy in Biological Engineering

at the

Massachusetts Institute of Technology

June 2014

Signature of Author Signature redacted
Department of Biological Engineering
May 20, 2014

Certified by Signature redacted
Peter C. Dedon
Professor of Biological Engineering
Thesis Supervisor

Accepted by Signature redacted
Forest M. White
Associate Professor of Biological Engineering
Chair, Graduate Program Committee

This thesis has been examined by the following doctoral advisory committee:

Peter C. Dedon
Professor of Biological Engineering
Principal Investigator, SMART Infectious Disease IRG
Thesis Supervisor

James G. Fox
Professor of Biological Engineering
Director, Division of Comparative Medicine
Committee Chair

Uttam L. RajBhandary
Lester Wolfe Professor in Molecular Biology

John S. Wishnok
Senior Research Scientist

Nucleic Acid Modifications in Bacterial Pathogens – Impact on Pathogenesis, Diagnosis, and Therapy

by

Brandon S. Russell

Submitted to the Department of Biological Engineering on May 23, 2014
in Partial Fulfillment of the Requirements for the Degree
of Doctor of Philosophy in Biological Engineering

Abstract

Nucleic acids are subject to extensive chemical modification by all organisms. These modifications display incredible structural diversity, and some are essential for survival. Intriguingly, several of these modifications are unique to bacteria, including many human pathogens. Given the enormous global disease burden due to bacterial infections, and the rapidly increasing rates of antibiotic resistance reported across the world, the need for research to address mechanisms of bacterial survival is more pressing than ever. The goal of this thesis was to determine the function of nucleic acid modifications in pathogenic bacteria, and to evaluate their impact on the three major stages of the infectious disease process: pathogenesis, diagnosis, and therapy.

We first used quantitative profiling of tRNA modifications to identify novel stress responses that help mediate host invasion in the world's most common pathogen, *Helicobacter pylori*. This work uncovered potentially novel targets for the development of new compounds that inhibit pathogenesis. We then developed a new animal model of mycobacterial lung infection that enables drug development and biomarker screening studies in standard laboratories without high-containment facilities. We showed that infection with *Mycobacterium bovis* bacille Calmette-Guérin produces a granulomatous lung disease in rats that recapitulates many of the important pathological features of human tuberculosis. This model also allowed us to test the utility of nucleic acid modifications as diagnostic biomarkers. Finally, we investigated the effect of the common, transferable bacterial DNA modification phosphorothioation on oxidative and antibiotic stress responses in several pathogens. We showed that phosphorothioation can reduce the effectiveness of antibiotic therapy, which may make it an environmental source of acquired antibiotic resistance.

These studies show that nucleic acid modifications play diverse roles in pathogenic bacteria, and that their modulation may be a promising target for developing new tools that can disrupt pathogenesis, improve diagnosis, and strengthen therapy.

Thesis Supervisor: Peter C. Dedon
Title: Professor of Biological Engineering

Acknowledgments

None of this work would have been possible the gracious and selfless support from a multitude of people. If I were to attempt to name everyone that has helped me along the way, I would likely never stop writing. To anyone that I have omitted through my own fault of memory, please accept my sincere apology.

First and foremost, I must thank my advisor, Professor Peter C. Dedon. From the first day that I met Pete when I was a wide-eyed undergraduate spending a summer at MIT, I knew that I had found a true mentor. Eight years later, with six of those as his graduate student, that feeling has never been stronger. I have never met a kinder, more sincere, or more generous person, and I am still humbled and inspired by his work ethic and intellectual authority. It's no surprise that the common refrain in our research group was always, "When does he sleep?" Pete has seen me through the ups and the downs of both research and life, and he was equally comfortable handling naïve questions from a neophyte scientist, intractable technical difficulties, and last-second requests for letters of support. Whether in quick chats in the hallway, late-night teleconferences across continents, or lengthy meetings in his office, talking and working with Pete was always a pleasure. The quality of his guidance, even when given in brief words, was unparalleled. Most importantly, Pete believed in me when I did not believe in myself, and for that I will always be deeply grateful.

I must also thank my committee members, Professor James Fox, Professor Uttam RajBhandary, and Dr. John "Pete" Wishnok. Their world-class expertise, gentle guidance, and difficult questions were essential to my growth as a researcher. As a budding organic chemist trying to combine veterinary science, molecular biology, and analytical chemistry into a coherent piece of work, I could not have done this without them. If only I had known years ago just what they meant when they called my thesis proposal "ambitious."

I owe a deep debt of gratitude to all the members of the Dedon Laboratory, both past and present. If Pete and my committee showed me the path, then my fellow lab members walked it with me. I thank Dr. Clement Chan, Dr. Ramesh Indrakanti, Dr. Kok Seong Lim, Dr. Erin Prestwich, and Dr. Dan Su for many long sessions teaching me the unintuitive finer points of analytical instruments and method development. I thank Dr. Megan McBee for cheerfully

tackling the unenviable task of teaching me both laboratory animal science and immunology. I thank Bo Cao, Dr. Michael DeMott, and Dr. Stefanie Kellner for joining me in trying to tease apart the gory details of sulfur in DNA. I thank our many undergraduate researchers, in particular Emily Kolenbrander, Sasilada Sirirungruang, Aislyn Schlack, and Seb Smick, for their tireless efforts. Finally, I thank Yok Hian Chionh, Dr. Vasileios Dendroulakis, Dr. Bahar Edrissi, Chen Gu, Watthanachai Jumpathong, Dr. Aswin Mangerich, Dr. Susovan Mohapatra, and Dr. Joy Pang for friendship, laughter, commiseration, and the occasional beer on Friday afternoons.

I am also thankful to all the members of the Division of Comparative Medicine for their patient training and assistance in numerous projects. In particular, I thank Dr. Zhongming Ge, Melissa Mobley, Dr. Sureshkumar Muthupalani, Dr. Nicola Parry, Joanna Richards, Nate Rogers, Dr. Alexander Sheh, and Gladys Valeriano.

I am indebted to all the members of the Department of Biological Engineering (BE) for giving me a graduate experience above and beyond what I ever could have imagined. I thank Professor Doug Lauffenburger for the leadership and vision to create a department as wonderful as BE. I thank all the administrative and support magicians behind the scenes that keep things running smoothly, especially Dan Darling, Dalia Fares, Susan Jaskela, and Aran Parillo. I thank all of the professors that have imparted to me even a tiny fraction of their expertise. In particular, I thank Professor John Essigmann and Professor Bevin Engelward for making lectures and discussions so engaging, challenging, and exciting that I still miss them.

I am thankful to all my fellow graduate students in the BE department. The camaraderie and support provided by BE students is perhaps the program's strongest feature. I am especially thankful to the members of my cohort that began in 2008, in particular Jim Abshire, Christina Birch, Tim Curran, and David Hagen. I am beyond proud to call these people my friends, and I could not have gotten through the program without their support. From all-nighters in "The Dungeon" wrangling MATLAB scripts, to quiet talks over coffee when we felt alone in the midst of it all, they were always there for me.

I am equally thankful to the great friends that I have made outside of BE. In particular I must thank Patrick Ho, Dr. Karan Mistry, Dr. Ben Rissing, Anne Wasson, Sarah Wilder, and Dr. John Wu for years of excitement, laughter, and on some occasions, tears. Boston has been home not

simply because I've had an address here, but because I've had such truly wonderful people to call my friends. The jokes, the puns, the small talk, the deep conversations, the easy questions, the difficult news, the late nights, the early mornings, the good food, the better drinks, and the moments both long and short that we've spent together have meant the world to me.

I am immensely proud to count myself among the membership of MIT Emergency Medical Services. I thank all the members, past and present, that made my time there so meaningful. They are truly among the finest, most hard-working people I've ever had the privilege to meet. Working with MIT-EMS is among the most rewarding things I've ever done in my life, and the friendships I formed there will stay with me wherever I go.

I have been incredibly fortunate to have a family that has supported, encouraged, and believed in me with all their hearts every day that I have been alive. It's hard to think of how anyone could keep a straight face when a nerdy eight-year-old boy's favorite activity is pretending to a famous scientist giving an interview on the national news, but somehow my family did it. I cannot say enough to communicate how grateful I am to all of them for their support. From the bottom of my heart I thank Amy and Rudy Smith; Charlotte and Buddy Allen; and Leah, David, Zachary, Jacob, and Isabelle Bridges. Without each and every one of them, none of what I've done would have been possible. A special thanks is due to Buddy, whose infectious curiosity and unwavering encouragement helped make me the scientist I am today.

The light of my life for the past four years has been my partner, Alexander McAdams. To say that she is the reason I get out of bed each morning would be no exaggeration, and not just because she sets the alarm. I have never met, and I doubt I ever will meet, anyone as driven, dedicated, intelligent, quick-witted, insightful, and compassionate as she is. Every day that we're together, she challenges me, supports me, and makes me strive to be a better person. She makes me laugh like no one else ever has, and I still get butterflies in my stomach when I look at her. She has proofread more jargon-filled run-on sentences than any writer should ever have to, and she somehow never lost her patience or sense of humor in dealing with the late nights, erratic hours, and doomed experiments. We have been together through my lowest lows and highest highs, and I struggle to imagine either my tragedies or my triumphs without her by my side. I love her more than anything, and it is my sincerest wish that we never spend a day apart.

This thesis is dedicated in loving memory to my late mother, Kimberly Russell, and my late grandmother, Shirley Russell. They were the strongest, most passionate people that I've ever known. Their constant, loving guidance made me who I am, and I miss them every day. Whatever I do in life will always pale in comparison to everything that they did for me.

Table of Contents

1. Background

1.1. Introduction and motivation

This research was motivated by the synthesis of two observations. The first observation is that nucleic acids, the fundamental biopolymers responsible for storing and translating the genetic code, are subject to extensive chemical modification [1-5]. Beyond the common canonical nucleosides are a host of more than 100 currently known structures [6], which are enzymatically synthesized following transcription [7], and can be found in all types of RNA, as well as DNA [8]. These modifications display a striking amount of structural diversity, and can differ from canonical nucleosides in the base, sugar, and/or backbone moiety [9, 10]. Their diversity is matched by their ubiquity, as these kinds of modifications occur in all known organisms, with some shared across all domains of life, and others restricted to particular subsets of organisms, including bacteria [11, 12]. Despite their evolutionary conservation and importance for life, the functions of these various modifications are often undefined, with research conducted and activities defined in a piecemeal fashion. This lack of systematic evaluation presents a large source of untapped data that we can investigate.

The second observation is that infectious diseases constitute a significant fraction of the global burden of disease [13, 14]. Infectious diseases account for three of the ten leading causes of death [15] and more than 30% of the lost disability-adjusted life years worldwide [16]. Of particular concern is the continued spread of antibiotic resistance, which has been increasing for years without a concomitant increase in the number of new antimicrobials [17-20]. There is thus a pressing need for research to address the spread, diagnosis, and treatment of infectious diseases. Taken together, these observations underlie the fundamental goal of this research: to define the role of nucleic acid modifications in bacterial pathogens. We will first examine the nature of RNA and DNA modifications, then look to the disease landscapes of the bacteria studied, and finally conclude by outlining the specific aims of this thesis.

1.2. Nucleic acid modifications

Modified derivatives of the canonical nucleic acid components of RNA and DNA are very common, and play important roles in a variety of processes. We studied two broad categories of

modified nucleic acids: noncanonical ribonucleosides in RNA and phosphorothioates in DNA. One important feature shared by these modifications is that they possess both well characterized and poorly understood functions, thus making them attractive topics for systematic study. We will briefly examine the salient features of each category.

1.2.1. RNA modifications

Endogenous RNA molecules are extensively modified in order to reach their final active forms. These modifications are both diverse and ubiquitous, taking many forms and performing many tasks. Here we briefly review their synthesis, location, and function.

1.2.1.1. Structure and biosynthesis

Beyond the four canonical ribonucleosides typically found in RNA, more than 100 modified nucleosides have been discovered from all phylogenetic domains of life [6, 9, 21]. These modifications have diverse structures, and can range from simple isomerizations or methylations up to the addition of multiple heavy atoms, or the linking of other biomolecules like amino acids [22-24]. The structures of some common modifications are shown in **Figure 1-1**.

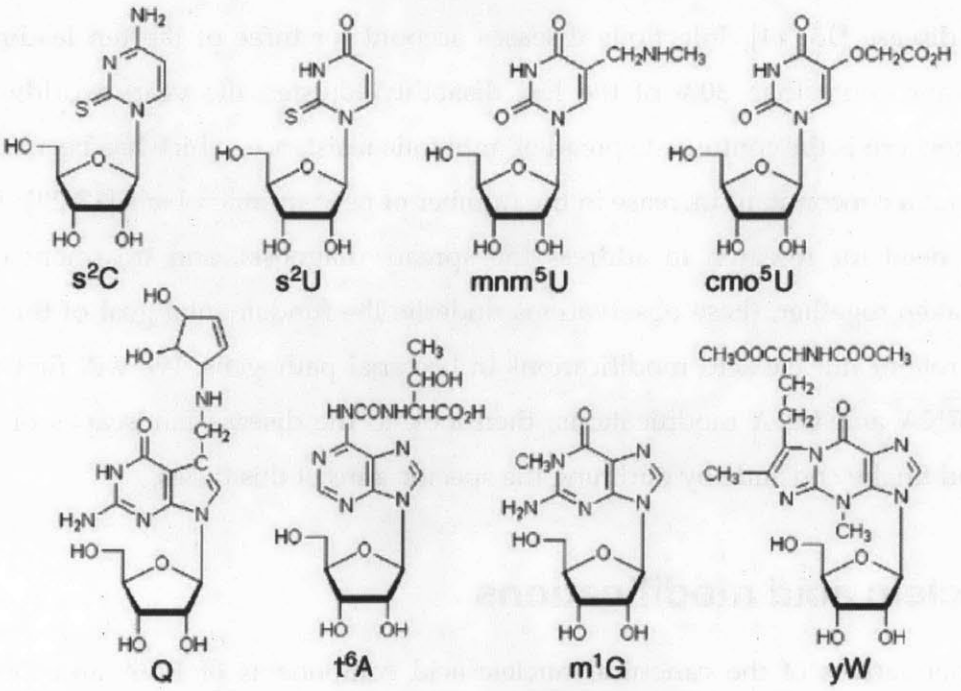

Figure 1-1: Structures of several common RNA modifications. Modifications derived from all four canonical nucleosides are shown. Figure adapted from [28].

Synthesis of these modifications generally occurs post-transcriptionally, using the canonical nucleosides as substrates (though some, including inosine and queuosine, are incorporated into RNA in their modified forms [25]). Depending on the complexity of the modification, a single enzyme or several interdependent enzymes might be required for synthesis. An example of the multi-step synthesis of a complex "hypermodified" adenosine derivative is shown in **Figure 1-2**. Modification enzymes are dependent on the position of the substrate nucleoside, so several enzymes are required to synthesize the same modification in different molecular contexts, which helps explain why there can be many more modification genes than there are genes for the RNA templates [26]. Dozens of pathways and enzymes involved in RNA modification have now been identified [7], including whole enzyme families such as the Trm proteins (tRNA methyl transferases) [27].

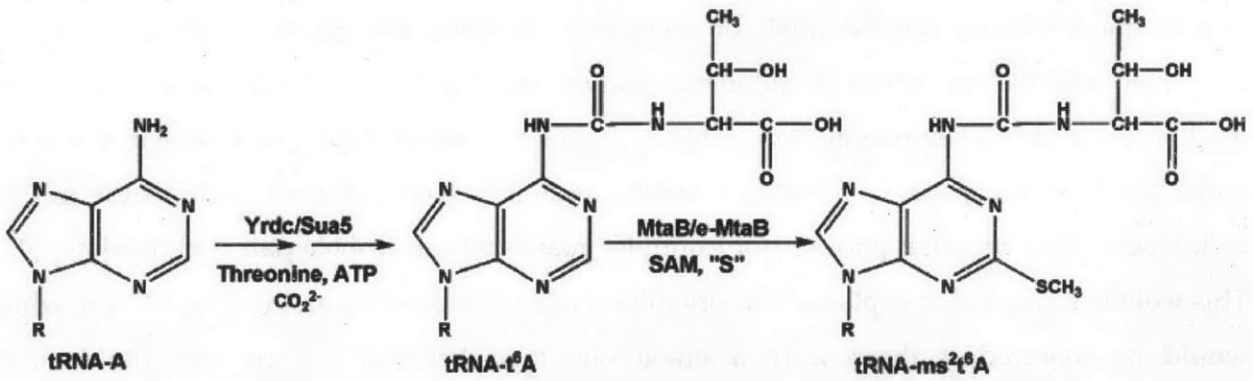

Figure 1-2: Biosynthesis of a hypermodified adenosine derivative. The product of these reactions, ms^2t^6A, is found at position 37 in tRNAs from all organisms, and is formed by a pair of universally conserved protein families. Figure adapted from [29].

1.2.1.2. RNA modifications in tRNA

Modified ribonucleosides are found in virtually all types of non-coding RNA [30], but they are most abundant in transfer RNA (tRNA), the adapter molecule linking the genetic code to the amino acid pool. Typical tRNA molecules are 75 to 90 nt long, and usually contain an average of eight modifications (though this is highly variable) [25]. These modifications can occur at virtually any position in the tRNA, but are especially common at positions 34 (the wobble position) and 37 (flanking the 3'-end of the anticodon loop), as shown in **Figure 1-3** [8, 31]. Modifications of all four canonical nucleosides have been discovered, but uridine and adenosine derivatives are especially common [6, 7, 9, 21]. In some organisms the number of

genes coding for tRNA modifying enzymes can be four-times greater than the number coding for the tRNAs themselves, making up as much as 1% of the genome [7, 25, 26, 32].

Given their abundance and conversation across organisms, it is not surprising that tRNA modifications have a variety of critical functions. One of the earliest observations was that they can modulate base pairing and pi-stacking in ways that stabilize tRNA secondary and tertiary structure [33, 34]. This may explain the high frequency and diversity of modifications seen in archaea, particularly extremophiles [11, 12, 35]. Modifications also help maintain the ribosomal reading frame and reduce the rate of translational frameshift mutations that occur through tRNA slippage, as unmodified tRNAs induce pausing and increase the error rate [26, 36]. Modifications can also serve as markers of proper tRNA maturation, and cells are capable of specifically degrading or enzymatically discriminating tRNAs that lack modifications [37-39]. Finally, modifications are essential for accurately decoding the genome, through both the expansion and the restriction of codon recognition [40, 41]. In expanding codon recognition, modifications play a key role in the wobble hypothesis, in which the 5′ nucleoside in the tRNA anticodon loop is capable of forming a wobble base pair with a 3′ nucleoside in the mRNA codon other than its usual partner (for example, guanosine can wobble pair with uridine) [42]. This wobble base pairing explains how organisms can have fewer than 61 coding tRNAs, which would be required if there were a one-to-one ratio between codons and tRNAs [43]. Modifications play a role in the wobble hypothesis by expanding the number of possible non-canonical base pairings (for example, the adenosine derivative inosine can pair with adenosine, cytosine, or guanosine) [28, 40, 44-49].

In contrast, modifications can also ensure accurate translation by restricting codon recognition, such as in the case of bacterial and archaeal translation of isoleucine codons. Isoleucine is part of the AUN codon box (where N represents any canonical nucleoside), which is unique in that three of its members—AUU, AUC, AUA—code for isoleucine, while only AUG codes for methionine [22]. Normally, given the wobble hypothesis, any tRNA capable of pairing with AUG would also pair with AUA. To avoid this problem, bacteria and archaea modify the wobble cytosine of the CAU isoleucine tRNA so that it pairs only with A, not with G [41]. In short, tRNA modifications are absolutely essential for normal function in all organisms.

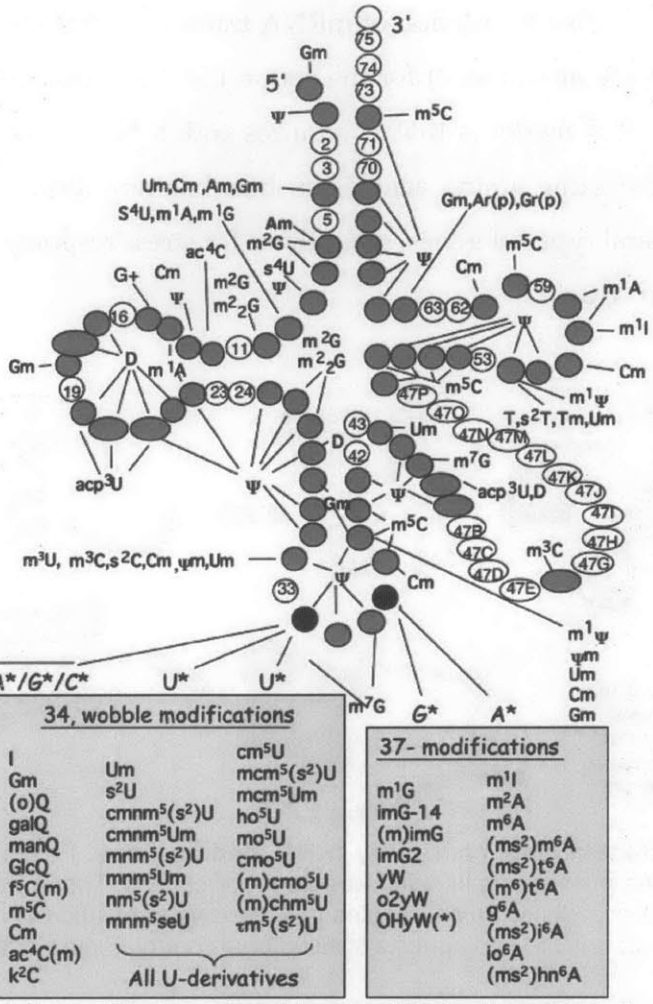

Figure 1-3: Distribution of modified nucleosides in tRNA. A variety of modifications have been identified at virtually all positions in tRNA (gray circles), with only a few positions not known to be modified (white circles). Positions 34 and 37 are most frequently modified (black circles). Figure adapted from [8].

1.2.1.3. Translational control by tRNA modifications

One feature shared by the diverse functions described above is that they are all relatively "static"; that is, while they are necessary for proper cellular function, they do not participate in dynamic processes. This view has shifted recently due to an emerging model in which tRNA modifications play a critical role in cellular responses to stress. Originally described in *Saccharomyces cerevisiae* exposed to alkylation stress [50], the model is conceptually illustrated in **Figure 1-4** [51]. As with many of the functions described above, the key feature in this model is that wobble-modified tRNAs have increased binding affinity for certain codons. Following stress, the proportion of modified tRNAs increases, either through increased activity of tRNA modifying enzymes, or through selective degradation of unmodified tRNAs [39]. This altered

tRNA pool results in selective translation of mRNA transcripts that are enriched (relative to the other codons for the same amino acid) for the codon that the modified tRNA selectively binds [48]. A key feature of this model is that it requires codon bias, a nonrandom distribution of multiple codons for the same amino acid. Such bias has now been demonstrated in several organisms and for several types of genes, often those for stress response proteins that need to be rapidly induced for survival [52].

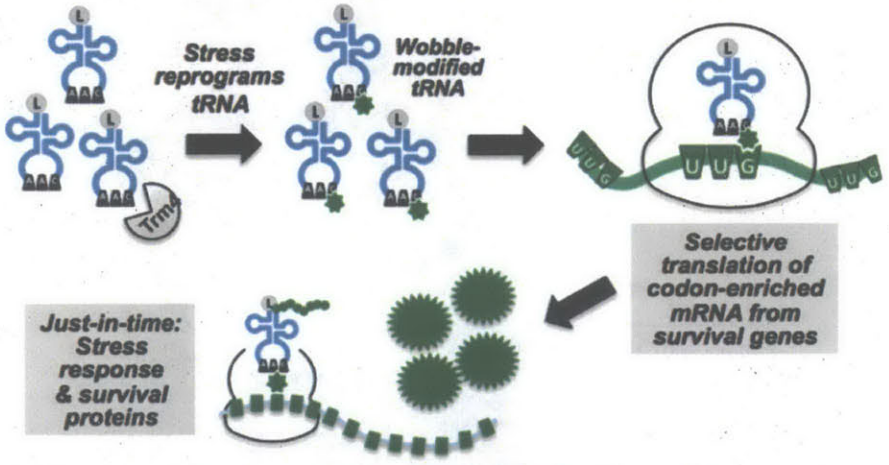

Figure 1-4: Model for translational control by tRNA modifications. Following stress, cells alter their tRNA pool to enrich tRNAs possessing specific wobble modifications. These wobble-modified tRNAs bind more efficiently to particular codons, which enables the selective translation of mRNA transcripts enriched in those codons. The result is rapid and specific translational control. Figure adapted from [51].

The dynamic nature of tRNA modifications has been confirmed by experiments showing that toxicants with distinct molecular mechanisms induce reprogramming of modifications in unique ways that bias the translation of specific survival proteins [53]. This model has now been corroborated by numerous experiments showing that loss of specific tRNA modifying enzymes confers sensitivity to the associated exposures [54-56]. We recently described a general platform for quantitative tRNA modification profiling that allows for the discovery of such translational control systems in any organism [57]. While these systems have so far been described only in eukaryotes, the ubiquitous nature of the machinery led us to hypothesize that they are present in all domains of life. In particular, such mechanisms may play important roles in pathogenic bacteria, modulating key processes such as immune evasion and antibiotic resistance.

1.2.2. DNA phosphorothioation

Phosphorothioation is a unique nucleic acid modification. It is both the only known endogenous sulfur-containing DNA modification, and the only known endogenous DNA backbone modification. While it was first described as an *in vitro*, synthetic creation, its presence in living organisms is now well established. Here we briefly review the structure, biosynthesis, distribution, and function of DNA phosphorothioation.

1.2.2.1. Chemical structure and characteristics

Phosphorothioate is a chemical modification of DNA in which one of the nonbridging oxygen atoms in the phosphate backbone is replaced with a sulfur atom, forming a bond known as a phosphorothioate (PT), shown in **Figure 1-5**. PT bonds were originally created several decades ago using synthetic organic chemistry on oligonucleotide substrates [58], and were the subject of much research owing to their unique properties. PT bonds are highly resistant to degradation by nucleases [59, 60], and their presence was used to stabilize oligonucleotides for intracellular delivery as antisense effectors [61]. At the same time, PT-containing DNA structures maintain normal interactions with a wide variety of enzymes, which opened the possibility for their use as competitive inhibitors [62, 63]. Interestingly, PT-containing DNA is also highly immunogenic, and has often been used as a vaccine adjuvant [64, 65]. The exact immunostimulatory motif is unknown [66, 67], but this property would gain new meaning decades after it was first observed, as described below.

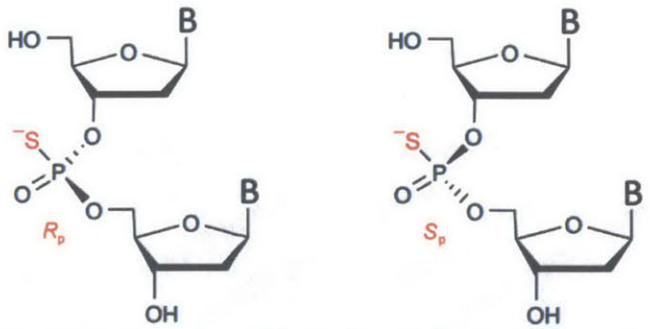

Figure 1-5: Structure of the DNA phosphorothioate bond. Replacing a nonbridging phosphate oxygen with sulfur (highlighted in red) creates a phosphorothioate bond. Both the R_p and S_p diastereomers (labeled in red) are shown. B: any purine or pyrimidine nucleobase.

1.2.2.2. Biosynthesis and *dnd* genes

An unusual phenotype in which the DNA of certain bacteria degraded during electrophoresis was first reported in 1988 [68]. Further studies showed that the degradation was associated with a site-specific DNA modification, and the gene cluster responsible was identified, isolated, and named *dnd* (for DNA degradation) [69-71]. Eventually a set of five genes, *dndA-E*, was shown to mediate the phenotype by addition of a sulfur-containing motif into the DNA [71]. Surprisingly, in 2007 the *dnd* gene cluster was shown to incorporate sulfur into DNA in the form of a sequence- and stereo-specific PT bond, providing the first known example of an endogenous DNA backbone modification [10].

Several studies have helped define the biochemical functions of the *dnd* gene products, and our current understanding of the cluster is shown in **Figure 1-6**. DndA is a cysteine desulfurase similar to the *Escherichia coli* protein IscS, and is capable of assembling DndC as a 4Fe-4S cluster protein [72]. Surprisingly, more than half of the *dnd* clusters that have been characterized lack *dndA*, with its activity complemented by a native gene linked to the *dnd* cluster (such as IscS in *E. coli* DH10B) [73]. In addition to its role as an 4Fe-4S cluster, DndC has been shown to have pyrophosphatase activity and is predicted to have 3'-phosphoadenosine-5'-phosphosulfate (PAPS) reductase activity [72, 74, 75]. DndB is predicted to have a 4Fe-4S cluster binding domain, as well as homology to DNA repair ATPases, and it has also been implicated as a possible transcription factor or protein regulator based on the observation that its loss increases PT incorporation [71, 76, 77]. DndD has ATPase and DNA nicking activity, as demonstrated by functional characterization of the *Pseudomonas fluorescens* homolog SpfD [78]. Finally, DndE has been shown to be a nicked DNA binding protein with an additional undefined fold [79, 80].

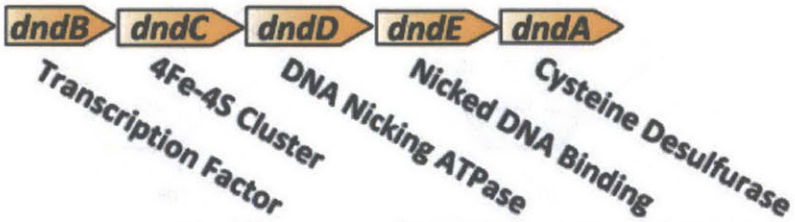

Figure 1-6: Organization of the *dnd* gene cluster. Putative functions for each gene product are shown, based on sequence homology, crystal structures, and/or biochemical characterization. The most complete version of the cluster is shown, though several organisms lack *dndA*. Figure adapted from [81].

1.2.2.3. Phylogenetic distribution and horizontal gene transfer

One of the most striking features of the *dnd* gene cluster is that it is found in a wide variety of unrelated bacteria, as shown in **Figure 1-7**. PT modifications have been found in more than 200 species, including many human pathogens [82-84]. There is now ample evidence that the *dnd* cluster is acquired by horizontal gene transfer. All of the characterized *dnd* clusters are located within much larger mobile genetic elements, such as chromosomal islands and plasmids, which display striking diversity [76]. The content of the *dnd* clusters themselves also vary greatly, as demonstrated by the observation that different organisms insert the PT bond at different DNA consensus sequences [85]. Members of the same species will often differ in their genomic island content and *dnd* status, supporting the conclusion that *dnd* transfer occurs independently and repeatedly, rather than through large scale vertical transfer [76].

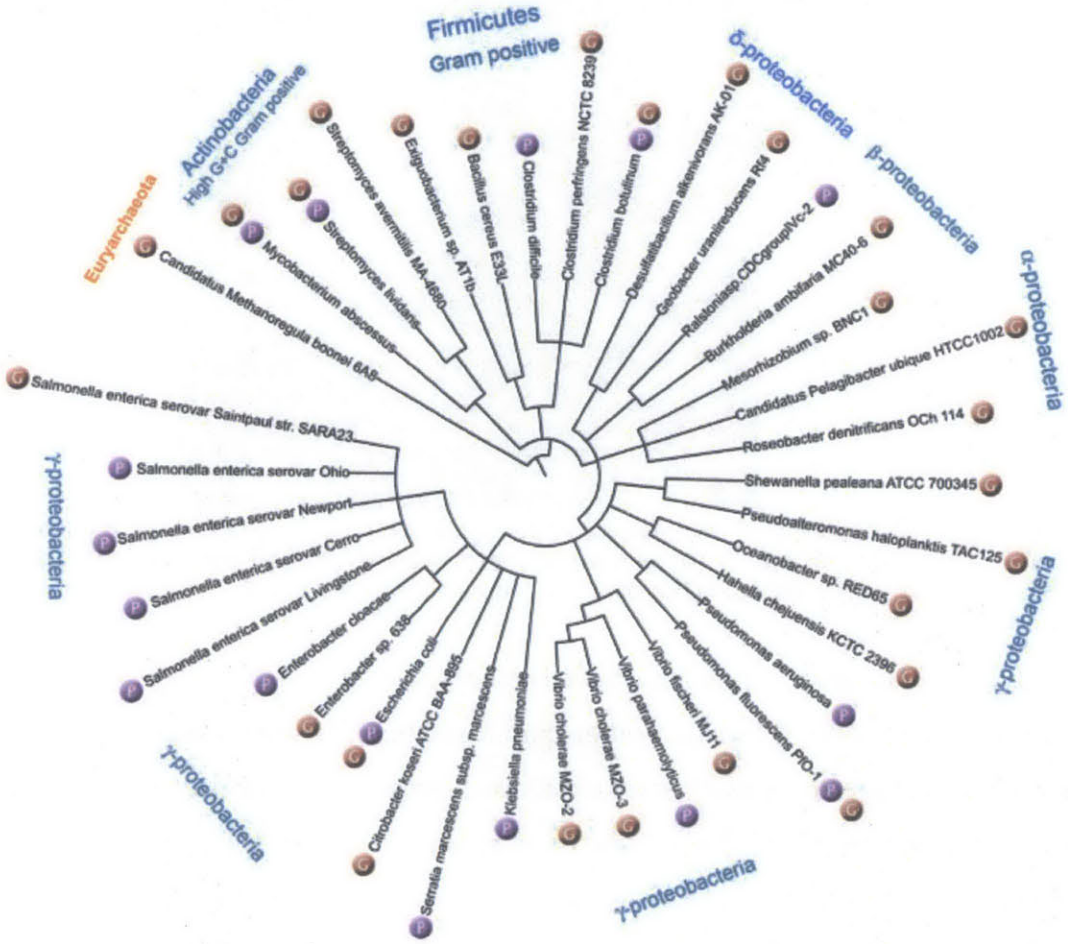

Figure 1-7: Phylogenetic tree of bacterial species containing phosphorothioate (PT) modifications. The presence of PT modifications was determined by sequencing of *dnd* genes (brown circles), presence of the PT-related DNA degradation phenotype (purple circles), or both. Figure adapted from [76].

1.2.2.4. Putative functions

Phosphorothioation systems share some similarities with methylation-based restriction-modification systems, such as sequence-specific insertion and discrete levels of modifications [85]. Thus it was hypothesized that the *dnd* cluster might function as a novel restriction system, or as a type of bacterial "immunity" similar to a CRISPR-Cas system [81]. This hypothesis was confirmed by the observation that PT-positive bacteria restrict the incorporation of a plasmid lacking sulfur, but PT-negative bacteria do not (**Figure 1-8**) [86]. Subsequent analysis revealed that restriction was mediated by a set of three genes, *dndF-H*, associated with the *dndA-E* cluster.

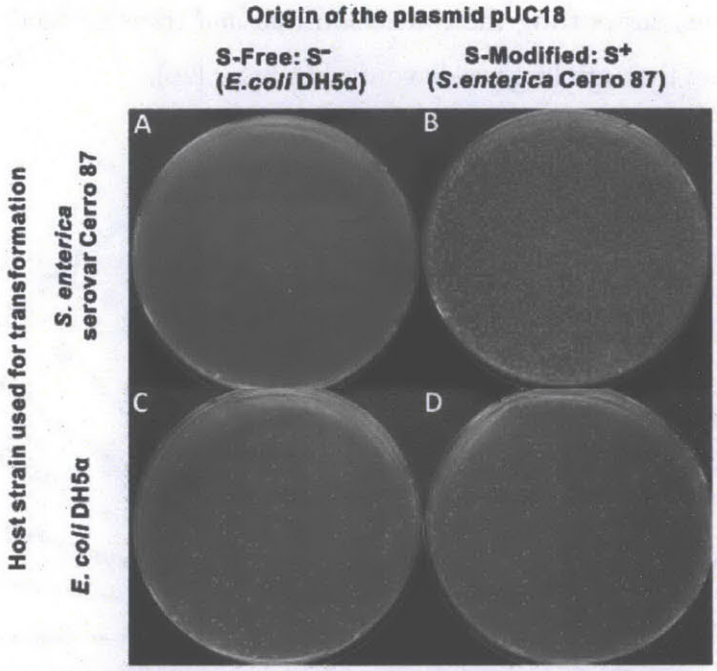

Figure 1-8: Restriction activity of *dnd* genes. Bacteria containing the restriction genes *dndF-H* (A and B) will restrict a plasmid lacking PT (A) but will accept the same plasmid containing PT (B). Bacteria lacking *dndF-H* (C and D) will accept either plasmid. Figure adapted from [86].

Surprisingly, however, many organisms have been discovered in which only *dndA-E* is present, pointing to the existence of a function other than restriction. Recent reports demonstrated that PT-positive bacteria are more resistant to oxidative stress in the form of hydrogen peroxide (**Figure 1-9**), and hypothesized that PT serves as an antioxidant [87]. Finally, there is evidence that some enzymes specifically recognize and interact with PT modifications, which has led to the hypothesis that PT may play a role in the control of gene expression [88, 89]

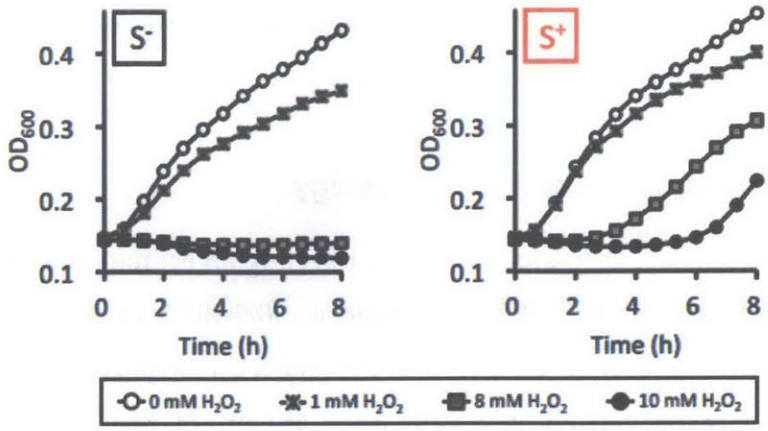

Figure 1-9: Hydrogen peroxide resistance conferred by *dnd* genes. Bacteria containing a functional *dnd* gene cluster and the associated PT modifications grow more robustly during exposure to H_2O_2 than bacteria without PT. Figure adapted from [87].

1.3. Bacterial pathogens

Bacterial infections constitute a substantial global disease burden, and are among the leading causes of death and disability worldwide [15, 16]. We chose to focus on *Helicobacter pylori* and the *Mycobacterium tuberculosis* complex, which are interesting not only for their ubiquity—the first and second most common infections in the world, respectively—but also for their unique disease processes, complex host interactions, and significant unmet needs. Here we will briefly review the key features of each disease.

1.3.1. *Helicobacter pylori*

H. pylori is a spiral, flagellated, Gram negative, microaerophilic bacterium that colonizes the human stomach [90]. Helical bacteria were first described in the stomachs of dogs and people more than 100 years ago [91], but these findings were frequently dismissed as contaminants due to the harsh nature of the stomach environment [92]. This assumed sterility remained largely dogma until Australian physician Robin Warren reported the discovery of an unidentified bacillus in the stomachs of patients with active gastritis [93]. After collaborator Barry Marshall infected himself by drinking a pure culture of *H. pylori* [94], the bacterium was recognized as the causative agent of chronic gastritis. Marshall and Warren were awarded the 2005 Nobel Prize in Physiology or Medicine for their discovery, and *H. pylori* is now recognized as the cause of a significant public health burden through its association with gastritis, peptic ulcer disease, and

increased risk of gastric cancer [90, 95-98]. Here we briefly review the epidemiology, pathogenesis, and unmet needs in *H. pylori* disease.

1.3.1.1. Disease presentation and epidemiology

H. pylori is the world's most successful pathogen, infecting an estimated three billion people, or half the global population [99]. The vast majority (80-90%) of those people harbor an asymptomatic and often undiagnosed infection that causes subclinical chronic inflammation, a condition known as gastritis [100]. The remaining 10-20% of people develops peptic ulcer disease. While ulcers were traditionally dismissed as more annoying than dangerous, *H. pylori* infection is a severe problem because it is strongly associated with the development of gastric cancer, which is the second leading cause of cancer death worldwide [95, 97, 98, 100-103]. The exact mechanism linking *H. pylori* infection to gastric cancer is unknown [104, 105], but the causal link is so well established that *H. pylori* became the first infectious disease to be classified as a definite carcinogen by the International Agency for Research on Cancer [106].

As shown in **Figure 1-10**, the distribution of *H. pylori* infections is highly variable along geographic and socioeconomic axes, with prevalence estimated to be <40% in most developed countries compared to >80% in many developing countries [100]. Age also has a significant impact, even in developed countries, with prevalence estimates varying from ~10% for children under 10 to >60% for adults over 50 [107]. The strong association with age is thought to reflect a selection bias of populations exposed to poor hygiene practices early in life, rather than increasing infection over the lifetime of an individual [108]. The majority of *H. pylori* infections occur during childhood, especially before five years of age [109], and the infection is known to persist for life without treatment [110]. Despite these high numbers, worldwide prevalence has been decreasing for several years, which likely reflects improved sanitation and nutrition programs [107]. In support of this conclusion, the incidence rates for *H. pylori* are very low in developed countries, but have remained relatively stable in developing countries [111, 112].

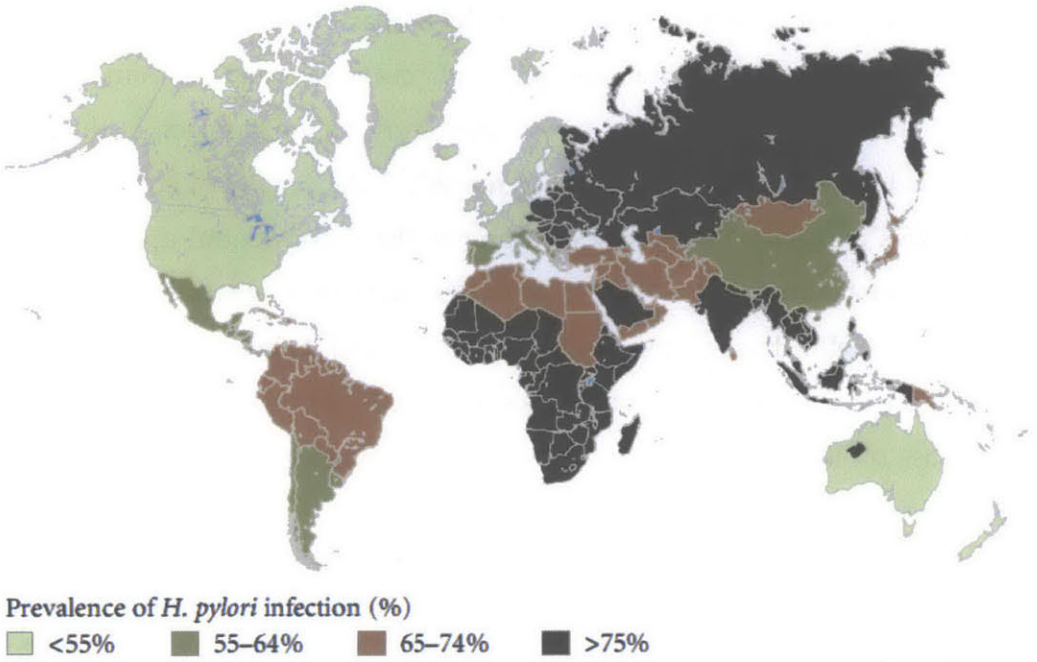

Figure 1-10: Epidemiology of *H. pylori* infection. The total estimated prevalence of *H. pylori* infection as of 2011 shows that many regions have more than 75% of people infected. Figure adapted from [100].

Notably, despite decades of research, the exact mechanisms of *H. pylori* transmission and acquisition are still unknown, and are the subject of significant debate within the field [99, 100, 108, 113]. No natural reservoir has been identified, and person-to-person transmission is generally accepted as the most likely explanation [113]. This belief is consistent with the repeated observation that living with family members harboring *H. pylori* is a significant risk factor for infection, especially among children with infected mothers or older siblings [109, 111, 112]. The fecal-oral, oral-oral, and gastric-oral routes have all been proposed, but none has ever been definitively proven.

1.3.1.2. Pathophysiology and host response

H. pylori infection is unique in that its pathology is not driven solely or even primarily by secreted toxins, but rather by a complex interplay between the bacterium and the host. A complete description of these interactions is beyond the scope of this work, but is available in several excellent review articles [97, 100, 114-116]. Here we will briefly summarize the initiation of infection and the development of pathology, paying special attention the most important pathogen and host features.

H. pylori is exquisitely well adapted to its niche in the human stomach, and is able to invade and colonize despite encountering numerous physical, chemical, and immunological barriers (**Figure 1-11**). The first barrier *H. pylori* faces upon entry to the stomach is the highly acidic nature of the gastric lumen, which has a pH of roughly 2 under normal conditions. *H. pylori* is able to survive this exposure by rapidly escaping to the more neutral epithelial layer of the stomach. The chemotaxis receptor TlpB orients the bacterium toward the epithelial layer, multiple flagella propel it through the gastric secretions, and its helical shape allows it to bore into the dense gastric mucus with a screw-like motion. In addition, *H. pylori* expresses large amounts of urease on its surface, which converts urea to ammonia and creates a pH-buffering envelope around the bacteria.

Once *H. pylori* reaches the epithelial layer, numerous adhesins such as SabA allow the bacteria to attach to the epithelial cells, and in some cases invade between the tight junctions [100] or into the epithelial cells [117]. After attaching to the epithelial layer, *H. pylori* passively evades the innate and adaptive immune responses through a variety of unique characteristics. Members of the toll-like receptor (TLR) family normally recognize common components of bacterial pathogens—such as cell surface lipopolysaccharides (LPS) or flagellar proteins—but they fail to do so in the case of *H. pylori*. LPS from *H. pylori* is tetra-acylated (rather than hexa-acylated as in most Gram negative organism), and its structure closely mimics that of the Lewis blood group antigens found on the surface of host cells, so it is not recognized by TLR4 [115]. Similarly, the main *H. pylori* flagellar protein FlaA harbors an N-terminal mutation that prevents its recognition by TLR5 [115]. Finally, the bacterium is capable of coating itself with host proteins, including cholesterol and plasminogen, which further enables it to evade detection by TLRs [118].

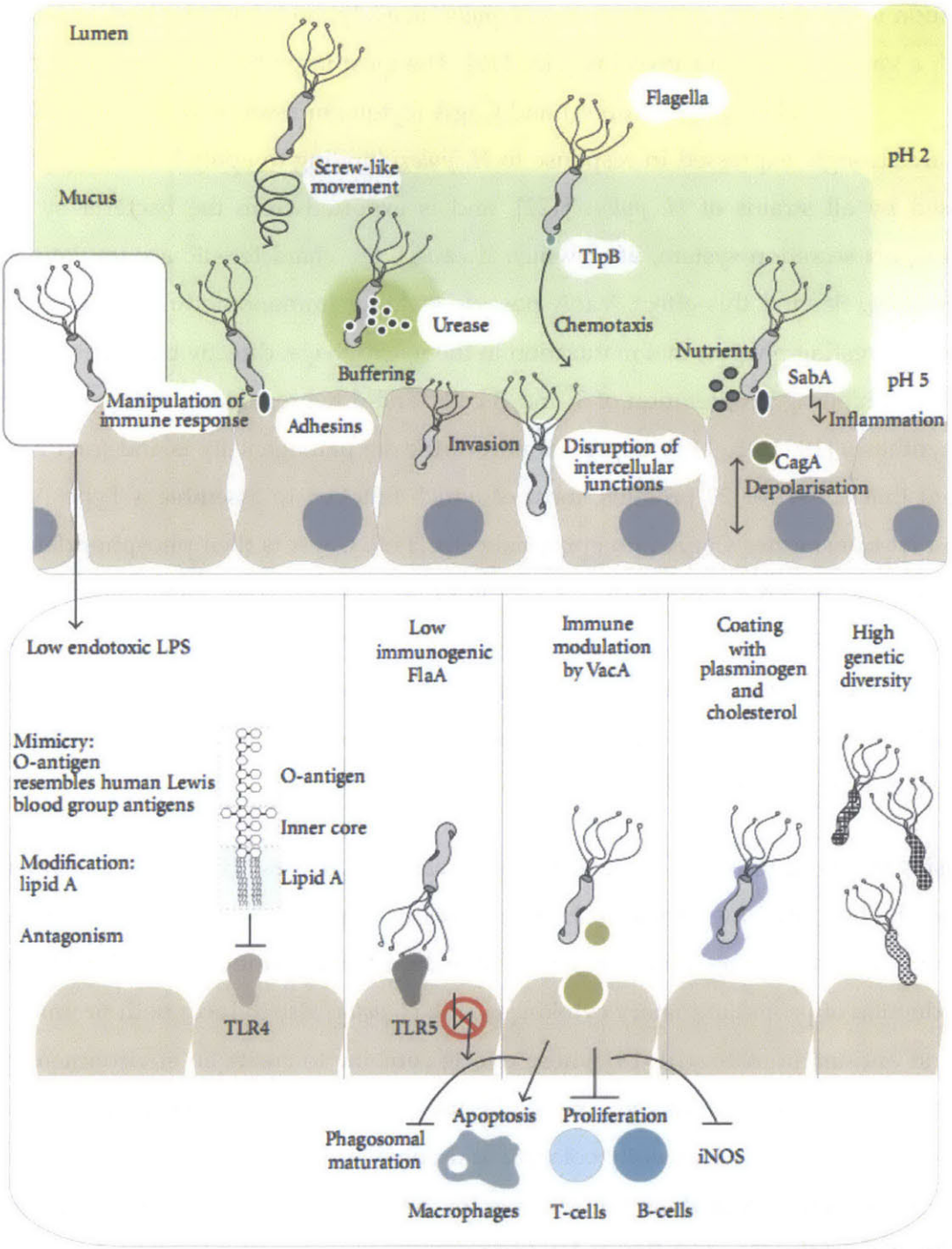

Figure 1-11: Mechanisms of invasion, colonization, and immune evasion in *H. pylori*. *H. pylori* uses a variety of processes to invade the human stomach. Its flegalla and helical shape allow it to escape the lumen and burrow into the gastric mucosa, under the guidance of TlpB. Cell surface ureases produce ammonia and buffer the local pH around the bacterium, and adhesins like SabA allow it to bind to and even invade the host epithelial cells. After adhesion, *H. pylori* passively evades the immune response via protein mutations and genetic diversity. The virulence factor CagA induces the release of nutrients from host cells, while VacA actively suppresses the immune response. Figure adapted from [100].

In addition to these passive mechanisms, *H. pylori* actively modulates the host immune system through a variety of effector proteins [115, 119]. The most important of these are the virulence factors VacA (vacuolating cytotoxin A) and CagA (cytotoxin associated gene A) [120], both of which are strongly expressed in response to *H. pylori* binding to epithelial cells [121]. VacA is expressed by all strains of *H. pylori* [122], and is exported from the bacteria by a Type V autotransport secretion system, after which it causes the characteristic accumulation of large vesicles [123]. Beyond this effect, VacA possesses strong immunomodulatory activity, and is capable of arresting phagosomal maturation in the macrophage, directly triggering macrophage apoptosis, inhibiting proliferation of T and B cells, and downregulating iNOS (inducible nitric oxide synthase) [100, 115, 119]. CagA is a part of the *cag* pathogenicity island (*cag*PAI), a 37-kb fragment that codes for 29 proteins, most of which function to assemble a Type IV secretion system that translocates CagA into epithelial cells [119]. CagA is then phosphorylated by host Src kinase, after which it induces drastic changes in cell morphology, including depolarization, elongation, and tight junction disruption [100]. These changes trigger the release of nutrients that *H. pylori* requires for robust growth. In addition, CagA induces transcription of oncogenes through STAT3, which may explain the stronger association with gastric cancer seen in CagA-positive (i.e. Type I) strains of *H. pylori* [104].

Surprisingly, in addition to these immune evasion strategies, *H. pylori* also intentionally activates the host immune response. *H. pylori* uses its Type IV secretion system to translocate peptidoglycan into the epithelial cell, which activates the transcription factor NF-κB and drives the production of proinflammatory cytokines [115]. *H. pylori* also induces both proinflammatory IL-1β and anti-inflammatory IL-18, whose effects combine to create an environment that both promotes bacterial persistence and continually induces host cell damage [124]. Together, these factors enable *H. pylori* to efficiently colonize and persistently damage the human stomach. The complexity of these interactions underscores the need for further research to strengthen our understanding of the *H. pylori* disease landscape.

1.3.1.3. Disease management and unmet needs

The extreme prevalence of *H. pylori* infection reflects the fact that there are significant barriers to effective disease management. The first barrier is diagnosis. A variety of tests that vary

significantly in cost and invasiveness are available, including: blood, stool, and urine antigen tests; serological antibody titer tests; urea breath tests; and endoscopic biopsies [125]. However, despite the seeming abundance of options, the vast majority (~90%) of *H. pylori* infections remained undiagnosed because they do not produce overt symptoms [99, 108, 111]. Proposals to attempt blanket or indiscriminate *H. pylori* eradication in asymptomatic populations have not been supported because of evidence that *H. pylori* eradication can predispose individuals to esophageal cancer [126]. This paradox reveals a striking gap in our understanding of *H. pylori* carcinogenesis: both its presence and its absence are associated with cancer, and the particular pathogen and host factors that drive disease partitioning are still not completely understood [127]. Thus the first major unmet need in *H. pylori* management is a more complete understanding of the molecular mechanisms of carcinogenesis and disease partitioning. Given *H. pylori*'s heavy reliance on post-transcriptional regulation [128], as well as the numerous emerging examples of translational control by RNA modifications [129, 130], nucleic acid modifications make an attractive avenue of research into this process.

In patients where disease is confirmed and eradication is indicated (such as in those with overt symptoms, or those already predisposed to gastric cancer [101]), there are still barriers to disease management. Standard therapy calls for triple or quadruple treatment, combining two antibiotics with a proton pump inhibitor and sometimes a bismuth compound [131]. While this is generally effective, eradication can fail, necessitating repeat treatment. In addition, antibiotic resistance is widespread, growing, and able to greatly reduce the effectiveness of first- and second-line therapies [132-134]. The problem of antibiotic resistance is further enhanced by multiple synergies. The first synergy is that more virulent strains of *H. pylori* are more likely to acquire and transmit antibiotic resistance [135]. The second synergy is that *H. pylori* displays an extreme level of genetic diversity, is naturally competent, and will readily take up and incorporate environmental DNA, all of which drive the rapid spread of resistance mutations [126]. The final synergy is that antibiotic treatment can actually induce phenotypic resistance by driving *H. pylori* into a nonreplicative state (**Figure 1-12**) [136]. Thus the second major unmet need is the development of novel antibiotics, particularly those that disrupt novel targets or virulence factors. Again, given the emerging examples of critical RNA modifications [53] and the potential resistance associated with phosphorothioation [87], nucleic acid modifications make attractive targets for addressing this need.

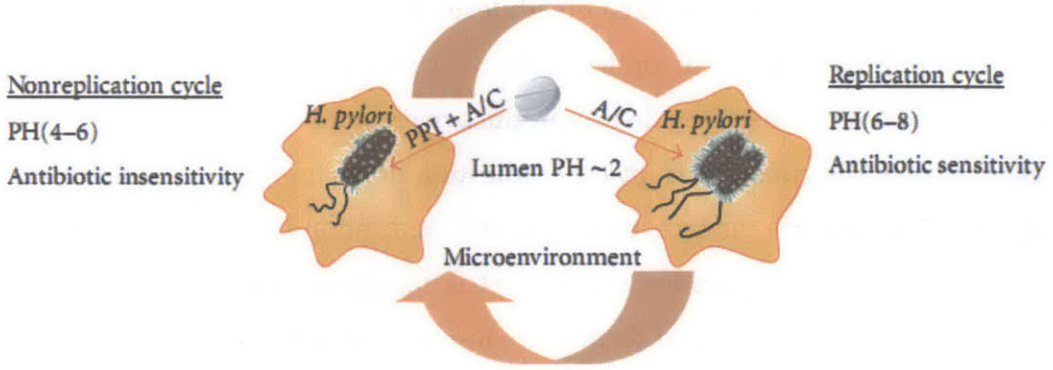

Figure 1-12: Synergy between antibiotic treatment and phenotypic resistance in *H. pylori*. Low pH induces a nonreplicative state in *H. pylori* that is phenotypically resistant to antibiotics. Antibiotic treatment can promote this resistance by decreasing the bacterial burden, which in turn lowers the gastric pH by disrupting the acid-suppressing activities of *H. pylori*. Figure adapted from [136].

1.3.2. *Mycobacterium tuberculosis* complex

The *Mycobacterium tuberculosis* complex refers to a group of closely related and genetically very similar mycobacterial species that cause tubercular (granuloma-forming) disease in a variety of organisms. The most well known and best characterized member of the complex is the titular *M. tuberculosis* (Mtb), the causative agent of most cases of human tuberculosis (TB). First described by Robert Koch over 100 years ago [137], Mtb infection continues to constitute a significant portion of the global burden of disease, and there is a pressing need for research to address all stages of the disease process. Here we briefly review the epidemiology, pathogenesis, and unmet needs in Mtb infection.

1.3.2.1. Disease presentation and epidemiology

TB is a chronic, highly contagious, sometimes fatal disease caused by infection with the bacterium Mtb. TB is most strongly associated with lung disease, and is usually spread by infected individual though the production of aerosolized droplets from coughing or sneezing [138]. TB is the second most common infection in the world, affecting an estimated two billion people, or one-third of the global population [139]. The vast majority of these people (~90%) have an asymptomatic and often undiagnosed infection referred to as latent TB. These individuals are not infectious, as the bacteria are successfully contained by the immune system. Roughly 10% of new infections progress to active TB, a severe and contagious form of the disease in which bacteria actively replicate within the lungs [140]. In severe cases the bacteria

can escape the lungs and disseminate to other organs, causing a host of debilitating symptoms [141]. In addition to immediate development of active disease, there is also the possibility of reactivation or progression, in which a person harboring a latent infection develops active disease [142]. Without treatment, both latent and active TB will persist for the life of the host. The transition from latent to active disease is highly dependent on a variety of host factors, and carries a lifetime risk of 5-10% [143].

The World Health Organization estimates that there are nine million new cases of active TB each year, which includes both primary active infections and reactivation of latent infections. There are also an estimated 1.5 million deaths each year [139]. Recent data indicate that TB is responsible for the loss of nearly 50 million disability adjusted life years worldwide annually, making it one of the top 15 causes of death and disability [16]. The global distribution of TB is heavily biased along both geographical and socioeconomic axes, as shown in **Figure 1-13**. A group of 22 high burden countries, nearly all of them in Sub-Saharan Africa and Southeast Asia, account for more than 80% of all TB cases [139]. Comorbidities such as HIV/AIDS and malnutrition are especially common in these regions, as are risk factors such as overcrowding and delayed diagnosis, all of which exacerbate the spread and progression of the disease.

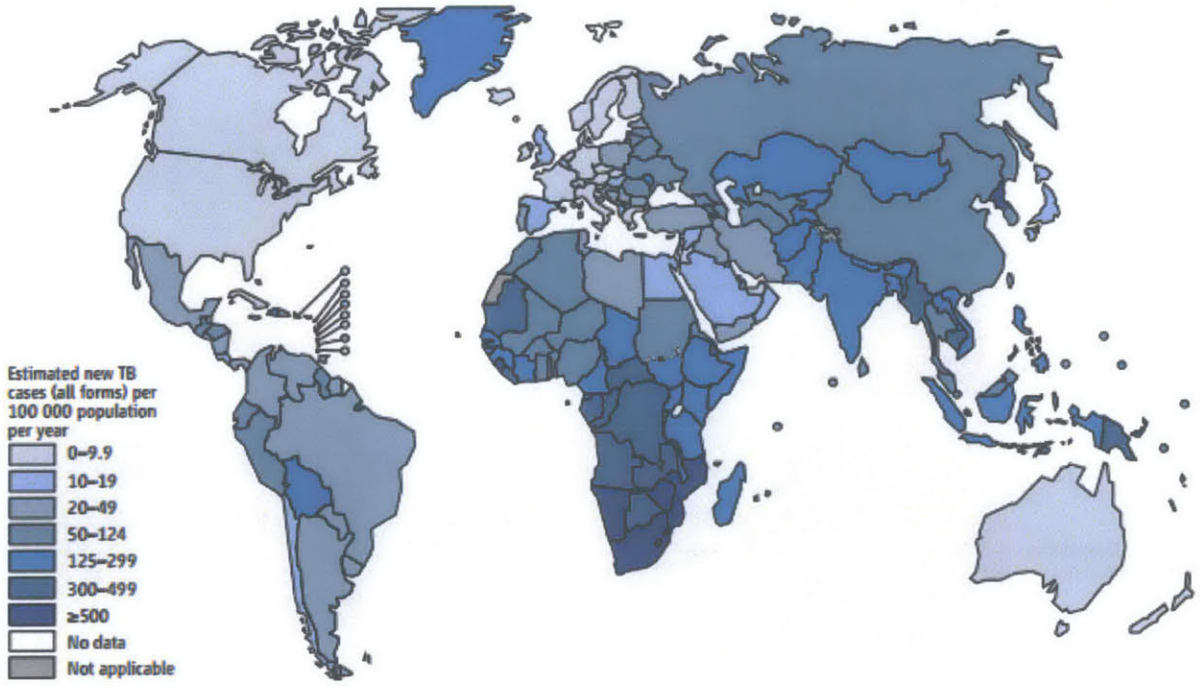

Figure 1-13: Epidemiology of tuberculosis. 2012 estimated incidence rates for new cases of active tuberculosis (both primary and reactivation) are shown. Figure adapted from [139].

1.3.2.2. Pathophysiology and host response

The disease process and presentation in TB is the result of an exceedingly complex, bidirectional interaction between the bacteria and the host. Dozens of virulence factors and host components are involved, many of which are poorly characterized [144-146]. A complete description of the process is beyond the scope of this work, but is described in detail in two recent, excellent reviews [143, 147]. Here we will briefly examine the initiation and progression of the disease, highlighting the most important pathogen and host factors.

The overall process of Mtb infection and TB development is outlined in **Figure 1-14** [148]. Aerosolized droplets containing live bacteria are inspired by an individual and travel into the lungs and settle in the alveolar spaces [141]. From there, bacteria are taken up by immune cells through phagotcytosis [138]. These immune cells are primarily resident alveolar macrophages, but neutrophils and dendritic cells are also capable of taking up the bacteria [143]. Phagocytosis activates the host immune response, which results in the migration of a variety of cell types to the site of infection [138, 143]. These cells surround the bacteria in an attempt to prevent replication and dissemination, which results in the characteristic formation of granulomas [149]. Over time granulomas may lose vascularization and become necrotic, and subsequent disruption can releases live bacteria, which results in active disease and transmission [150].

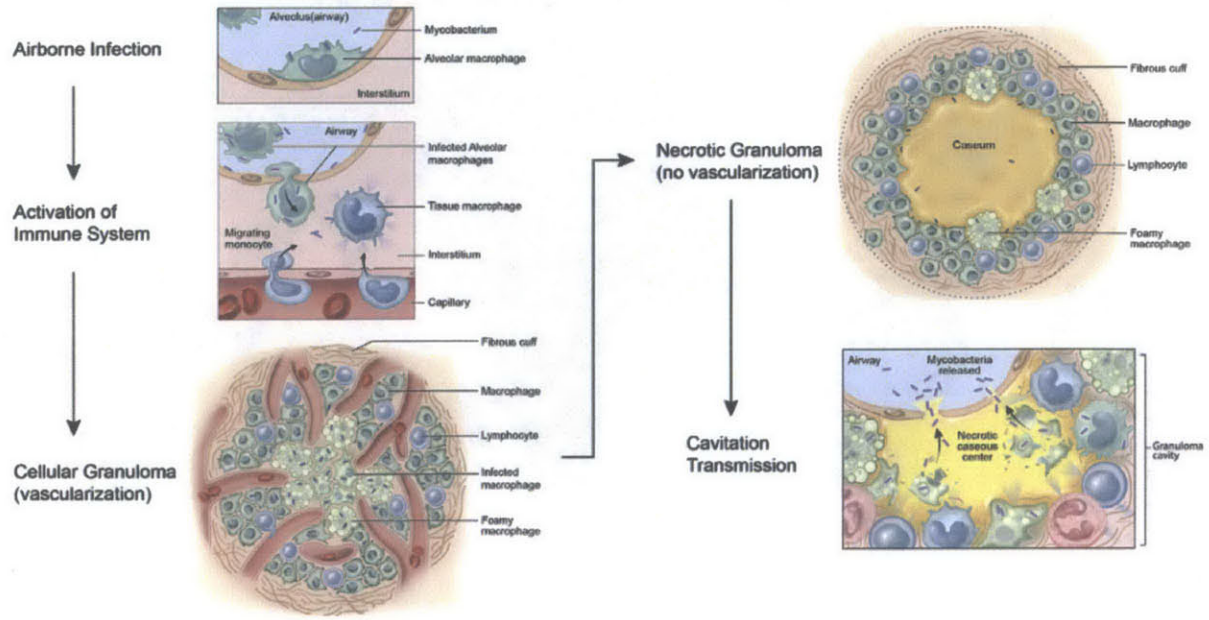

Figure 1-14: Process of tuberculosis infection. The development of tuberculosis involves several steps. After bacteria enter the lungs, they are engulfed by innate immune cells, which trigger an immune

response. Invasion of a variety of immune cells leads to the formation of a granuloma, which over time can become necrotic and lead to release of bacteria. Figure adapted from [148].

The molecular mechanisms driving this process are incredibly complex, and depend on both pathogen and host factors. The initial invasion of the bacteria into macrophages is mediated by a variety of host cell surface receptors, including complement receptors and the mannose receptor [143]. At the same time, bacterial lipids in the cell envelope interact with the macrophage surface, and enhance both binding and phagocytosis [151]. This reflects Mtb's role as an intracellular pathogen and its preferred niche inside macrophages. After phagocytosis, bacteria are contained within an intracellular compartment known as a phagosome. Under normal circumstances, the phagosome is highly toxic, and uses iNOS, NADPH oxidase, and an ATP-driven proton pump to generate reactive oxygen and nitrogen species (RONS), including nitric oxide (NO), superoxide (O_2^-), peroxynitrite ($ONOO^-$), and hydrogen peroxide (H_2O_2) (**Figure 1-15A**). In addition, the phagosome is capable of fusing with the lysosome, an acidified vacuole containing more than 50 proteases, hydrolases, and nucleases. This fusion produces a mature phagolysosome, which is capable of degrading nearly any cellular material (**Figure 1-15B**). However, Mtb is able to halt these processes [141, 147, 152].

Mtb uses a Type II secretion system to express a variety of RONS detoxifying enzymes [147], including the superoxide dismutase SodA and the catalase KatG, all of which counteract the effects of the phagosome [153, 154]. The proteins responsible for detoxifying the phagosome (both confirmed and putative) are shown in **Figure 1-15A**. In addition, Mtb releases a variety of molecules, including complex lipid derivatives of the cell envelope and kinases that target host proteins, which disrupt macrophage signaling pathways and prevent lysosomal fusion and formation of the mature phagolysosome [155-157]. The full set of confirmed and putative phagosomal arresting proteins is shown in **Figure 1-15B**. Mtb lipids are also capable of driving infected macrophages toward necrosis, which facilitates the spread of bacteria [155]. Thus, Mtb reengineers the phagosome into a permissive environment for replication and survival [158].

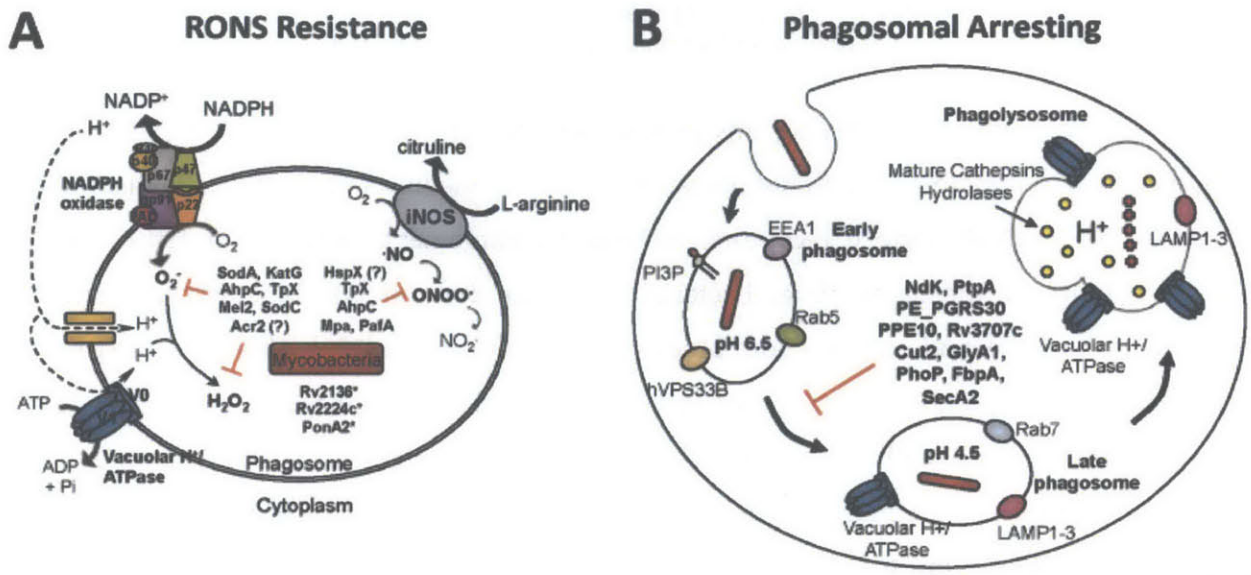

Figure 1-15: Factors promoting *M. tuberculosis* survival inside macrophages. *M. tuberculosis* survives inside macrophages by detoxifying reactive oxygen and nitrogen species (RONS) (A) and by preventing formation of the phagolysosome (B). Figure adapted from [43].

The extent of this restructuring is underscored by evidence that Mtb actively drives recruitment of macrophages to the site of infection, in order to gain access to new hosts [159, 160]. After establishing its niche, Mtb continues to alter the host function by means of a unique Type VII secretion system [161], which it uses to transport effector proteins across the waxy cell envelope and into the host macrophage [147]. The best characterized of these proteins is ESAT-6, which is known to be involved in granuloma formation [149, 162, 163], and has been implicated in processes including macrophage lysis, granuloma disruption, and transmission [164-168].

In addition to these pathogen factors, a variety of host factors modulate the progression of TB (**Figure 1-16**). Following phagocytosis, infected macrophages may undergo either apoptosis or necrosis, depending on the particular balance of signaling lipids. Apoptosis is a host defense mechanism that allows other resident immune cells, such as dendritic cells, to take up the bacteria and act as antigen presenting cells (APCs) to trigger the adaptive immune response [169]. Phagocytosis also leads to the production of many cytokines and antimicrobial peptides, which were recently shown to play a greater role in control than previously believed [160].

The three most important cytokines in TB are TNF-α, IL-12p40, and IFN-γ [143]. Infected macrophages produce large amounts of TNF-α and IL-12p40, both of which are critical determinants of the outcome of Mtb infection [143]. TNF-α plays a major role in infection

control and granuloma maintenance, and its downregulation is associated with increased pathology and transmission [170]. IL-12p40 induces dendritic cells to translocate to the mediastinal draining lymph node [138, 143], where they act as APCs and drive the differentiation of naïve T cells into the T_H1 cells that are characteristic of Mtb infection [171]. These T_H1 cells then migrate back to the lung, where they secrete large amounts of IFN-γ, a potent activator of macrophages that maintains the inflammatory environment. In addition to their role in controlling the disease, host factors also play a critical role in the development of severe pathology and the transmission of the disease, through the action of host matrix metalloproteinases [150, 172, 173]. Overall, the immunopathology of TB represents a complex interplay between pathogen and host factors, and underscores the continued gap in our understanding and need for more research.

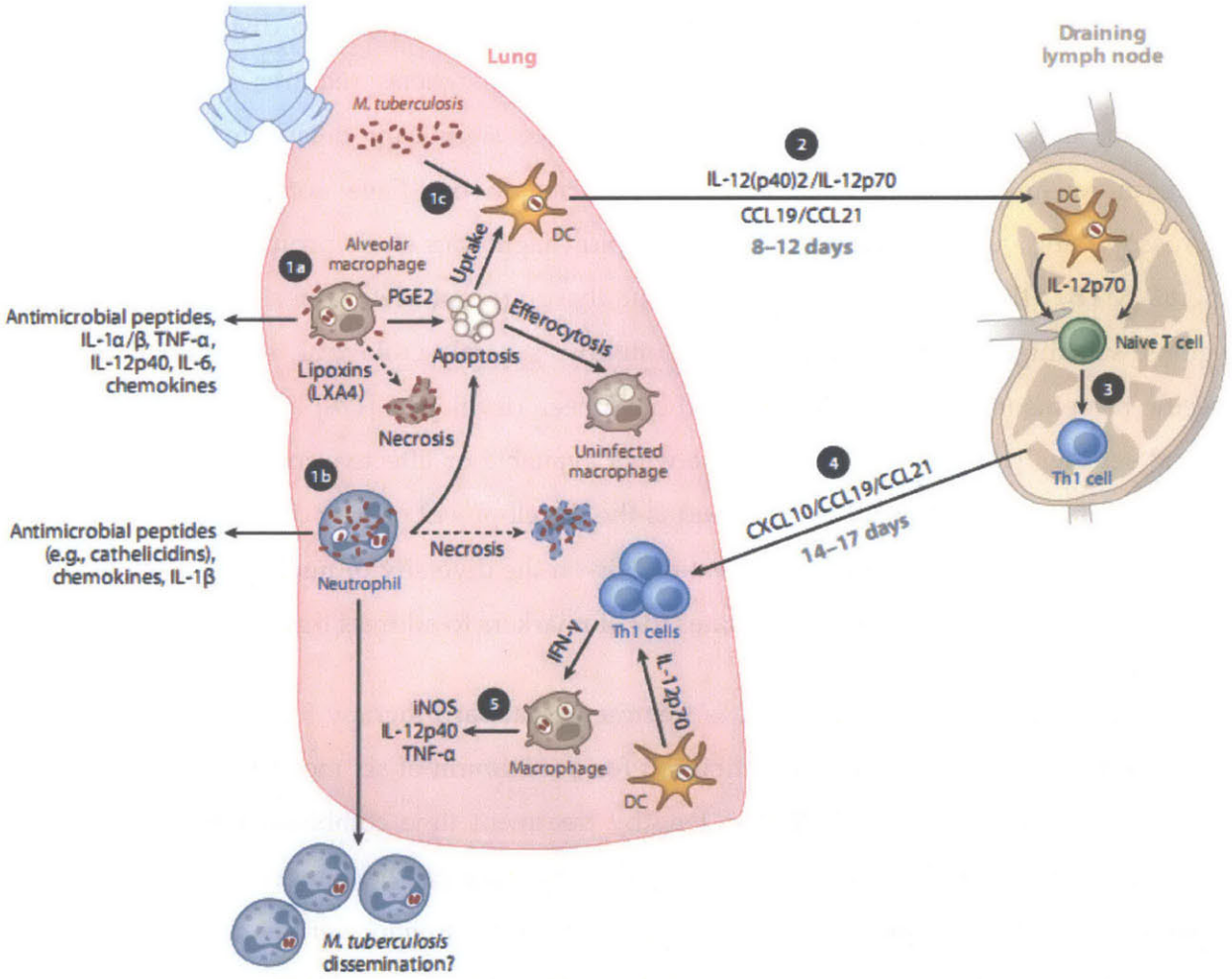

Figure 1-16: Host immune response to *M. tuberculosis* infection. Following infection, bacteria are taken up by macrophages and neutrophils, which then release a host of cytokines that drive the immune

response. After 8-12 days, dendritic cells migrate to the local lymph nodes and trigger a T_H1 type response. After 14-17 days, activated T_H1 cells migrate back to the lungs to maintain the inflammatory environment. Figure adapted from [143].

1.3.2.3. Disease management and unmet needs

Effective management of TB is hampered by a number of factors. The first barrier is accurately diagnosing the disease, which is often difficult due to the asymptomatic nature of most infections and the nonspecific symptoms of active disease [140]. The most commonly used diagnostic techniques also face significant limitations. Tuberculin skin testing (also called the Mantoux test or purified protein derivative (PPD) test) is used as a rapid screen for the presence of antibodies against mycobacterial proteins [174], but will return a false positive result in patients that have received the BCG vaccine [175], which makes it unsuitable in most parts of the world. Sputum smear microscopy is commonly used, but can only detect infection after a relatively high bacterial burden has been established, and is unable to distinguish Mtb from other non-tuberculous mycobacteria [176]. Definitive diagnosis requires sputum culturing, which can take more than a month and introduce significant delays to treatment [143]. Furthermore, an estimated 30-50% of TB patients do not have access to either sputum microscopy and culturing [139]. Some new rapid diagnostics show promise, in particular the Xpert® MTB/RIF PCR-based assay [177], but these are not always available or practical in regions with high disease burden [137]. Similarly, several serological tests that detect Mtb-specific proteins (such as the 85B antigen) have been developed [178] and are widely used in clinical settings [179], but these are not always available or effective in low resource settings [180-182]. Thus the first major unmet need is the development of new diagnostics, particularly those amenable to rapid, noninvasive testing. Given the diversity of nucleic acid modifications in bacteria, they make attractive candidates for biomarkers to address this need.

After diagnosis, the next major hurdle is treatment. Standard therapy for TB requires a patient to take a daily cocktail of multiple antibiotics for a minimum of six months, and sometimes as long as two years [137, 140, 143]. The lengthy treatment time combined with the nontrivial toxicities associated with most TB drugs—which have remained unchanged for decades [183]—makes noncompliance a significant problem. In turn, noncompliance drives the development of drug resistance, which is a growing concern as rates continue to increase [184]. Multi-drug resistant TB (MDR-TB), which is resistant to the two first-line drugs isoniazid and rifampicin,

now accounts for almost 4% of new TB cases each year, and more than 20% of new cases in those previously treated [139]. There is also growing evidence that MDR-TB strains are capable of acquiring compensatory mutations that allow them to retain full growth fitness when compared to non-MDR-TB strains, which could further exacerbate their spread [185]. Thus the second major unmet need is the development of novel antibiotics, particularly those that disrupt novel targets. Given the widespread examples of translational control by RNA modifications, they make attractive candidates for such drug targets. Additionally, given the potential influence of phosphorothioation on stress resistance [87], as well as the frequency with which PTs are observed in mycobacterial species [82], nucleic acid modifications may represent a critical axis along which to fight drug resistance.

Finally, to complicate matters further, drug development for TB poses a particularly difficult set of challenges [148]. The unique structures of both the Mtb bacterium and the TB granuloma make the process of delivering a drug to the target exceedingly difficult [186]. As shown in **Figure 1-17**, an anti-TB drug must travel from the general circulation to the granuloma (which may be poorly vascularized), then into the caseum and phagosome (which may each be encapsulated by different cellular structures), then into the bacteria (which may not be actively growing [187]), and finally to the sub-cellular target molecule. This problem of access and delivery has a significant impact on the drug discovery process, as it means that the standard pharmacokinetic parameters used to guide compound development do not correlate with efficacy against TB [148]. There is now a growing recognition that lead optimization and drug candidate screening for TB must be conducted using *in vivo* models that accurately recapitulate the granuloma structure [188]. Thus the final major unmet need is the development of better, cheaper, easier to use animal models that are suitable for drug development [189].

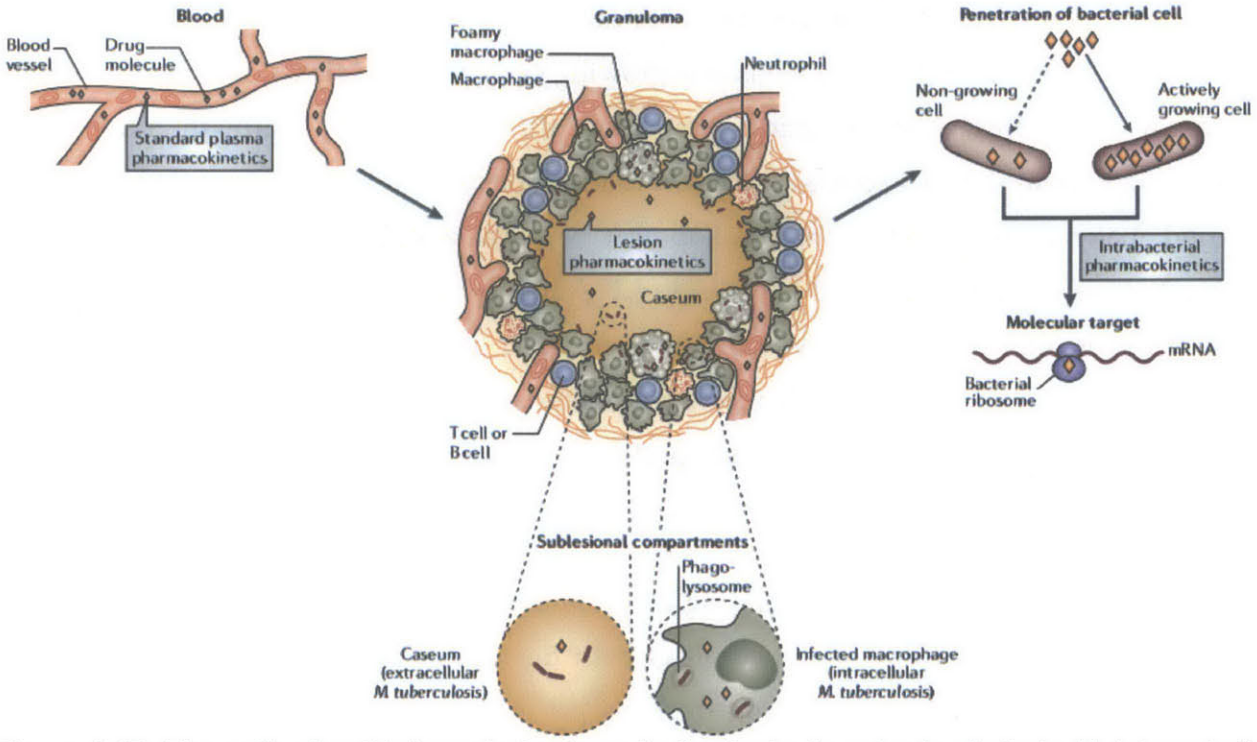

Figure 1-17: The path of anti-tuberculosis drugs in the body. In order to eliminate *M. tuberculosis* infection, drugs must penetrate a series of poorly vascularized and difficult to access compartments, including the granuloma, the caseum, the phagosome, and the bacterium. Figure adapted from [186].

1.4. Thesis outline and specific aims

This thesis was inspired by the ubiquity, diversity, and poorly characterized functional landscape of nucleic acid modifications, combined with the significant global disease burden posed by bacterial infections. The broad goal of this research was to define the function of nucleic acid modifications in bacterial pathogens, looking across three broad segments of the disease process: pathogenesis, diagnosis, and therapy. Toward this goal, we devised three specific aims. The first aim, described in Chapter 2, was to define the function of tRNA modifications in the pathogenesis and innate immune evasion of the gastric pathogen *H. pylori*. The second aim, described in Chapter 3, was to develop a novel animal model of Mtb complex lung infection that would allow for testing the utility of nucleic acid modifications as diagnostic biomarkers. The third aim, described in Chapter 4, was to determine the general, transferable effect of DNA phosphorothioation on growth fitness and resistance to therapy in several model bacterial pathogens. Together these studies advance our understanding of and increase our resources against bacterial diseases, a contribution that is summarized in Chapter 5.

1.5. References

1. A.J. Louie, E.P. Candido, G.H. Dixon (1974) *Enzymatic modifications and their possible roles in regulating the binding of basic proteins to DNA and in controlling chromosomal structure.* **Cold Spring Harb Symp Quant Biol** 38: 803-819.
2. D.W. Russell, R.K. Hirata (1989) *The detection of extremely rare DNA modifications. Methylation in dam- and hsd- Escherichia coli strains.* **J Biol Chem** 264(18): 10787-10794.
3. L. Tosi, A. Granieri, E. Scarano (1972) *Enzymatic DNA modifications in isolated nuclei from developing sea urchin embryos.* **Exp Cell Res** 72(1): 257-264.
4. D. Söll (1971) *Enzymatic modification of transfer RNA.* **Science** 173(3994): 293-299.
5. R. Reddy, T.S. Ro-Choi, D. Henning, H. Shibata, Y.C. Choi, H. Busch (1972) *Modified nucleosides of nuclear and nucleolar low molecular weight ribonucleic acid.* **J Biol Chem** 247(22): 7245-7250.
6. J. Rozenski, P.F. Crain, J.A. Mccloskey (1999) *The RNA Modification Database: 1999 update.* **Nucleic Acids Res** 27(1): 196-197.
7. S. Dunin-Horkawicz, A. Czerwoniec, M.J. Gajda, M. Feder, H. Grosjean, J.M. Bujnicki (2006) *MODOMICS: A database of RNA modification pathways.* **Nucleic Acids Res** 34(Database issue): D145-149.
8. H. Grosjean. *DNA and RNA Modification Enzymes: Structure, Mechanism, Function and Evolution*. Molecular Biology Intelligence Unit. 2009, Austin, TX: Landes Bioscience.
9. W.A. Cantara, P.F. Crain, J. Rozenski, J.A. Mccloskey, K.A. Harris, X. Zhang, F.A. Vendeix, D. Fabris, P.F. Agris (2011) *The RNA Modification Database, RNAMDB: 2011 update.* **Nucleic Acids Res** 39(Database issue): D195-201.
10. L. Wang, S. Chen, T. Xu, K. Taghizadeh, J.S. Wishnok, X. Zhou, D. You, Z. Deng, P.C. Dedon (2007) *Phosphorothioation of DNA in bacteria by dnd genes.* **Nat Chem Biol** 3(11): 709-710.
11. C.G. Edmonds, P.F. Crain, R. Gupta, T. Hashizume, C.H. Hocart, J.A. Kowalak, S.C. Pomerantz, K.O. Stetter, J.A. Mccloskey (1991) *Posttranscriptional modification of tRNA in thermophilic archea (archeabacteria).* **J Bacteriol** 173(10): 3138-3148.
12. J.A. Mccloskey, D.E. Graham, S. Zhou, P.F. Crain, M. Ibba, J. Konisky, D. Söll, G.J. Olsen (2001) *Post-transcriptional modification in archaeal tRNAs: Identities and phylogenetic relations of nucleotides from mesophilic and hyperthermophilic Methanococcales.* **Nucleic Acids Res** 29(22): 4699-4706.
13. A.S. Fauci, D.M. Morens (2012) *The perpetual challenge of infectious diseases.* **N Engl J Med** 366(5): 454-461.
14. C.J. Murray, A.D. Lopez (2013) *Measuring the global burden of disease.* **N Engl J Med** 369(5): 448-457.
15. World Health Organization (2011) *The top 10 causes of death.* WHO Fact Sheet N°310. Last updated July 2013. Accessed on 8 April 2014. Available from: http://www.who.int/mediacentre/factsheets/fs310/en/.
16. Institute for Health Metrics and Evaluation (2010) *GBD Compare.* Global Burden of Disease Visualizations. Last updated March 2013. Accessed on 8 April 2014. Available from: http://viz.healthmetricsandevaluation.org/gbd-compare/.
17. G.L. French (2010) *The continuing crisis in antibiotic resistance.* **Int J Antimicrob Agents** 36(Suppl 3): S3-7.

18. I.M. Gould (2010) *Coping with antibiotic resistance: The impending crisis.* **Int J Antimicrob Agents** 36(Suppl 3): S1-2.
19. S.T. Shulman (2013) *The antibiotic crisis.* **Pediatr Ann** 42(7): 260-261.
20. J.H. Rex (2014) *ND4BB: Addressing the antimicrobial resistance crisis.* **Nat Rev Microbiol** 12(4): 231-232.
21. P.A. Limbach, P.F. Crain, J.A. Mccloskey (1994) *Summary: The modified nucleosides of RNA.* **Nucleic Acids Res** 22(12): 2183-2196.
22. Y. Ikeuchi, A. Soma, T. Ote, J. Kato, Y. Sekine, T. Suzuki (2005) *Molecular mechanism of lysidine synthesis that determines tRNA identity and codon recognition.* **Mol Cell** 19(2): 235-246.
23. C.E. Dumelin, Y. Chen, A.M. Leconte, Y.G. Chen, D.R. Liu (2012) *Discovery and biological characterization of geranylated RNA in bacteria.* **Nat Chem Biol** 8(11): 913-919.
24. W.E. Kowtoniuk, Y. Shen, J.M. Heemstra, I. Agarwal, D.R. Liu (2009) *A chemical screen for biological small molecule–RNA conjugates reveals CoA-linked RNA.* **Proc Natl Acad Sci USA** 106(19): 7768-7773.
25. G.R. Björk. *The Role of Modified Nucleosides in tRNA Interactions*, in *Transfer RNA in Protein Synthesis*, D. Hatfield, B.J. Lee, and R.M. Pirtle, Editors. 1992, CRC Press: Boca Raton, FL.
26. G.R. Björk, J.M.B. Durand, T.G. Hagervall, R. Leipuvien≐, H.K. Lundgren, K. Nilsson, P. Chen, Q. Qian, J. Urbonavičius (1999) *Transfer RNA modification: Influence on translational frameshifting and metabolism.* **FEBS Lett** 452(1–2): 47-51.
27. A. Alexandrov, E.J. Grayhack, E.M. Phizicky (2005) *tRNA m^7G methyltransferase Trm8p/Trm82p: evidence linking activity to a growth phenotype and implicating Trm82p in maintaining levels of active Trm8p.* **RNA** 11(5): 821-830.
28. E.M. Gustilo, F.A. Vendeix, P.F. Agris (2008) *tRNA's modifications bring order to gene expression.* **Curr Opin Microbiol** 11(2): 134-140.
29. S. Arragain, S.K. Handelman, F. Forouhar, F.Y. Wei, K. Tomizawa, J.F. Hunt, T. Douki, M. Fontecave, E. Mulliez, M. Atta (2010) *Identification of eukaryotic and prokaryotic methylthiotransferase for biosynthesis of 2-methylthio-N^6-threonylcarbamoyladenosine in tRNA.* **J Biol Chem** 285(37): 28425-28433.
30. Y.H. Chionh, C.H. Ho, D. Pruksakorn, I. Ramesh Babu, C.S. Ng, F. Hia, M.E. Mcbee, D. Su, Y.L. Pang, C. Gu, H. Dong, E.G. Prestwich, P.Y. Shi, P.R. Preiser, S. Alonso, P.C. Dedon (2013) *A multidimensional platform for the purification of non-coding RNA species.* **Nucleic Acids Res** 41(17): e168.
31. G.R. Björk, J.U. Ericson, C.E.D. Gustafsson, T.G. Hagervall, Y.H. Jonsson, P.M. Wikstrom (1987) *Transfer RNA modification.* **Annu Rev Biochem** 56(1): 263-285.
32. P.P. Chan, T.M. Lowe (2009) *GtRNAdb: A database of transfer RNA genes detected in genomic sequence.* **Nucleic Acids Res** 37(Database issue): D93-97.
33. D.R. Davis (1995) *Stabilization of RNA stacking by pseudouridine.* **Nucleic Acids Res** 23(24): 5020-5026.
34. Y. Motorin, M. Helm (2010) *tRNA stabilization by modified nucleotides.* **Biochemistry** 49(24): 4934-4944.
35. J.A. Kowalak, J.J. Dalluge, J.A. Mccloskey, K.O. Stetter (1994) *The role of posttranscriptional modification in stabilization of transfer RNA from hyperthermophiles.* **Biochemistry** 33(25): 7869-7876.

36. J. Urbonavičius, Q. Qian, J.M.B. Durand, T.G. Hagervall, G.R. Björk (2001) *Improvement of reading frame maintenance is a common function for several tRNA modifications.* **EMBO J** 20(17): 4863-4873.
37. L.A. Sylvers, K.C. Rogers, M. Shimizu, E. Ohtsuka, D. Soll (1993) *A 2-thiouridine derivative in $tRNA^{Glu}$ is a positive determinant for aminoacylation by Escherichia coli glutamyl-tRNA synthetase.* **Biochemistry** 32(15): 3836-3841.
38. N. Pardi, H. Muramatsu, D. Weissman, K. Kariko (2013) *In vitro transcription of long RNA containing modified nucleosides.* **Methods Mol Biol** 969: 29-42.
39. A. Alexandrov, I. Chernyakov, W. Gu, S.L. Hiley, T.R. Hughes, E.J. Grayhack, E.M. Phizicky (2006) *Rapid tRNA decay can result from lack of nonessential modifications.* **Mol Cell** 21(1): 87-96.
40. Eva m. Novoa, M. Pavon-Eternod, T. Pan, L. Ribas de pouplana (2012) *A role for tRNA modifications in genome structure and codon usage.* **Cell** 149(1): 202-213.
41. C. Köhrer, D. Mandal, K.W. Gaston, H. Grosjean, P.A. Limbach, U.L. Rajbhandary (2014) *Life without $tRNA^{Ile}$-lysidine synthetase: Translation of the isoleucine codon AUA in Bacillus subtilis lacking the canonical $tRNA_2^{Ile}$.* **Nucleic Acids Res** 42(3): 1904-1915.
42. M. Pollak (1968) *An examination of the energetics of Crick's wobble hypothesis.* **J Theor Biol** 19(3): 241-246.
43. F.H. Crick (1966) *Codon–anticodon pairing: The wobble hypothesis.* **J Mol Biol** 19(2): 548-555.
44. P.F. Agris, F.A. Vendeix, W.D. Graham (2007) *tRNA's wobble decoding of the genome: 40 years of modification.* **J Mol Biol** 366(1): 1-13.
45. J.A. Martinez Gimenez, G.T. Saez, R.T. Seisdedos (1998) *On the function of modified nucleosides in the RNA world.* **J Theor Biol** 194(4): 485-490.
46. C. Yarian, H. Townsend, W. Czestkowski, E. Sochacka, A.J. Malkiewicz, R. Guenther, A. Miskiewicz, P.F. Agris (2002) *Accurate translation of the genetic code depends on tRNA modified nucleosides.* **J Biol Chem** 277(19): 16391-16395.
47. P.F. Agris (2008) *Bringing order to translation: The contributions of transfer RNA anticodon-domain modifications.* **EMBO Rep** 9(7): 629-635.
48. E.M. Novoa, L. Ribas De Pouplana (2012) *Speeding with control: Codon usage, tRNAs, and ribosomes.* **Trends Genet** 28(11): 574-581.
49. W.A. Cantara, F.V.T. Murphy, H. Demirci, P.F. Agris (2013) *Expanded use of sense codons is regulated by modified cytidines in tRNA.* **Proc Natl Acad Sci USA** 110(27): 10964-10969.
50. U. Begley, M. Dyavaiah, A. Patil, J.P. Rooney, D. Direnzo, C.M. Young, D.S. Conklin, R.S. Zitomer, T.J. Begley (2007) *Trm9-catalyzed tRNA modifications link translation to the DNA damage response.* **Mol Cell** 28(5): 860-870.
51. P.C. Dedon, T.J. Begley (2014) *A system of RNA modifications and biased codon use controls cellular stress response at the level of translation.* **Chem Res Toxicol** 27(3): 330-337.
52. C.T. Chan, Y.L. Pang, W. Deng, I.R. Babu, M. Dyavaiah, T.J. Begley, P.C. Dedon (2012) *Reprogramming of tRNA modifications controls the oxidative stress response by codon-biased translation of proteins.* **Nat Commun** 3: 937.
53. C.T. Chan, M. Dyavaiah, M.S. Demott, K. Taghizadeh, P.C. Dedon, T.J. Begley (2010) *A quantitative systems approach reveals dynamic control of tRNA modifications during cellular stress.* **PLoS Genet** 6(12): e1001247.

54. A. Patil, M. Dyavaiah, F. Joseph, J.P. Rooney, C.T. Chan, P.C. Dedon, T.J. Begley (2012) *Increased tRNA modification and gene-specific codon usage regulate cell cycle progression during the DNA damage response.* **Cell Cycle** 11(19): 3656-3665.
55. A. Patil, C.T. Chan, M. Dyavaiah, J.P. Rooney, P.C. Dedon, T.J. Begley (2012) *Translational infidelity-induced protein stress results from a deficiency in Trm9-catalyzed tRNA modifications.* **RNA Biol** 9(7): 990-1001.
56. D. Fu, J.A. Brophy, C.T. Chan, K.A. Atmore, U. Begley, R.S. Paules, P.C. Dedon, T.J. Begley, L.D. Samson (2010) *Human AlkB homolog ABH8 Is a tRNA methyltransferase required for wobble uridine modification and DNA damage survival.* **Mol Cell Biol** 30(10): 2449-2459.
57. D. Su, C.T. Chan, C. Gu, K.S. Lim, Y.H. Chionh, M.E. Mcbee, B.S. Russell, I.R. Babu, T.J. Begley, P.C. Dedon (2014) *Quantitative analysis of ribonucleoside modifications in tRNA by HPLC-coupled mass spectrometry.* **Nat Protoc** 9(4): 828-841.
58. F. Eckstein (1970) *Nucleoside phosphorothioates.* **J Am Chem Soc** 92(15): 4718-4723.
59. S.D. Putney, S.J. Benkovic, P.R. Schimmel (1981) *A DNA fragment with an α-phosphorothioate nucleotide at one end is asymmetrically blocked from digestion by exonuclease III and can be replicated in vivo.* **Proc Natl Acad Sci USA** 78(12): 7350-7354.
60. B.V. Potter, F. Eckstein (1984) *Cleavage of phosphorothioate-substituted DNA by restriction endonucleases.* **J Biol Chem** 259(22): 14243-14248.
61. T.M. Woolf, C.G. Jennings, M. Rebagliati, D.A. Melton (1990) *The stability, toxicity and effectiveness of unmodified and phosphorothioate antisense oligodeoxynucleotides in Xenopus oocytes and embryos.* **Nucleic Acids Res** 18(7): 1763-1769.
62. F. Eckstein, H. Sternbach (1967) *Nucleoside 5'-O-phosphorothioates as inhibitors for phosphatases.* **Biochim Biophys Acta** 146(2): 618-619.
63. A.W. Murray, M.R. Atkinson (1968) *Adenosine 5'-phosphorothioate: A nucleotide analog that is a substrate, competitive inhibitor, or regulator of some enzymes that interact with adenosine 5'-phosphate.* **Biochemistry** 7(11): 4023-4029.
64. S.A. Halperin, G. Van Nest, B. Smith, S. Abtahi, H. Whiley, J.J. Eiden (2003) *A phase I study of the safety and immunogenicity of recombinant hepatitis B surface antigen co-administered with an immunostimulatory phosphorothioate oligonucleotide adjuvant.* **Vaccine** 21(19-20): 2461-2467.
65. S.A. Halperin, B.J. Ward, M. Dionne, J.M. Langley, S.A. Mcneil, B. Smith, D. Mackinnon-Cameron, W.L. Heyward, J.T. Martin (2013) *Immunogenicity of an investigational hepatitis B vaccine (hepatitis B surface antigen co-administered with an immunostimulatory phosphorothioate oligodeoxyribonucleotide) in nonresponders to licensed hepatitis B vaccine.* **Hum Vaccin Immunother** 9(7): 1438-1444.
66. Q. Zhao, D. Yu, S. Agrawal (1999) *Site of chemical modifications in CpG containing phosphorothioate oligodeoxynucleotide modulates its immunostimulatory activity.* **Bioorg Med Chem Lett** 9(24): 3453-3458.
67. F. Brugnolo, F. Annunziato, S. Sampognaro, C. Manuelli, L. Cosmi, S. Romagnani, E. Maggi, P. Parronchi (2001) *Phosphorothioate oligonucleotides: Looking for the motif(s) possessing immunostimulatory activities in humans.* **Adv Exp Med Biol** 495: 261-264.
68. X. Zhou, Z. Deng, J.L. Firmin, D.A. Hopwood, T. Kieser (1988) *Site-specific degradation of Streptomyces lividans DNA during electrophoresis in buffers contaminated with ferrous iron.* **Nucleic Acids Res** 16(10): 4341-4352.

69. M. Evans, F.S. Kaczmarek, K. Stutzman-Engwall, P. Dyson (1994) *Characterization of a Streptomyces-lividans-type site-specific DNA modification system in the avermectin-producer Streptomyces avermitilis permits investigation of two novel giant linear plasmids, pSA1 and pSA2.* **Microbiology** 140(6): 1367-1371.
70. P. Dyson, M. Evans (1998) *Novel post-replicative DNA modification in Streptomyces: Analysis of the preferred modification site of plasmid pIJ101.* **Nucleic Acids Res** 26(5): 1248-1253.
71. X. Zhou, X. He, J. Liang, A. Li, T. Xu, T. Kieser, J.D. Helmann, Z. Deng (2005) *A novel DNA modification by sulphur.* **Mol Microbiol** 57(5): 1428-1438.
72. D. You, L. Wang, F. Yao, X. Zhou, Z. Deng (2007) *A novel DNA modification by sulfur: DndA is a NifS-like cysteine desulfurase capable of assembling DndC as an iron−sulfur cluster protein in Streptomyces lividans.* **Biochemistry** 46(20): 6126-6133.
73. X. An, W. Xiong, Y. Yang, F. Li, X. Zhou, Z. Wang, Z. Deng, J. Liang (2012) *A novel target of IscS in Escherichia coli: Participating in DNA phosphorothioation.* **PLoS One** 7(12): e51265.
74. X. An, X. Zhou, Z. Wang, Z. Deng, J. Liang (2013) *[Cloning, expression and purification of dptC, a DNA phosphorothioate modification related gene from Salmonella enterica serovar Cerro 87].* **Wei Sheng Wu Xue Bao** 53(10): 1111-1116.
75. X. An, X. Zhou, Z. Wang, Z. Deng, J. Liang (2013) *[Mutagenesis of cysteine residues in dptC from Salmonella enterica serovar Cerro 87 and its effects on DNA phosphorothioate modification].* **Wei Sheng Wu Xue Bao** 53(2): 204-209.
76. H.Y. Ou, X. He, Y. Shao, C. Tai, K. Rajakumar, Z. Deng (2009) *dndDB: A database focused on phosphorothioation of the DNA backbone.* **PLoS One** 4(4): e5132.
77. J. Liang, Z. Wang, X. He, J. Li, X. Zhou, Z. Deng (2007) *DNA modification by sulfur: Analysis of the sequence recognition specificity surrounding the modification sites.* **Nucleic Acids Res** 35(9): 2944-2954.
78. F. Yao, T. Xu, X. Zhou, Z. Deng, D. You (2009) *Functional analysis of spfD gene involved in DNA phosphorothioation in Pseudomonas fluorescens Pf0-1.* **FEBS Lett** 583(4): 729-733.
79. W. Hu, C. Wang, J. Liang, T. Zhang, Z. Hu, Z. Wang, W. Lan, F. Li, H. Wu, J. Ding, G. Wu, Z. Deng, C. Cao (2012) *Structural insights into DndE from Escherichia coli B7A involved in DNA phosphorothioation modification.* **Cell Res** 22(7): 1203-1206.
80. F. Chen, K. Lin, Z. Zhang, L. Chen, X. Shi, C. Cao, Z. Wang, J. Liang, Z. Deng, G. Wu (2011) *Purification, crystallization and preliminary X-ray analysis of the DndE protein from Salmonella enterica serovar Cerro 87, which is involved in DNA phosphorothioation.* **Acta Crystallogr Sect F Struct Biol Cryst Commun** 67(Pt 11): 1440-1442.
81. K.S. Makarova, Y.I. Wolf, E.V. Koonin (2013) *Comparative genomics of defense systems in archaea and bacteria.* **Nucleic Acids Res** 41(8): 4360-4377.
82. Y. Zhang, M.A. Yakrus, E.A. Graviss, N. Williams-Bouyer, C. Turenne, A. Kabani, R.J. Wallace, Jr. (2004) *Pulsed-field gel electrophoresis study of Mycobacterium abscessus isolates previously affected by DNA degradation.* **J Clin Microbiol** 42(12): 5582-5587.
83. U. Romling, B. Tummler (2000) *Achieving 100% typeability of Pseudomonas aeruginosa by pulsed-field gel electrophoresis.* **J Clin Microbiol** 38(1): 464-465.
84. S.T. Howard, K.L. Newman, S. Mcnulty, B.A. Brown-Elliott, R. Vasireddy, L. Bridge, R.J. Wallace, Jr. (2013) *Insertion site and distribution of a genomic island conferring*

DNA phosphorothioation in the Mycobacterium abscessus complex. **Microbiology** 159(Pt 11): 2323-2332.

85. L. Wang, S. Chen, K.L. Vergin, S.J. Giovannoni, S.W. Chan, M.S. Demott, K. Taghizadeh, O.X. Cordero, M. Cutler, S. Timberlake, E.J. Alm, M.F. Polz, J. Pinhassi, Z. Deng, P.C. Dedon (2011) *DNA phosphorothioation is widespread and quantized in bacterial genomes.* **Proc Natl Acad Sci USA** 108(7): 2963-2968.
86. T. Xu, F. Yao, X. Zhou, Z. Deng, D. You (2010) *A novel host-specific restriction system associated with DNA backbone S-modification in Salmonella.* **Nucleic Acids Res** 38(20): 7133-7141.
87. X. Xie, J. Liang, T. Pu, F. Xu, F. Yao, Y. Yang, Y.L. Zhao, D. You, X. Zhou, Z. Deng, Z. Wang (2012) *Phosphorothioate DNA as an antioxidant in bacteria.* **Nucleic Acids Res** 40(18): 9115-9124.
88. W.A. Loenen, E.A. Raleigh (2014) *The other face of restriction: Modification-dependent enzymes.* **Nucleic Acids Res** 42(1): 56-69.
89. G. Liu, H.Y. Ou, T. Wang, L. Li, H. Tan, X. Zhou, K. Rajakumar, Z. Deng, X. He (2010) *Cleavage of phosphorothioated DNA and methylated DNA by the Type IV restriction endonuclease ScoMcrA.* **PLoS Genet** 6(12): e1001253.
90. J.G. Kusters, A.H. Van Vliet, E.J. Kuipers (2006) *Pathogenesis of Helicobacter pylori infection.* **Clin Microbiol Rev** 19(3): 449-490.
91. J.W. Konturek (2003) *Discovery by Jaworski of Helicobacter pylori and its pathogenetic role in peptic ulcer, gastritis and gastric cancer.* **J Physiol Pharmacol** 54 Suppl 3: 23-41.
92. B.J. Marshall. *One hundred years of discovery and rediscovery of Helicobacter pylori and its association with peptic ulcer disease*, in *Helicobacter pylori: Physiology and Genetics*, H.L.T. Mobley, G.L. Mendz, and S.L. Hazell, Editors. 2001: Washington (DC).
93. J.R. Warren (1983) *Unidentified curved bacilli on gastric epithelium in active chronic gastritis.* **Lancet** 1(8336): 1273-1273.
94. B.J. Marshall (2008) *Helicobacter pylori—a Nobel pursuit?* **Can J Gastroenterol** 22(11): 895-896.
95. N. Uemura, S. Okamoto, S. Yamamoto, N. Matsumura, S. Yamaguchi, M. Yamakido, K. Taniyama, N. Sasaki, R.J. Schlemper (2001) *Helicobacter pylori infection and the development of gastric cancer.* **N Engl J Med** 345(11): 784-789.
96. K.E.L. Mccoll (2010) *Helicobacter pylori infection.* **N Engl J Med** 362(17): 1597-1604.
97. D.B. Polk, R.M. Peek, Jr. (2010) *Helicobacter pylori: Gastric cancer and beyond.* **Nat Rev Cancer** 10(6): 403-414.
98. L.E. Wroblewski, R.M. Peek, Jr., K.T. Wilson (2010) *Helicobacter pylori and gastric cancer: Factors that modulate disease risk.* **Clin Microbiol Rev** 23(4): 713-739.
99. R.A. Feldman, A.J.P. Eccersley, J.M. Hardie (1998) *Epidemiology of Helicobacter pylori: Acquisition, transmission, population prevalence and disease-to-infection ratio.* **Br Med Bull** 54(1): 39-53.
100. B. Bauer, T.F. Meyer (2011) *The human gastric pathogen Helicobacter pylori and its association with gastric cancer and ulcer disease.* **Ulcers** 2011: 1-23.
101. P. Malfertheiner, P. Sipponen, M. Naumann, P. Moayyedi, F. Megraud, S.D. Xiao, K. Sugano, O. Nyren (2005) *Helicobacter pylori eradication has the potential to prevent gastric cancer: A state-of-the-art critique.* **Am J Gastroenterol** 100(9): 2100-2115.

102. D.M. Parkin, F. Bray, J. Ferlay, P. Pisani (2002) *Global cancer statistics, 2002.* **CA-Cancer J Clin** 55(2): 74–108.
103. D. Forman, D.G. Newell, F. Fullerton, J.W.G. Yarnell, A.R. Stacey, N. Wald, F. Sitas (1991) *Association between infection with Helicobacter pylori and risk of gastric cancer: Evidence from a prospective investigation.* **BMJ** 302: 1302-1305.
104. F. Farinati, R. Cardin, V.M. Russo, G. Busatto, M. Franco, M. Rugge (2003) *Helicobacter pylori CagA status, mucosal oxidative damage and gastritis phenotype: A potential pathway to cancer?* **Helicobacter** 8(3): 227-234.
105. P. Lonkar, P.C. Dedon (2011) *Reactive species and DNA damage in chronic inflammation: Reconciling chemical mechanisms and biological fates.* **Int J Cancer** 128(9): 1999-2009.
106. International Agency for Research on Cancer Working Group on the Evaluation of Carcinogenic Risks to Humans. *Helicobacter pylori*, in *Schistosomes, Liver Flukes and Helicobacter pylori*. 1994, IARC: Lyon, France. p. 177-240.
107. D. Rothenbacher, H. Brenner (2003) *Burden of Helicobacter pylori and H. pylori-related diseases in developed countries: Recent developments and future implications.* **Microb Infect** 5(8): 693-703.
108. L.M. Brown (2000) *Helicobacter pylori: Epidemiology and routes of transmission.* **Epidemiol Rev** 22(2): 283-297.
109. M. Rowland, L. Daly, M. Vaughan, A. Higgins, B. Bourke, B. Drumm (2006) *Age-specific incidence of Helicobacter pylori.* **Gastroenterology** 130(1): 65-72; quiz 211.
110. D.E. Berg, P.S. Hoffman, B.J. Appelmelk, J.G. Kusters (1997) *The Helicobacter pylori genome sequence: Genetic factors for long life in the gastric mucosa.* **Trends Microbiol** 5(12): 468-474.
111. P. Lehours, O. Yilmaz (2007) *Epidemiology of Helicobacter pylori infection.* **Helicobacter** 12 Suppl 1: 1-3.
112. K. Muhsen, M. Jurban, S. Goren, D. Cohen (2012) *Incidence, age of acquisition and risk factors of Helicobacter pylori infection among Israeli Arab infants.* **J Trop Pediatr** 58(3): 208-213.
113. M.J. Blaser (2006) *Who are we? Indigenous microbes and the ecology of human diseases.* **EMBO Rep** 7(10): 956-960.
114. T.P. Cid, M.C. Fernandez, S. Benito Martinez, N.L. Jones (2013) *Pathogenesis of Helicobacter pylori infection.* **Helicobacter** 18 Suppl 1: 12-17.
115. N.R. Salama, M.L. Hartung, A. Muller (2013) *Life in the human stomach: Persistence strategies of the bacterial pathogen Helicobacter pylori.* **Nat Rev Microbiol** 11(6): 385-399.
116. Y. Yamaoka (2010) *Mechanisms of disease: Helicobacter pylori virulence factors.* **Nat Rev Gastroenterol Hepatol** 7(11): 629-641.
117. A. Dubois, T. Boren (2007) *Helicobacter pylori is invasive and it may be a facultative intracellular organism.* **Cell Microbiol** 9(5): 1108-1116.
118. A. Ljungh (2000) *Helicobacter pylori interactions with plasminogen.* **Methods** 21(2): 151-157.
119. S. Suerbaum, P. Michetti (2002) *Helicobacter pylori infection.* **N Engl J Med** 347(15): 1175-1186.
120. S. Yamazaki, A. Yamakawa, T. Okuda, M. Ohtani, H. Suto, Y. Ito, Y. Yamazaki, Y. Keida, H. Higashi, M. Hatakeyama, T. Azuma (2005) *Distinct diversity of vacA, cagA,*

and cagE genes of Helicobacter pylori associated with peptic ulcer in Japan. **J Clin Microbiol** 43(8): 3906-3916.
121. Raghwan, R. Chowdhury (2014) *Host cell contact induces fur-dependent expression of virulence factors CagA and VacA in Helicobacter pylori.* **Helicobacter** 19(1): 17-25.
122. M.K. Tummuru, T.L. Cover, M.J. Blaser (1994) *Mutation of the cytotoxin-associated cagA gene does not affect the vacuolating cytotoxin activity of Helicobacter pylori.* **Infect Immun** 62(6): 2609-2613.
123. S.L. Palframan, T. Kwok, K. Gabriel (2012) *Vacuolating cytotoxin A (VacA), a key toxin for Helicobacter pylori pathogenesis.* **Front Cell Infect Microbiol** 2: 92.
124. I. Hitzler, A. Sayi, E. Kohler, D.B. Engler, K.N. Koch, W.D. Hardt, A. Muller (2012) *Caspase-1 has both proinflammatory and regulatory properties in Helicobacter infections, which are differentially mediated by its substrates IL-1β and IL-18.* **J Immunol** 188(8): 3594-3602.
125. D. Vaira, N. Vakil (2001) *Blood, urine, stool, breath, money, and Helicobacter pylori.* **Gut** 48: 287-289.
126. M.S. Dorer, S. Talarico, N.R. Salama (2009) *Helicobacter pylori's unconventional role in health and disease.* **PLoS Pathog** 5(10): e1000544.
127. L.E. Wroblewski, R.M. Peek, Jr. (2013) *Helicobacter pylori in gastric carcinogenesis: Mechanisms.* **Gastroenterol Clin North Am** 42(2): 285-298.
128. F.M. Barnard, M.F. Loughlin, H.P. Fainberg, M.P. Messenger, D.W. Ussery, P. Williams, P.J. Jenks (2003) *Global regulation of virulence and the stress response by CsrA in the highly adapted human gastric pathogen Helicobacter pylori.* **Mol Microbiol** 51(1): 15-32.
129. F. Bauer, A. Matsuyama, J. Candiracci, M. Dieu, J. Scheliga, D.A. Wolf, M. Yoshida, D. Hermand (2012) *Translational control of cell division by Elongator.* **Cell Rep** 1(5): 424-433.
130. C. Chen, S. Tuck, A.S. Bystrom (2009) *Defects in tRNA modification associated with neurological and developmental dysfunctions in Caenorhabditis elegans Elongator mutants.* **PLoS Genet** 5(7): e1000561.
131. P. Bytzer, J.F. Dahlerup, J.R. Eriksen, D. Jarbøl, S. Rosenstock, S. Wildt (2011) *Diagnosis and treatment of Helicobacter pylori infection.* **Dan Med Bull** 58(4): C4271.
132. L. Fischbach, E.L. Evans (2007) *Meta-analysis: The effect of antibiotic resistance status on the efficacy of triple and quadruple first-line therapies for Helicobacter pylori.* **Aliment Pharmacol Ther** 26(3): 343-357.
133. F. Megraud (2004) *H. pylori antibiotic resistance: Prevalence, importance, and advances in testing.* **Gut** 53(9): 1374-1384.
134. M.C. Camargo, A. Garcia, A. Riquelme, W. Otero, C.A. Camargo, T. Hernandez-Garcia, R. Candia, M.G. Bruce, C.S. Rabkin (2014) *The Problem of Helicobacter pylori resistance to antibiotics: A systematic review in Latin America.* **Am J Gastroenterol** 109(4): 485-495.
135. A. Khan, A. Farooqui, H. Manzoor, S.S. Akhtar, M.S. Quraishy, S.U. Kazmi (2012) *Antibiotic resistance and cagA gene correlation: A looming crisis of Helicobacter pylori.* **World J Gastroenterol** 18(18): 2245-2252.
136. W. Wu, Y. Yang, G. Sun (2012) *Recent insights into antibiotic resistance in Helicobacter pylori eradication.* **Gastroenterol Res Pract** 2012: 723183.

137. S. Keshavjee, P.E. Farmer (2012) *Tuberculosis, drug resistance, and the history of modern medicine.* **N Engl J Med** 367(10): 931-936.
138. N.W. Schluger, W.N. Rom (1998) *The host immune response to tuberculosis.* **Am J Respir Crit Care Med** 157: 679-691.
139. World Health Organization. *Global Tuberculosis Report.* 2013.
140. A. Zumla, M. Raviglione, R. Hafner, C.F. Von Reyn (2013) *Tuberculosis.* **N Engl J Med** 368(8): 745-755.
141. I. Smith (2003) *Mycobacterium tuberculosis pathogenesis and molecular determinants of virulence.* **Clin Microbiol Rev** 16(3): 463-496.
142. P.L. Lin, J.L. Flynn (2010) *Understanding latent tuberculosis: A moving target.* **J Immunol** 185(1): 15-22.
143. A. O'garra, P.S. Redford, F.W. Mcnab, C.I. Bloom, R.J. Wilkinson, M.P. Berry (2013) *The immune response in tuberculosis.* **Annu Rev Immunol** 31: 475-527.
144. L.S. Meena, Rajni (2010) *Survival mechanisms of pathogenic Mycobacterium tuberculosis $H_{37}Rv$.* **FEBS J** 277(11): 2416-2427.
145. N. Chandra, D. Kumar, K. Rao (2011) *Systems biology of tuberculosis.* **Tuberculosis** 91(5): 487-496.
146. J. Mcfadden, D.J.V. Beste, A.M. Kierzek (Eds.) *Systems Biology of Tuberculosis.* 2013, Springer: New York.
147. M.A. Forrellad, L.I. Klepp, A. Gioffre, J. Sabio Y Garcia, H.R. Morbidoni, M. De La Paz Santangelo, A.A. Cataldi, F. Bigi (2013) *Virulence factors of the Mycobacterium tuberculosis complex.* **Virulence** 4(1): 3-66.
148. V. Dartois, C.E. Barry, 3rd (2013) *A medicinal chemists' guide to the unique difficulties of lead optimization for tuberculosis.* **Bioorg Med Chem Lett** 23(17): 4741-4750.
149. B.M. Saunders, W.J. Britton (2007) *Life and death in the granuloma: Immunopathology of tuberculosis.* **Immunol Cell Biol** 85(2): 103-111.
150. P.T. Elkington, J.M. D'armiento, J.S. Friedland (2011) *Tuberculosis immunopathology: The neglected role of extracellular matrix destruction.* **Sci Transl Med** 3(71): 71ps76.
151. C.D. Gaynor, F.X. Mccormack, D.R. Voelker, S.E. Mcgowan, L.S. Schlesinger (1995) *Pulmonary surfactant protein A mediates enhanced phagocytosis of Mycobacterium tuberculosis by a direct interaction with human macrophages.* **J Immunol** 155(11): 5343-5351.
152. S. Ehrt, D. Schnappinger (2007) *Mycobacterium tuberculosis virulence: lipids inside and out.* **Nat Med** 13(3): 284-285.
153. K.H. Bhat, A. Das, A. Srikantam, S. Mukhopadhyay (2013) *PPE2 protein of Mycobacterium tuberculosis may inhibit nitric oxide in activated macrophages.* **Ann NY Acad Sci** 1283: 97-101.
154. D. Liao, Q. Fan, L. Bao (2013) *The role of superoxide dismutase in the survival of Mycobacterium tuberculosis in macrophages.* **Jpn J Infect Dis** 66(6): 480-488.
155. S.M. Behar, C.J. Martin, C. Nunes-Alves, M. Divangahi, H.G. Remold (2011) *Lipids, apoptosis, and cross-presentation: links in the chain of host defense against Mycobacterium tuberculosis.* **Microbes Infect** 13(8-9): 749-756.
156. P.C. Karakousis, W.R. Bishai, S.E. Dorman (2004) *Mycobacterium tuberculosis cell envelope lipids and the host immune response.* **Cell Microbiol** 6(2): 105-116.
157. L.M. Rocha-Ramirez, I. Estrada-Garcia, L.M. Lopez-Marin, E. Segura-Salinas, P. Mendez-Aragon, D. Van Soolingen, R. Torres-Gonzalez, R. Chacon-Salinas, S. Estrada-

Parra, C. Maldonado-Bernal, C. Lopez-Macias, A. Isibasi (2008) *Mycobacterium tuberculosis lipids regulate cytokines, TLR-2/4 and MHC class II expression in human macrophages.* **Tuberculosis** 88(3): 212-220.

158. M. Podinovskaia, W. Lee, S. Caldwell, D.G. Russell (2013) *Infection of macrophages with Mycobacterium tuberculosis induces global modifications to phagosomal function.* **Cell Microbiol** 15(6): 843-859.
159. E. Guirado, L.S. Schlesinger, G. Kaplan (2013) *Macrophages in tuberculosis: Friend or foe.* **Semin Immunopathol** 35(5): 563-583.
160. H. Bruns, S. Stenger (2014) *New insights into the interaction of Mycobacterium tuberculosis and human macrophages.* **Future Microbiol** 9: 327-341.
161. A.M. Abdallah, N.C. Gey Van Pittius, P.A. Champion, J. Cox, J. Luirink, C.M. Vandenbroucke-Grauls, B.J. Appelmelk, W. Bitter (2007) *Type VII secretion—mycobacteria show the way.* **Nat Rev Microbiol** 5(11): 883-891.
162. L.E. Swaim, L.E. Connolly, H.E. Volkman, O. Humbert, D.E. Born, L. Ramakrishnan (2006) *Mycobacterium marinum infection of adult zebrafish causes caseating granulomatous tuberculosis and is moderated by adaptive immunity.* **Infect Immun** 74(11): 6108-6117.
163. H.E. Volkman, T.C. Pozos, J. Zheng, J.M. Davis, J.F. Rawls, L. Ramakrishnan (2010) *Tuberculous granuloma induction via interaction of a bacterial secreted protein with host epithelium.* **Science** 327(5964): 466-469.
164. S.C. Derrick, S.L. Morris (2007) *The ESAT6 protein of Mycobacterium tuberculosis induces apoptosis of macrophages by activating caspase expression.* **Cell Microbiol** 9(6): 1547-1555.
165. W. Liu, Y. Peng, Y. Yin, Z. Zhou, W. Zhou, Y. Dai (2014) *The involvement of NADPH oxidase-mediated ROS in cytokine secretion from macrophages induced by Mycobacterium tuberculosis ESAT-6.* **Inflammation**.
166. S.K. Pathak, S. Basu, K.K. Basu, A. Banerjee, S. Pathak, A. Bhattacharyya, T. Kaisho, M. Kundu, J. Basu (2007) *Direct extracellular interaction between the early secreted antigen ESAT-6 of Mycobacterium tuberculosis and TLR2 inhibits TLR signaling in macrophages.* **Nat Immunol** 8(6): 610-618.
167. A. Welin, D. Eklund, O. Stendahl, M. Lerm (2011) *Human macrophages infected with a high burden of ESAT-6-expressing M. tuberculosis undergo caspase-1- and cathepsin B-independent necrosis.* **PLoS One** 6(5): e20302.
168. L. Zhang, H. Zhang, Y. Zhao, F. Mao, J. Wu, B. Bai, Z. Xu, Y. Jiang, C. Shi (2012) *Effects of Mycobacterium tuberculosis ESAT-6/CFP-10 fusion protein on the autophagy function of mouse macrophages.* **DNA Cell Biol** 31(2): 171-179.
169. S.M. Behar, C.J. Martin, M.G. Booty, T. Nishimura, X. Zhao, H.X. Gan, M. Divangahi, H.G. Remold (2011) *Apoptosis is an innate defense function of macrophages against Mycobacterium tuberculosis.* **Mucosal Immunol** 4(3): 279-287.
170. V. Kindler, A.-P. Sappino, G.E. Grau, P.-F. Piguet, P. Vassalli (1989) *The inducing role of tumor necrosis factor in the development bactericidal granulomas during BCG infection.* **Cell** 56: 731-740.
171. X. Bai, S.E. Wilson, K. Chmura, N.E. Feldman, E.D. Chan (2004) *Morphometric analysis of Th_1 and Th_2 cytokine expression in human pulmonary tuberculosis.* **Tuberculosis** 84(6): 375-385.

172. P.T. Elkington, T. Shiomi, R. Breen, R.K. Nuttall, C.A. Ugarte-Gil, N.F. Walker, L. Saraiva, B. Pedersen, F. Mauri, M. Lipman, D.R. Edwards, B.D. Robertson, J. D'armiento, J.S. Friedland (2011) *MMP-1 drives immunopathology in human tuberculosis and transgenic mice.* **J Clin Invest** 121(5): 1827-1833.
173. P. Salgame (2011) *MMPs in tuberculosis: granuloma creators and tissue destroyers.* **J Clin Invest** 121(5): 1686-1688.
174. G. Rabalais, G. Adams, B. Stover (1991) *PPD skin test conversion in health-care workers after exposure to Mycobacterium tuberculosis infection in infants.* **Lancet** 338(8770): 826.
175. J.H. Joncas, R. Robitaille, T. Gauthier (1975) *Interpretation of the PPD skin test in BCG-vaccinated children.* **Can Med Assoc J** 113(2): 127-128.
176. P. Desikan (2013) *Sputum smear microscopy in tuberculosis: is it still relevant?* **Indian J Med Res** 137(3): 442-444.
177. G. Theron, J. Peter, R. Meldau, H. Khalfey, P. Gina, B. Matinyena, L. Lenders, G. Calligaro, B. Allwood, G. Symons, U. Govender, M. Setshedi, K. Dheda (2013) *Accuracy and impact of Xpert MTB/RIF for the diagnosis of smear-negative or sputum-scarce tuberculosis using bronchoalveolar lavage fluid.* **Thorax** 68(11): 1043-1051.
178. R. Dayal, A. Singh, V.M. Katoch, B. Joshi, D.S. Chauhan, P. Singh, G. Kumar, V.D. Sharma (2008) *Serological diagnosis of tuberculosis.* **Indian J Pediatr** 75(12): 1219-1221.
179. P. Aggarwal, D. Aggarwal (2013) *Serological test for tuberculosis: so near yet so far.* **J Infect** 67(3): 241-242.
180. S. Singh, J. Singh, S. Kumar, K. Gopinath, V. Balooni, N. Singh, K. Mani (2012) *Poor performance of serological tests in the diagnosis of pulmonary tuberculosis: evidence from a contact tracing field study.* **PLoS One** 7(7): e40213.
181. D.W. Dowdy, K.R. Steingart, M. Pai (2011) *Serological testing versus other strategies for diagnosis of active tuberculosis in India: a cost-effectiveness analysis.* **PLoS Med** 8(8): e1001074.
182. K.R. Steingart, A. Ramsay, D.W. Dowdy, M. Pai (2012) *Serological tests for the diagnosis of active tuberculosis: Relevance for India.* **Indian J Med Res** 135(5): 695-702.
183. R. Osborne (2013) *First novel anti-tuberculosis drug in 40 years.* **Nat Biotechnol** 31(2): 89-91.
184. G.B. Migliori, A. Matteelli, D. Cirillo, M. Pai (2008) *Diagnosis of multidrug-resistant tuberculosis and extensively drug-resistant tuberculosis: Current standards and challenges.* **Can J Infect Dis Med Microbiol** 19(2): 169-172.
185. N. Casali, V. Nikolayevskyy, Y. Balabanova, S.R. Harris, O. Ignatyeva, I. Kontsevaya, J. Corander, J. Bryant, J. Parkhill, S. Nejentsev, R.D. Horstmann, T. Brown, F. Drobniewski (2014) *Evolution and transmission of drug-resistant tuberculosis in a Russian population.* **Nat Genet** 46(3): 279-286.
186. V. Dartois (2014) *The path of anti-tuberculosis drugs: From blood to lesions to mycobacterial cells.* **Nat Rev Microbiol** 12(3): 159-167.
187. E.J. Muñoz-Elías, J. Timm, T. Botha, W.T. Chan, J.E. Gomez, J.D. Mckinney (2005) *Replication dynamics of Mycobacterium tuberculosis in chronically infected mice.* **Infect Immun** 73(1): 546-551.

188. E. Guirado, L.S. Schlesinger (2013) *Modeling the Mycobacterium tuberculosis granuloma – the critical battlefield in host immunity and disease.* **Front Immunol** 4(98).
189. U.D. Gupta, V.M. Katoch (2005) *Animal models of tuberculosis.* **Tuberculosis** 85(5-6): 277-293.

2. The role of tRNA modifications in *Helicobacter pylori* stress response

2.1. Introduction and motivation

Helicobacter pylori is the world's most common infectious agent, colonizing an estimated three billion people [1, 2]. While *H. pylori* infection causes peptic ulcer disease in about 10% of cases [3], the majority of infections (~90%) are undiagnosed and asymptomatic, persisting undetected for the life of the host [4-6]. The asymptomatic infection is not benign, however, as it always induces gastritis and chronic inflammation [7]. This inflammation is thought to be one component [8] of the striking causal link between *H. pylori* infection and gastric cancer [9-14], for which it has long been recognized as a definite ("Group 1") carcinogen by the International Agency for Research on Cancer [15]. Gastric cancer is the fourth most commonly diagnosed form of cancer and the second leading cause of cancer deaths worldwide, accounting for roughly 700,000 deaths annually [16]. The distribution of both *H. pylori* and gastric cancer is heavily biased along geographic and socioeconomic axes, with countries in the developing world bearing a disproportionate burden of disease [7, 16, 17]; *H. pylori* infection rates in Southeast Asia and South America can reach 90% [6]. Several studies have demonstrated a reduced risk of gastric cancer following eradication of *H. pylori* [18], so there is a significant global health incentive to address *H. pylori* infections.

Effective management of *H. pylori* faces several barriers, beginning with diagnosis. A variety of diagnostic methods that differ in invasiveness, cost, and reliability are available, including serology, stool antigen tests, urea breath tests, and endoscopic biopsies [19]. Despite the apparent abundance of tests, the lack of overt symptoms in most people means that the vast majority of cases still go undetected [20]. Once disease is detected, standard therapy includes multiple antibiotics in combination with a proton-pump inhibitor and a bismuth compound, which is often successful in eradication [21]. However, eradication can fail, and reinfection or recurrence of symptoms is sometimes encountered [3]. In addition, there is growing evidence that antibiotic resistance is widespread and becoming more common, and that resistance severely curtails the effectiveness of even combination therapy [22-24]. There is also evidence that pathogenicity is correlated with resistance, and that more virulent strains are more likely to

develop resistance [25]. Finally, *H. pylori* displays a striking degree of genetic diversity even within a single colony [26], which can enhance the spread of resistance. There is thus a pressing need to develop novel approaches to *H. pylori* treatment [7].

H. pylori is exquisitely adapted to life in the harsh niche of the human stomach, and it relies on a variety of immune evasion and stress response systems to persist in the stomach despite being exposed to a host of toxic chemicals [27-29]. Disrupting these survival systems provides an attractive target for antibiotics, as it might allow us to halt colonization altogether, thereby preventing the development of gastritis and avoiding the harmful effects of chronic inflammation. In evaluating potential targets for antibiotic development, we were inspired by the observation that *H. pylori* has a paucity of global transcriptional regulators, and that the majority of its regulation appears to take place post-transcriptionally [30]. Drawing on observations that tRNA modifications can control post-transcriptional responses by biasing the translation of certain mRNAs [31-36], we hypothesized that tRNA modifications might play a role in *H. pylori*'s survival in the stomach. To test this hypothesis, we applied a sophisticated liquid chromatography-coupled tandem mass spectrometry (LC-MS/MS) approach to quantify the changes in *H. pylori* tRNA modifications in response to common stresses encountered in the stomach. Our results revealed novel signatures of exposure and identified several modifications that are highly correlated with particular stresses.

2.2. Methods

2.2.1. Bacterial strains and culture conditions

Helicobacter pylori strain 26695 (ATCC 700392) was obtained as a frozen glycerol stock from Dr. Alexander Sheh (MIT Division of Comparative Medicine). All cultures were grown at 37 °C in a microaerophilic atmosphere designed to mimic the human stomach [27], as follows: cultures were sealed in vented anaerobic jars (BD GasPak); room air was evacuated to a pressure of -24 in/Hg; and jars were backfilled with a mixture of 10% H_2, 10% CO_2, and 80% N_2 (Airgas) to produce a final composition of approximately 8% H_2, 8% CO_2, 4% O_2, and 80% N_2. Plate cultures were grown on prepared tryptic soy agar supplemented with 5% defibrinated sheep blood (Hardy Diagnostics). Plates were passaged for no more than nine generations before

being rederived from frozen stocks. Each time frozen stocks were plated, duplicate platings were incubated in an aerobic environment to check for contamination; no growth was ever observed on aerobically incubated plates. Liquid cultures were grown in Brucella broth (BD) supplemented with 5% fetal bovine serum (Seradigm) and filter sterilized by passing through a 0.2 μm polyethylenesulfone membrane (Nalgene). Primary liquid cultures were prepared from plate cultures after 3 days of growth, and were grown in 50 ml volumes in 500 ml baffled flasks with loose caps. Primary liquid cultures were used for all experiments unless they failed to reach an OD_{600} of at least 1.0 after 20 h, in which case they were diluted 100-fold with fresh media and grown for an additional 20 h. If these secondary cultures failed to reach an OD_{600} of at least 1.0, they were discarded. Aliquots from all liquid cultures were plated and grown in an aerobic environment to check for contamination, and data from cultures that displayed aerobic growth were discarded.

2.2.2. Dose-response curves

Hydrochloric acid (HCl) was obtained from VWR, and hydrogen peroxide (H_2O_2) was obtained from Sigma. Working stocks of HCl were prepared from concentrated stock before each exposure. H_2O_2 concentration was checked before each exposure by measuring the absorbance at 240 nm and using a molar absorptivity of 43.6 $M^{-1}cm^{-1}$ [37], and the dose was adjusted as necessary to maintain consistency between experiments. Saturated overnight cultures of *H. pylori* (OD_{600}>1.0) were normalized to an OD_{600} of 0.5 with fresh media, then exposed in a 1 ml volume for 30 min at 37 °C while shaking in room air. Sham controls were treated with sterile deionized water (Millipore filtration system). After exposure, cultures were serially diluted and 100 μl aliquots were plated on blood agar plates, which were grown as described above. Colony forming units were counted after 3-5 days of growth (depending on exposure), and survival at each dose was expressed as a percentage of the sham treated control. Common phenotypic endpoints (LD_{20} and LD_{80} values for each toxicant) were calculated by plotting dose response curves and visually estimating (example in **Figure 2-S5**).

2.2.3. tRNA preparation

Saturated overnight cultures of *H. pylori* (OD_{600}>1.0) were normalized to an OD_{600} of 0.5 with fresh media and exposed to toxicants in a final volume of 50 ml at 37 °C while shaking in room

air. After exposure, cells were pelleted by centrifuging at 3,000 x *g* for 10 min, resuspended in 10 ml sterile Dulbecco's DPBS (Mediatech), then pelleted again by centrifuging at 3,000 x *g* for 10 min. The supernatant was discarded, and the cell pellet was homogenized in 1 ml TRI Reagent (Sigma) by repetitive pipetting. Total RNA was extracted according to the manufacturer's instructions. Small RNA (primarily tRNA) was then isolated using the Invitrogen PureLink Small RNA Kit. Isolated tRNA was checked for quantity and quality using an Agilent 2100 Bioanalyzer Small RNA Kit, which also confirmed the absence of small rRNA fragments or degradation products that could skew the modification profiles (example shown in **Figure 2-S1**). Isolated tRNA (50 µl total volume) was digested to single nucleosides by adding the following cocktail and incubating at 37 °C for 3 h: 1.0 µl of 1 mg/ml coformycin (DTP/NCI open chemical repository), 0.5 µl of 100 mM butylated hydroxytoluene (Sigma), 5.0 µl of 1 mg/ml tetrahydrouridine (EMD), 0.2 µl of 50 mM magnesium chloride, 0.5 µl of 1 M pH 7.9 Tris, 4.3 µl of 5 U/µl benzonase (Sigma), 2.1 µl of 0.1 U/µl phosphodiesterase I (Affymetrix), 0.3 µl of 17 U/µl alkaline phosphatase (Sigma). After digestion, enzymes were removed by passing the lysates through a 10 kDa molecular weight cutoff filter (VWR).

2.2.4. LC-MS/MS

Ribonucleosides were resolved using a Thermo Scientific Hypersil GOLD aQ reversed-phase column (150 x 2.1 mm, 3 µm particle size) with a flow rate of 0.4 ml/min at 36 °C. Solvent A was 0.1% formic acid in deionized water (Millipore filtration system) and solvent B was 0.1% formic acid in acetonitrile (Sigma). The column was eluted with the following gradient of solvent B: 0.00–6.00 min, 0%; 6.00–7.65 min, 0–1%; 7.65–9.35 min, 1–6%; 9.35–10.00 min, 6%; 10.00–12.00 min, 6–50%; 12.00–14.00 min, 50–75%; 14.00–17.00 min, 75%; 17.00–18.00 min, 75–100%; 18.00–21.00 min, 100%; 21.00–22.00 min, 100–0%; 22.00–28.00 min, 0%. The HPLC column was coupled to an Agilent 6430 Triple Quadrupole mass spectrometer with an electrospray ionization source, which was operated in positive ion mode with the first (Q1) and third (Q3) quadrupoles fixed to unit resolution. Instrument parameters were as follows: gas temperature, 350 °C; gas flow, 10 l/min; nebulizer pressure, 20 psi; capillary voltage, 3800 V; multiplier voltage, 650 V. Neutral loss (NL) scanning experiments used a constant fragmentor voltage of 100 V and a constant collision energy of 10 V, and Q3 was set to monitor for ions that lost a mass of 132 or 146 Da. This mass loss corresponds to the characteristic fragmentation of the glycosidic bond to form a

neutral sugar moiety (132 Da for ribose, 146 Da for 2'-O-methylribose) and a charged base fragment [38]. Given the low sensitivity of the NL method, a single injection of 8 μg of tRNA lysate was used. Dynamic multiple reaction monitoring (DMRM) mode was used to quantify the levels of modifications before and after treatment, using the optimized DMRM parameters shown in **Table 2-S1**. Mass spectrometer signal intensities for all species were normalized by dividing by the area under the curve (AUC) for adenosine (rA) measured by an inline diode array detector monitoring UV absorbance at 260 nm. We chose rA as the species to monitor because it has the highest molar absorptivity among ribonucleosides [39], and is uniformly distributed across *H. pylori* tRNA genes, with a standard deviation of 3% rA content across 36 genes [40]. The linearity of the relationship between rA concentration and AUC was established by an external calibration curve constructed from triplicate injections of 0.05, 0.10, 0.25, 1.00, 5.00, and 10.00 total nmol of rA standard, which revealed a linear relationship with an R^2-value >0.998 (**Figure 2-S2**). To determine the limit of detection (LOD) with respect to amount of tRNA, lysates containing 0.75, 1.50, and 3.00 total μg of tRNA were injected, and the abundance of the modification with the lowest signal intensity (m^2_2G) was monitored. This revealed an LOD of ~200 ng total tRNA (**Figure 2-S3**). All injections were above the LOD.

2.2.5. Data analysis

Mass spectrometer data files were analyzed with MassHunter Qualitative Analysis (Agilent). Basic data analysis and graphing was performed with Microsoft Excel. Hierarchical clustering was performed with Cluster 3.0 (http://bonsai.hgc.jp/~mdehoon/software/cluster/software.htm) and visualized with Java TreeView (http://jtreeview.sourceforge.net/). Principal component analysis was performed with Multibase (Numerical Dynamics).

2.3. Results

2.3.1. The spectrum of tRNA modifications in *H. pylori*

For our studies we chose to use the well characterized, genomically sequenced *H. pylori* strain 26695, which is a Type I strain known to carry the *cag* pathogenicity island and express the critical virulence factor VacA [41]. The first step in our analysis was to determine the spectrum of ribonucleoside modifications present in *H. pylori* tRNA. We used a recently developed,

highly sensitive LC-MS/MS technique to resolve and quantify modified ribonucleosides from tRNA lysates [42]. We used a combination of semi-targeted neutral loss scanning to identify potential ribonucleosides [38, 43] along with targeted multiple reaction monitoring experiments for tentatively identified species expected to occur in *H. pylori* [44]. Together these methods produced a set of 17 species, shown in **Figure 2-1**. Of these, 14 were definitively identified by comparison to synthetic standards (**Figure 2-S4**), and the remaining three were tentatively identified by m/z value and fragmentation pattern. Crude quantitative analysis reveals that the modifications vary over four orders of magnitude, with m^7G having the highest intensity, and $m^2{}_2G$ having the lowest. Broadly, modifications can be grouped by signal intensity as high (m^7G, m^1A, I, m^6A, m^5C), medium (D, m^2A, m^1G, Am, $m^6{}_2A$, t^6A, ms^2t^6A), and low (Ψ, m^6C, Gm, $m^2{}_2G$, i^6A). These intensities reflect both the actual abundance of the modification as well as its chemical and mass spectral properties. Because many types of RNA are known to contain modified nucleosides [45, 46], we used a microfluidic platform (Agilent Bioanalyzer) to examine all tRNA extracts prior to digestion and LC-MS/MS. This step confirmed the absence of RNA degradation fragments or intact short ribosomal RNA (rRNA) sequences, such as the 120 nt 5S rRNA (**Figure 2-S1**). Following identification of the spectrum of modifications, a dynamic multiple reaction monitoring (DMRM) method was developed, which contained optimized instrument parameters for maximum sensitivity in quantifying each ribonucleoside based on the characteristic m/z transition (**Table 2-S1**).

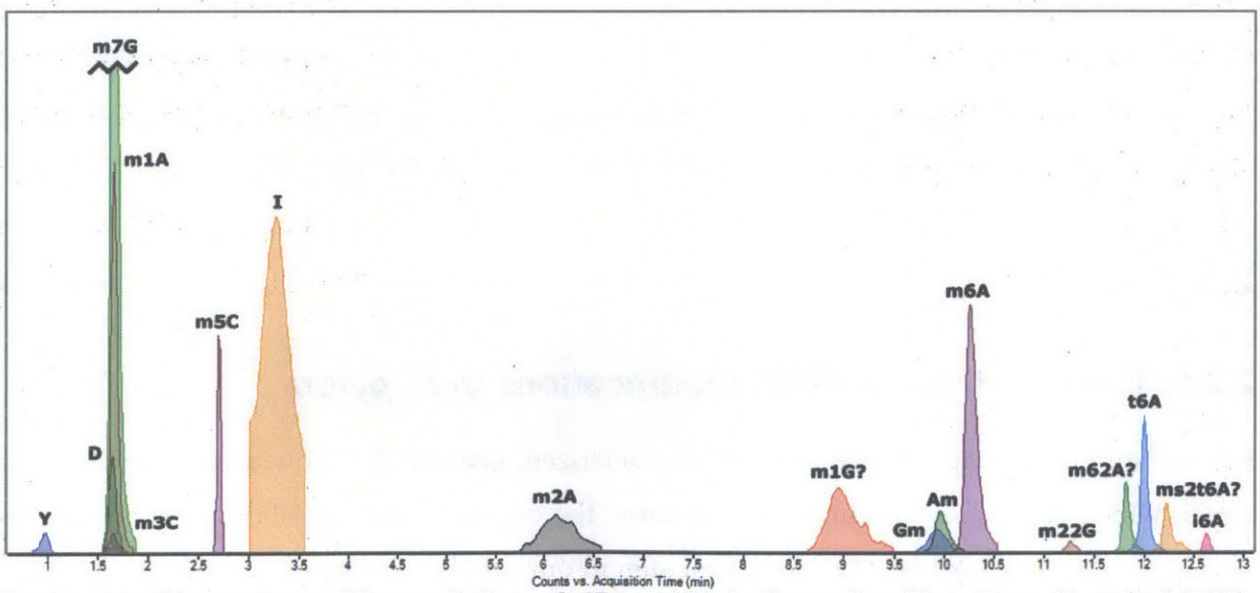

Figure 2-1: Chromatographic resolution of 17 modified ribonucleosides from *H. pylori* tRNA. Identities were confirmed by comparison to synthetic standards, unless denoted with a question mark,

which indicates a tentative identity based only on m/z value and fragmentation pattern. The y-axis is arbitrary, and the m^7G peak is truncated for better visibility of low-abundance species.

2.3.2. tRNA modification changes are toxicant-specific

Having established a spectrum of tRNA modifications in *H. pylori*, we then sought to determine their impact on its ability to colonize the human stomach. Because we were interested in stress response systems that support *H. pylori*'s ability to invade the stomach and evade the host innate immune response, we chose to study two toxicants that are essential for H. *pylori* to avoid. Hydrochloric acid (HCl) is the first barrier that *H. pylori* faces, as it must survive the low pH of the stomach long enough to invade the more neutral environment of the gastric mucosa [7, 29]. Hydrogen peroxide (H_2O_2) is a major component of the innate immune response, and is produced by neutrophils in an attempt to kill invading pathogens [8]. Interestingly, H_2O_2 production is also induced by *H. pylori* itself through the release of NAP (neutrophil activating protein), which may serve as a mechanism for increasing damage to the host tissue [12]. Together, HCl and H_2O_2 are the first two barriers to *H. pylori* colonization. Of course, *H. pylori* is well adapted to survive both these stresses, and produces large amounts of both urease and catalase to detoxify its microenvironment [28]. We sought to determine if tRNA modifications play a role in the regulation and production of these survival factors.

To ensure comparability between toxicants with distinct mechanisms of action, we constructed dose response curves to define common endpoints (**Figure 2-S5**). We then exposed *H. pylori* to low (LD_{20}) and high (LD_{80}) doses of each toxicant, along with sham-treated controls, and quantified the levels of 17 modified ribonucleosides (**Tables 2-S2** and **2-S3**). We calculated fold-change values between the treated and untreated groups, and applied multivariate statistical techniques to determine the impact of various modifications. As shown in **Figure 2-2**, hierarchical clustering accurately groups exposures by both dose and toxicant, with distinct and often inversely correlated patterns appearing for both HCl and H_2O_2 exposure. It is especially notable that the species strongly increased in HCl exposure (Gm, m^5C, i^6A, m^1A, m^3C, $m^6{}_2A$) are consistently decreased in H_2O_2 exposure, while those consistently increased in H_2O_2 exposure (I, m^6A, Am, ms^2t^6A, t^6A) are consistently decreased in HCl exposure. These data indicate that tRNA modifications can serve as biomarkers of exposure by correlating with specific stresses, and also point to potentially crucial functions of the highly increased modifications.

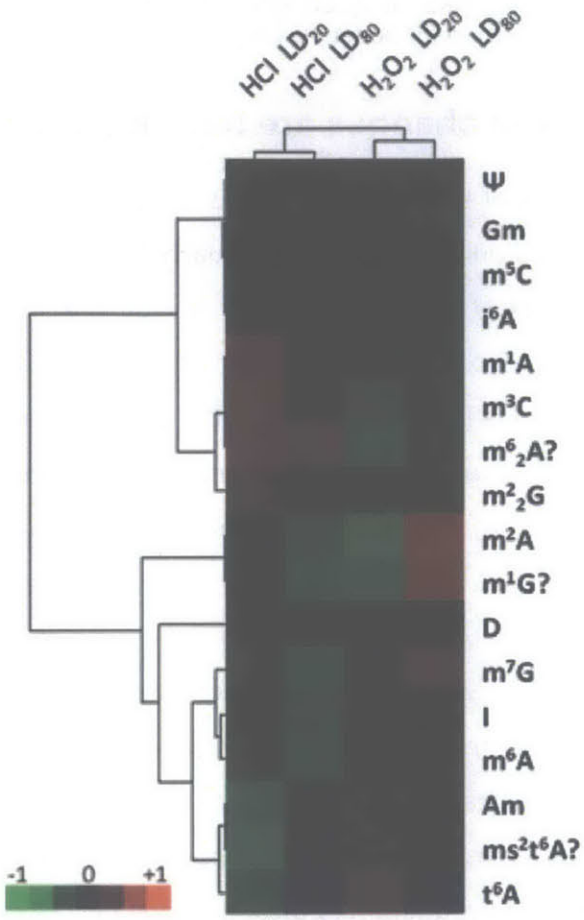

Figure 2-2: Hierarchical clustering of *H. pylori* ribonucleoside fold-changes after toxicant exposure. Ribonucleosides cluster by both toxicant and dose, revealing unique signatures. Data were $\log_2$ transformed, mean centered, and normalized prior to clustering with centroid linkage.

To better understand the relationship between modifications and stress response, we applied principal component analysis (PCA), a multivariate statistical technique that can reveal hidden correlations between multiply interacting pathways. PCA revealed clear separation between the two toxicants, with 89% of the variance captured by the first two principal components (PCs), which indicates excellent correlation (**Figure 2-3**). The score plot reveals that PC1 is primarily responsible for separating the low dose H_2O_2 samples from all the others. This may represent the fact that low dose H_2O_2 can function as an intracellular signaling molecule [47], or may be a result of *H. pylori*'s strong adaptation to persistent H_2O_2 exposure. In contrast, PC2 provides clear separation between both HCl exposures and the high dose H_2O_2. This separation likely reflects the fact that the two toxicants have different mechanisms of action, and are detoxified by distinct bacterial enzymes. By examining the loadings plot, we can determine which modifications contribute to each toxicant grouping. It appears that m^7G, m^6A, and ms^2t^6A are all

strongly correlated with the low dose H_2O_2, while m^2A and m^1G are strongly correlated with the high dose H_2O_2, and $m^6{}_2A$ and m^3C are strongly correlated with both HCl doses. These associations complement the hierarchical clustering results, and point to a potentially important role for tRNA modifications in the responses to both HCl and H_2O_2.

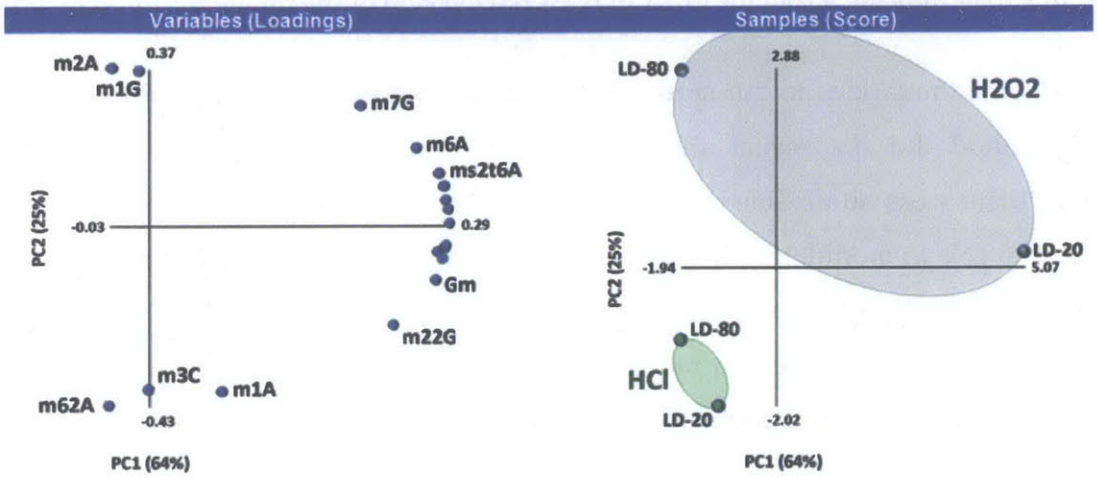

Figure 2-3: Principal component analysis of *H. pylori* ribonucleoside fold-changes after toxicant exposure. The loadings plot shows the ten modifications with the highest contribution to the variance seen in the score plot, revealing specific modifications associated with each toxicant. Data were mean centered and normalized prior to calculation.

2.4. Significance and future directions

The goal of these studies was to determine the role that tRNA modifications play in *H. pylori*'s stress responses and ability to survive the host immune system. Here we report that *H. pylori* restructures its tRNA modification spectrum in toxicant-specific ways. Our data show that H_2O_2 and HCl induce significant and divergent changes in the abundance of several tRNA modifications, and that the pattern of these changes is predictive of the exposure, with certain modifications highly correlated with each exposure.

Several well characterized tRNA modifications were identified as potentially important for *H. pylori*'s survival of HCl and H_2O_2 exposure, and their involvement may give us mechanistic insight. For example, we saw a very strong association between low dose H_2O_2 and m^7G, which has been shown to be essential for robust growth in yeast [48]. Similarly, m^6A is found in bacteria only on valine tRNA [49], which may point to a role in regulating specific proteins. Perhaps most excitingly, ms^2t^6A is commonly found at tRNA position 37 adjacent to the anticodon loop [50], where several modifications have been shown to participate in reading

frame maintenance and binding modulation [51-53]. Notably, $m^6{}_2A$ appears to be strongly associated with the response to HCl exposure. This modification was long thought to be specific to rRNA [54], but our group recently reported its discovery in the tRNA of *Mycobacterium bovis* bacille Calmette-Guérin [55]. As *M. bovis* also survives in a harsh inflammatory environment [56-58], this may indicate a role for $m^6{}_2A$ in bacterial evasion of the innate immune response.

There are some limitations to our study that must be acknowledged. Most obviously, our LC-MS/MS method did not reveal all the tRNA modifications that we expected to find. In particular, there were no uridine derivatives in our list, even though these are known to often play a critical role in modulating the binding of the wobble position of tRNA [51], and *H. pylori* possesses the gene for synthesis of 5-methylaminomethyl-2-thiouridine [59]. Similarly, we did not detect lysidine, which bacteria require for successful translation of isoleucine codons [60]. We attribute this failure to problems of sensitivity and insufficient material, as others have reported weak signals and difficult identification for modified uridines [35], and lysidine is known to occur on only a single tRNA [61]. Therefore we recognize that this list of modifications is not exhaustive, and that there may be other species that are critical for survival. We must also recognize the inherent limitation in using only a single strain of *H. pylori*, particularly given its genetic diversity [26] and the substantial phenotypic variation that is seen between strains [62]. However, these limitations do not detract from our overall findings, and provide guidance for future studies.

Moving forward, there are several important steps to expand on these findings and fully elucidate the impact on tRNA modifications on *H. pylori* stress response. The set of toxicants examined should be expanded to include all the common components of the innate immune response, particularly hypochlorite and nitric oxide [8, 63]. Once a complete set of potentially critical modifications is assembled, bioinformatics tools and published databases can be used to determine the biosynthetic pathways and enzymes involved in the synthesis of modifications of interest [46]. Knockout *H. pylori* strains deficient for particular tRNA modifications can then be constructed [64], and the survival of these knockouts can be compared to wild type strains to verify their importance [35]. Finally, the validated crucial modification pathways could be used as substrates for structure-guided drug discovery [65], which could lead to a new class treatments for *H. pylori*.

2.5. Supplementary material

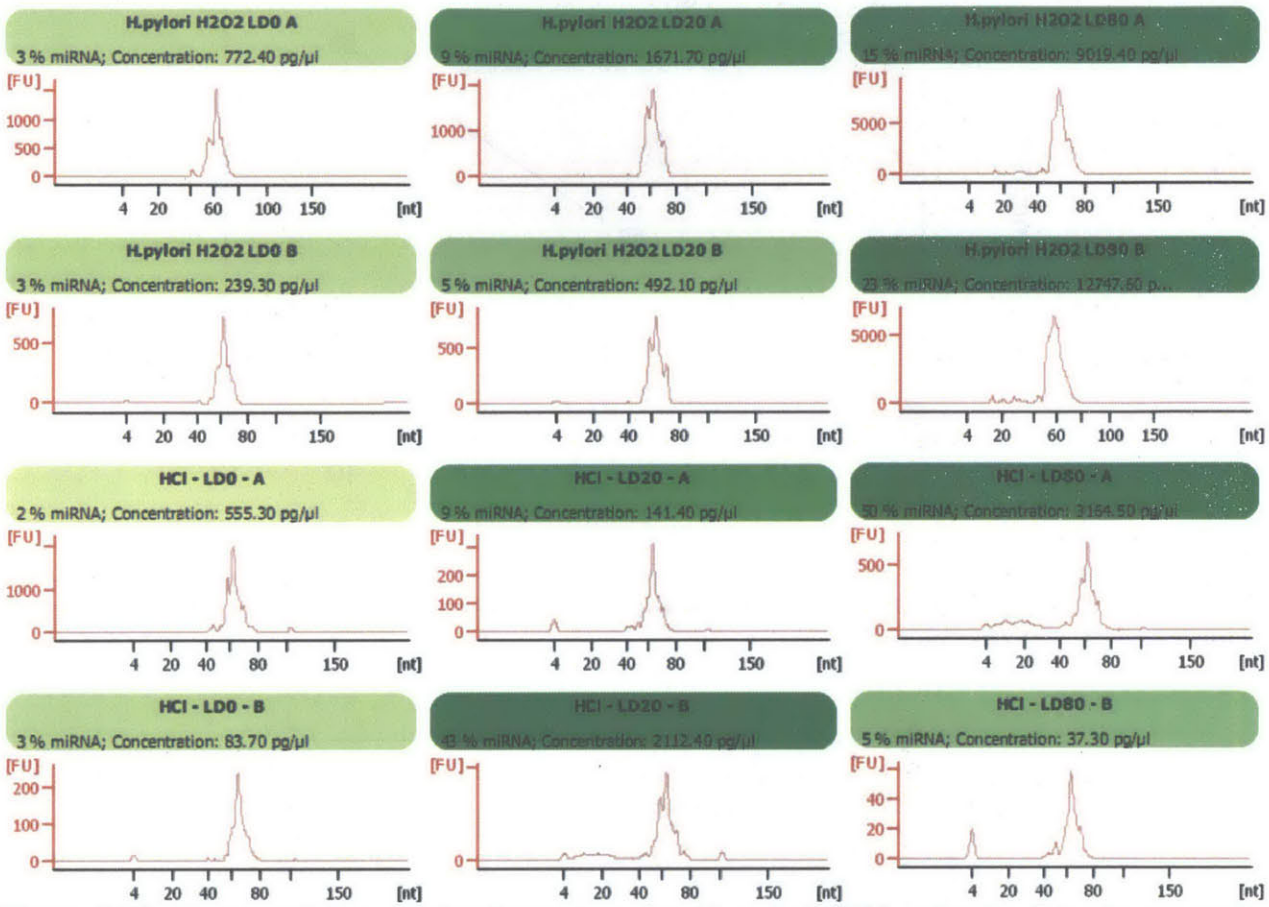

Figure 2-S1: Representative electropherograms for *H. pylori* tRNA extracts. Prior to enzymatic hydrolysis, all tRNA samples were quantified and evaluated for ribosomal RNA (rRNA) contamination using an Agilent Bioanalyzer. Representative tracings are shown, revealing very little degradation and no full-length 5S rRNA (120 nt).

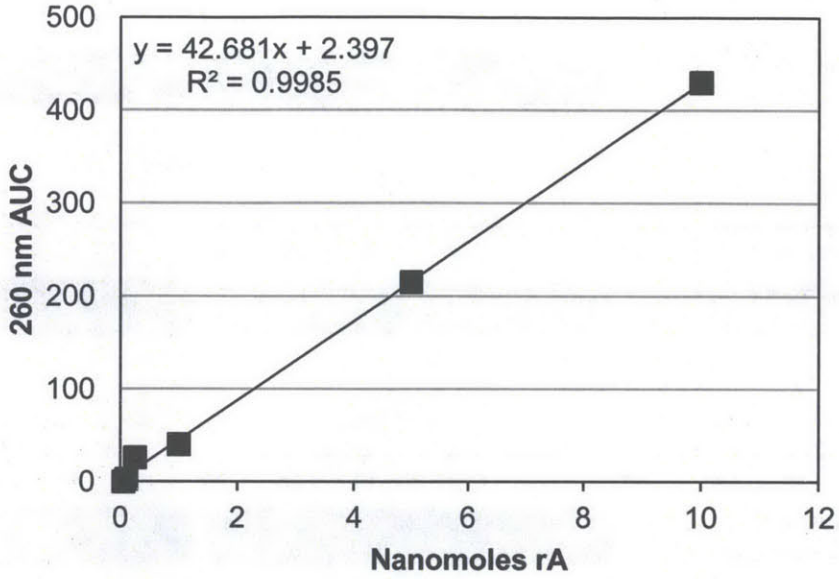

Figure 2-S2: UV calibration curve. To determine the linearity of the UV response, injections of 0.05, 0.10, 0.25, 1.00, 5.00, and 10.00 nmol of adenosine were performed. Each data point is the mean of three injections performed in random order.

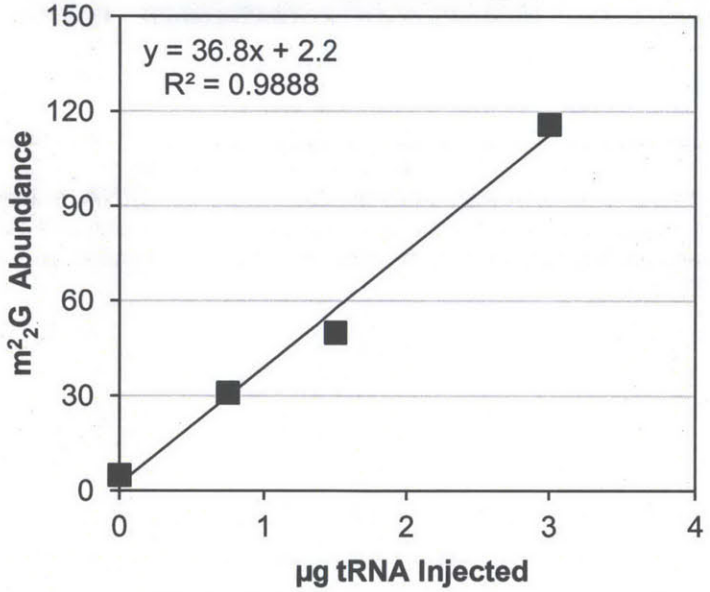

Figure 2-S3: Calibration curve and limit of detection for tRNA injections. To determine the minimum amount of tRNA needed to detect all identified ribonucleosides, injections of 0.75, 1.50, and 3.00 total µg of tRNA were performed, and the abundance of the species with the weakest signal (m^2_2G) was monitored. The limit of detection was 207 ng tRNA per injection.

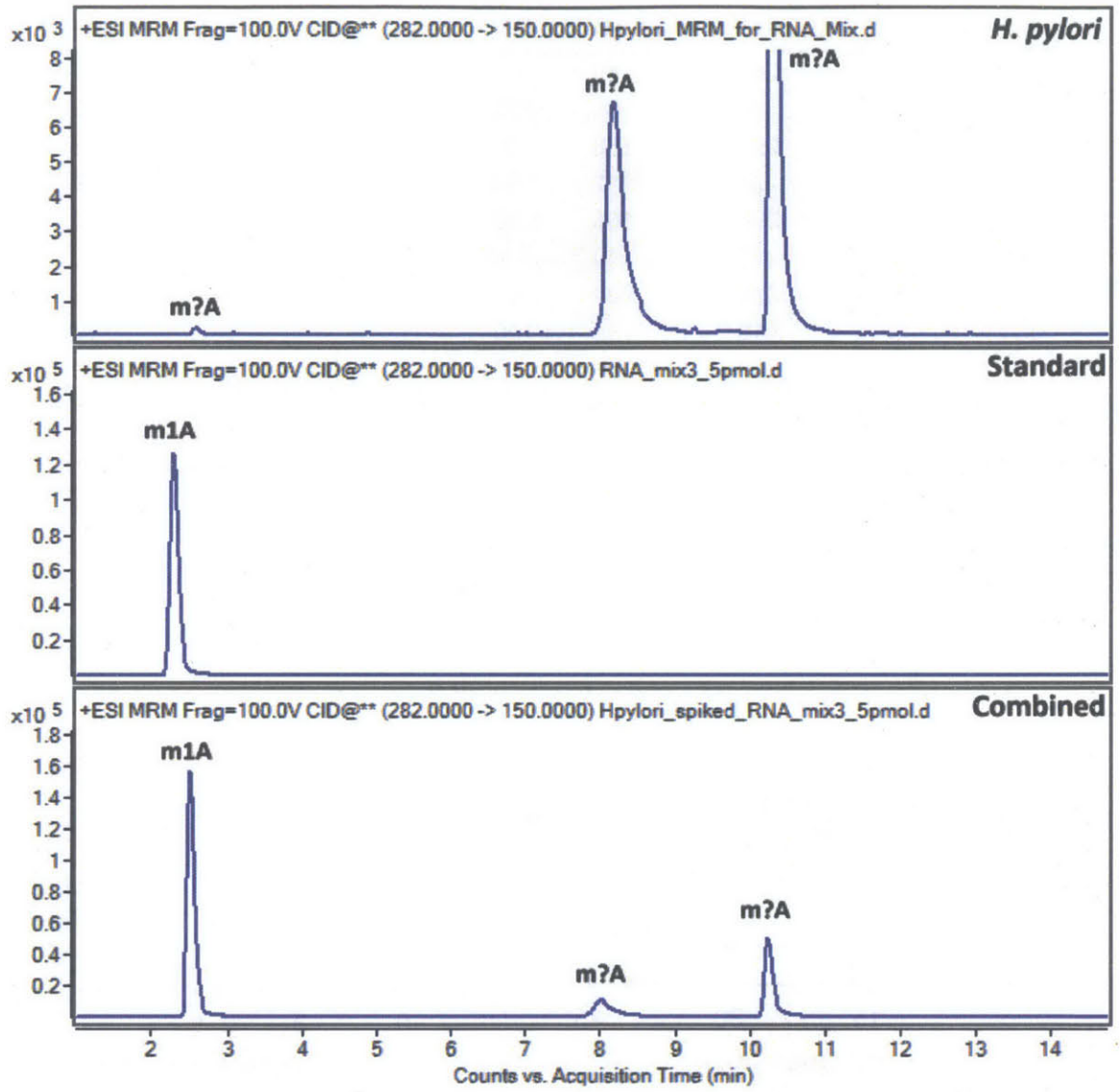

Figure 2-S4: Confirmation of m^1A identity by comparison to synthetic standard. The top panel shows three peaks with m/z transition corresponding to methyladenosine (m?A) in total *H. pylori* tRNA lysate. The middle panel shows a pure standard of m^1A, suggesting that the first peak is m1A. The bottom panel shows *H. pylori* tRNA spiked with the m^1A standard, confirming the peak identity. The y-axis scale between panels varies due to the standard being more concentrated than the tRNA extract. This process was repeated for all 14 confirmed species.

Name	Precursor	Product	F V	CE	CAV	RT	Delta
Ψ	245	191	80	10	7	1.6	2
D	247	115	80	8	7	1.6	2
m^5C, m^3C	258	126	80	8	7	2.3	2
I	269	137	80	10	7	4	2
Am	282	136	100	15	7	9.8	3
m^1A	282	150	100	16	7	2	2
m^2A	282	150	100	16	7	6.5	3

Name	Precursor	Product	F V	CE	CAV	RT	Delta
m^6A	282	150	100	16	7	10.3	2
$m^6{}_2A$?	296	164	100	16	7	11.8	2
m^1G?	298	166	90	10	7	9.3	3
Gm	298	152	80	7	7	10.1	2
m^7G	298	166	90	10	7	2	2
$m^2{}_2G$	312	180	100	8	7	11.2	2
i^6A	336	204	100	17	7	12.6	2
t^6A	413	281	100	8	7	12	2
ms^2t^6A?	459	327	100	8	7	12.2	2

Table 2-S1: Dynamic multiple reaction monitoring method for *H. pylori* ribonucleosides. Question marks indicate species tentatively identified only by m/z value and fragmentation pattern. Precursor: precursor ion (m/z), Product: product ion (m/z), FV: fragmentor voltage (V), CE: collision energy (V), CAV: cell accelerator voltage (V), RT: retention time (min), Delta: retention time window (min).

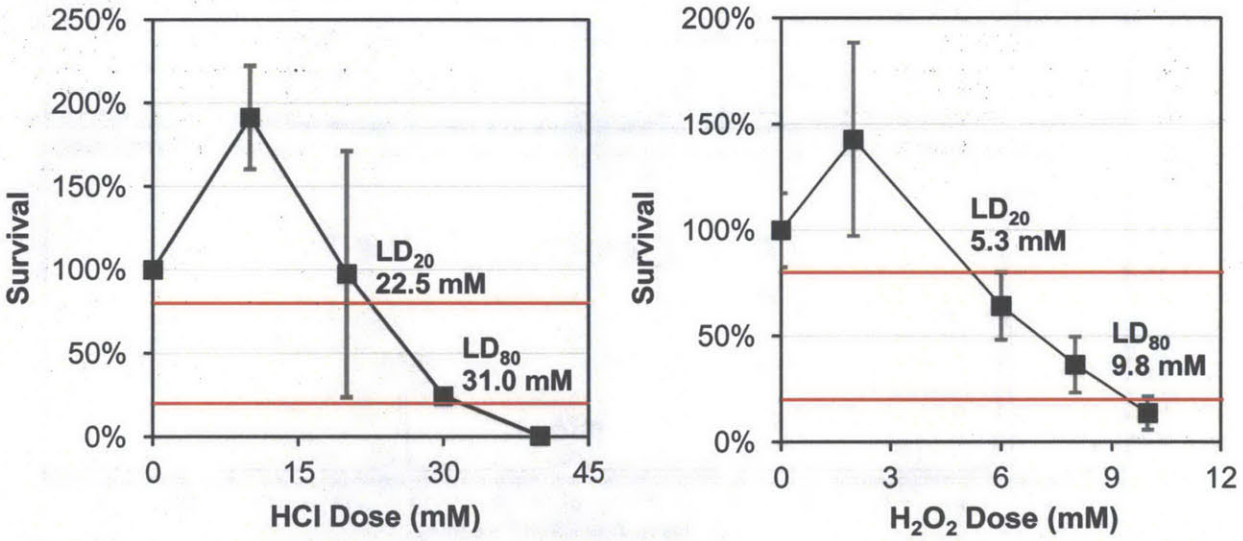

Figure 2-S5: *H. pylori* dose-response curves for hydrochloric acid and hydrogen peroxide. To ensure common phenotypic endpoints for exposures, dose-response curves were constructed for each toxicant. Red lines indicate 80% survival (LD_{20}) and 20% survival (LD_{80}). Data points at each dose are mean ± SD for at least three biological replicates.

rN	HCl LD_0		HCl LD_{20}			HCl LD_{80}		
	Mean	SD	Mean	SD	*t*-test	Mean	SD	*t*-test
D	5873.76	4801.87	17288.53	11027.75	0.251	5888.37	944.73	0.997
Ψ	67.56	45.56	*295.10*	*109.24*	*0.053*	162.48	104.52	0.304
m^7G	12192.89	3674.60	10140.22	6104.97	0.705	6631.37	2052.10	0.135
m^1A	40.29	23.89	547.54	351.99	0.112	*198.32*	*42.44*	*0.010*
m^3C	36.76	23.76	635.95	416.58	0.112	*191.66*	*91.92*	*0.082*
m^5C	39.07	20.95	81.98	28.99	0.165	97.36	71.62	0.331

rN	HCl LD_0		HCl LD_{20}			HCl LD_{80}		
	Mean	SD	Mean	SD	*t*-test	Mean	SD	*t*-test
I	1879.96	987.98	5554.18	2903.95	0.166	2198.08	1053.73	0.771
m^2A	3897.43	533.48	3692.79	2812.59	0.924	*2600.03*	*611.29*	*0.087*
m^1G?	3185.91	416.57	2873.47	1944.56	0.835	1623.02	*349.53*	*0.015*
Am	74.48	46.78	194.45	81.22	0.145	216.87	157.07	0.287
Gm	242.03	142.86	782.40	350.92	0.114	728.23	513.28	0.266
m^6A	6427.28	1469.65	6004.67	3624.64	0.886	4164.38	995.42	0.146
$m^2{}_2G$	22.87	11.44	398.07	253.45	0.105	130.42	*46.67*	*0.034*
$m^6{}_2A$?	56.16	31.59	1488.43	1845.91	0.334	708.00	710.28	0.265
t^6A	213.50	58.60	258.33	130.83	0.681	261.08	42.63	0.406
ms^2t^6A?	157.71	35.12	99.78	44.35	0.221	125.77	36.11	0.421
i^6A	26.64	25.19	100.33	49.28	0.133	125.47	83.14	0.183

Table 2-S2: Normalized abundances for 17 modified ribonucleosides in *H. pylori* after hydrochloric acid exposure. Triplicate injections of three biological replicates were normalized by amount of tRNA and averaged. Student's *t*-test (two-tailed, unpaired) was performed for each ribonucleosides species, comparing the treated cultures to negative controls. Modifications with $p<0.1$ are highlighted.

rN	H_2O_2 LD_0		H_2O_2 LD_{20}			H_2O_2 LD_{80}		
	Mean	SD	Mean	SD	*t*-test	Mean	SD	*t*-test
D	123.45	23.99	936.23	1036.47	0.330	132.37	24.74	0.733
Ψ	5.09	2.75	277.91	369.95	0.356	1.44	0.11	0.133
m^7G	2216.49	381.09	3010.37	1420.86	0.488	2590.11	389.52	0.387
m^1A	11.34	10.55	89.71	116.77	0.398	5.44	2.82	0.488
m^3C	4.77	3.10	29.61	38.34	0.413	1.67	0.54	0.236
m^5C	3.83	2.31	48.44	62.70	0.372	0.37	0.18	0.102
I	92.65	35.95	981.59	704.52	0.149	262.97	117.64	0.122
m^2A	492.07	89.74	451.18	190.41	0.797	*645.54*	*25.22*	*0.080*
m^1G?	274.81	69.21	247.16	26.87	0.626	368.08	13.16	0.134
Am	2.17	0.70	60.82	73.92	0.325	13.24	8.93	0.155
Gm	9.49	3.39	85.70	103.29	0.356	4.43	0.99	0.113
m^6A	1109.37	131.49	1932.11	800.83	0.225	1293.69	87.53	0.174
$m^2{}_2G$	1.77	0.70	41.57	56.54	0.376	1.08	0.39	0.292
$m^6{}_2A$?	6.56	2.85	56.70	60.79	0.309	5.25	1.67	0.605
t^6A	43.13	7.80	175.61	190.97	0.382	53.52	22.66	0.573
ms^2t^6A?	30.38	2.47	108.21	109.93	0.373	38.12	7.56	0.241
i^6A	1.56	0.91	26.51	35.34	0.375	0.66	0.42	0.275

Table 2-S3: Normalized abundances for 17 modified ribonucleosides in *H. pylori* after hydrogen peroxide exposure. Triplicate injections of three biological replicates were normalized by amount of tRNA and averaged. Student's *t*-test (two-tailed, unpaired) was performed for each ribonucleosides species, comparing the treated cultures to negative controls. Modifications with $p<0.1$ are highlighted.

2.6. References

1. R.A. Feldman, A.J.P. Eccersley, J.M. Hardie (1998) *Epidemiology of Helicobacter pylori: Acquisition, transmission, population prevalence and disease-to-infection ratio.* **Br Med Bull** 54(1): 39-53.
2. L.M. Brown (2000) *Helicobacter pylori: Epidemiology and routes of transmission.* **Epidemiol Rev** 22(2): 283-297.
3. K.E.L. Mccoll (2010) *Helicobacter pylori infection.* **N Engl J Med** 362(17): 1597-1604.
4. M. Woodward, C. Morrison, K. Mccoll (2000) *An investigation into factors associated with Helicobacter pylori infection.* **J Clin Epidemiol** 53(2): 175-181.
5. S. Suerbaum, P. Michetti (2002) *Helicobacter pylori infection.* **N Engl J Med** 347(15): 1175-1186.
6. D. Rothenbacher, H. Brenner (2003) *Burden of Helicobacter pylori and H. pylori-related diseases in developed countries: Recent developments and future implications.* **Microb Infect** 5(8): 693-703.
7. B. Bauer, T.F. Meyer (2011) *The human gastric pathogen Helicobacter pylori and its association with gastric cancer and ulcer disease.* **Ulcers** 2011: 1-23.
8. P. Lonkar, P.C. Dedon (2011) *Reactive species and DNA damage in chronic inflammation: Reconciling chemical mechanisms and biological fates.* **Int J Cancer** 128(9): 1999-2009.
9. N. Uemura, S. Okamoto, S. Yamamoto, N. Matsumura, S. Yamaguchi, M. Yamakido, K. Taniyama, N. Sasaki, R.J. Schlemper (2001) *Helicobacter pylori infection and the development of gastric cancer.* **N Engl J Med** 345(11): 784-789.
10. F. Farinati, R. Cardin, V.M. Russo, G. Busatto, M. Franco, M. Rugge (2003) *Helicobacter pylori CagA status, mucosal oxidative damage and gastritis phenotype: A potential pathway to cancer?* **Helicobacter** 8(3): 227-234.
11. W.K. Leung, S.R. Lin, J.Y. Ching, K.F. To, E.K. Ng, F.K. Chan, J.Y. Lau, J.J. Sung (2004) *Factors predicting progression of gastric intestinal metaplasia: Results of a randomised trial on Helicobacter pylori eradication.* **Gut** 53(9): 1244-1249.
12. O. Handa, Y. Naito, T. Yoshikawa (2010) *Helicobacter pylori: A ROS-inducing bacterial species in the stomach.* **Inflamm Res** 59(12): 997-1003.
13. D.B. Polk, R.M. Peek, Jr. (2010) *Helicobacter pylori: Gastric cancer and beyond.* **Nat Rev Cancer** 10(6): 403-414.
14. L.E. Wroblewski, R.M. Peek, Jr., K.T. Wilson (2010) *Helicobacter pylori and gastric cancer: Factors that modulate disease risk.* **Clin Microbiol Rev** 23(4): 713-739.
15. International Agency for Research on Cancer Working Group on the Evaluation of Carcinogenic Risks to Humans. *Helicobacter pylori*, in *Schistosomes, Liver Flukes and Helicobacter pylori*. 1994, IARC: Lyon, France. p. 177-240.
16. D.M. Parkin, F. Bray, J. Ferlay, P. Pisani (2002) *Global cancer statistics, 2002.* **CA-Cancer J Clin** 55(2): 74–108.

15. International Agency for Research on Cancer Working Group on the Evaluation of Carcinogenic Risks to Humans. *Helicobacter pylori*, in *Schistosomes, Liver Flukes and Helicobacter pylori*. 1994, IARC: Lyon, France. p. 177-240.
16. D.M. Parkin, F. Bray, J. Ferlay, P. Pisani (2002) *Global cancer statistics, 2002.* **CA-Cancer J Clin** 55(2): 74–108.
17. M.M. Khalifa, R.R. Sharaf, R.K. Aziz (2010) *Helicobacter pylori: A poor man's gut pathogen?* **Gut Pathog** 2(1): 2.
18. P. Malfertheiner, P. Sipponen, M. Naumann, P. Moayyedi, F. Megraud, S.D. Xiao, K. Sugano, O. Nyren (2005) *Helicobacter pylori eradication has the potential to prevent gastric cancer: A state-of-the-art critique.* **Am J Gastroenterol** 100(9): 2100-2115.
19. D. Vaira, N. Vakil (2001) *Blood, urine, stool, breath, money, and Helicobacter pylori.* **Gut** 48: 287-289.
20. M.J. Blaser (2006) *Who are we? Indigenous microbes and the ecology of human diseases.* **EMBO Rep** 7(10): 956-960.
21. P. Bytzer, J.F. Dahlerup, J.R. Eriksen, D. Jarbøl, S. Rosenstock, S. Wildt (2011) *Diagnosis and treatment of Helicobacter pylori infection.* **Dan Med Bull** 58(4): C4271.
22. W. Wu, Y. Yang, G. Sun (2012) *Recent insights into antibiotic resistance in Helicobacter pylori eradication.* **Gastroenterol Res Pract** 2012: 723183.
23. L. Fischbach, E.L. Evans (2007) *Meta-analysis: The effect of antibiotic resistance status on the efficacy of triple and quadruple first-line therapies for Helicobacter pylori.* **Aliment Pharmacol Ther** 26(3): 343-357.
24. F. Megraud (2004) *H. pylori antibiotic resistance: Prevalence, importance, and advances in testing.* **Gut** 53(9): 1374-1384.
25. A. Khan, A. Farooqui, H. Manzoor, S.S. Akhtar, M.S. Quraishy, S.U. Kazmi (2012) *Antibiotic resistance and cagA gene correlation: A looming crisis of Helicobacter pylori.* **World J Gastroenterol** 18(18): 2245-2252.
26. M.S. Dorer, S. Talarico, N.R. Salama (2009) *Helicobacter pylori's unconventional role in health and disease.* **PLoS Pathog** 5(10): e1000544.
27. G.L. Mendz, A.J. Shepley, S.L. Hazell, M.A. Smith (1997) *Purine metabolism and the microaerophily of Helicobacter pylori.* **Arch Microbiol** 168: 448-456.
28. D.E. Berg, P.S. Hoffman, B.J. Appelmelk, J.G. Kusters (1997) *The Helicobacter pylori genome sequence: Genetic factors for long life in the gastric mucosa.* **Trends Microbiol** 5(12): 468-474.
29. B.J. Marshall, L.J. Barrett, C. Prakash, R.W. Mccallum, R.L. Guerrant (1990) *Urea protects Helicobacter-(Campylobacter)-pylori from the bactericidal effect of acid.* **Gastroenterology** 99(3): 697-702.
30. F.M. Barnard, M.F. Loughlin, H.P. Fainberg, M.P. Messenger, D.W. Ussery, P. Williams, P.J. Jenks (2003) *Global regulation of virulence and the stress response by CsrA in the highly adapted human gastric pathogen Helicobacter pylori.* **Mol Microbiol** 51(1): 15-32.
31. P.C. Dedon, T.J. Begley (2014) *A system of RNA modifications and biased codon use controls cellular stress response at the level of translation.* **Chem Res Toxicol** 27(3): 330-337.
32. U. Begley, M.S. Sosa, A. Avivar-Valderas, A. Patil, L. Endres, Y. Estrada, C.T. Chan, D. Su, P.C. Dedon, J.A. Aguirre-Ghiso, T. Begley (2013) *A human tRNA methyltransferase*

9-like protein prevents tumour growth by regulating LIN9 and HIF1-α **EMBO Mol Med** 5(3): 366-383.

33. A. Patil, M. Dyavaiah, F. Joseph, J.P. Rooney, C.T. Chan, P.C. Dedon, T.J. Begley (2012) *Increased tRNA modification and gene-specific codon usage regulate cell cycle progression during the DNA damage response.* **Cell Cycle** 11(19): 3656-3665.
34. C.T. Chan, Y.L. Pang, W. Deng, I.R. Babu, M. Dyavaiah, T.J. Begley, P.C. Dedon (2012) *Reprogramming of tRNA modifications controls the oxidative stress response by codon-biased translation of proteins.* **Nat Commun** 3: 937.
35. C.T. Chan, M. Dyavaiah, M.S. Demott, K. Taghizadeh, P.C. Dedon, T.J. Begley (2010) *A quantitative systems approach reveals dynamic control of tRNA modifications during cellular stress.* **PLoS Genet** 6(12): e1001247.
36. U. Begley, M. Dyavaiah, A. Patil, J.P. Rooney, D. Direnzo, C.M. Young, D.S. Conklin, R.S. Zitomer, T.J. Begley (2007) *Trm9-catalyzed tRNA modifications link translation to the DNA damage response.* **Mol Cell** 28(5): 860-870.
37. A.G. Hildebraunt, I. Roots (1975) *Reduced nicotinamide adenine dinucleotide phosphate (NADPH)-dependent formation and breakdown of hydrogen peroxide during mixed function oxidation reactions in liver microsomes.* **Arch Biochem Biophys** 171(2): 385-397.
38. E.L. Esmans, D. Broes, I. Hoes, F. Lemiere, K. Vanhoutte (1998) *Liquid chromatography–mass spectrometry in nucleoside, nucleotide and modified nucleotide characterization.* **J Chromatogr A** 794: 109-127.
39. M.J. Cavaluzzi, P.N. Borer (2004) *Revised UV extinction coefficients for nucleoside-5'-monophosphates and unpaired DNA and RNA.* **Nucleic Acids Res** 32(1): e13.
40. P.P. Chan, T.M. Lowe (2009) *GtRNAdb: A database of transfer RNA genes detected in genomic sequence.* **Nucleic Acids Res** 37(Database issue): D93-97.
41. T. Resende, D.M. Correia, M. Rocha, I. Rocha (2013) *Re-annotation of the genome sequence of Helicobacter pylori 26695.* **J Integr Bioinform** 10(3): 233.
42. D. Su, C.T. Chan, C. Gu, K.S. Lim, Y.H. Chionh, M.E. Mcbee, B.S. Russell, I.R. Babu, T.J. Begley, P.C. Dedon (2014) *Quantitative analysis of ribonucleoside modifications in tRNA by HPLC-coupled mass spectrometry.* **Nat Protoc** 9(4): 828-841.
43. F. Teichert, S. Winkler, H.C. Keun, W.P. Steward, A.J. Gescher, P.B. Farmer, R. Singh (2011) *Evaluation of urinary ribonucleoside profiling for clinical biomarker discovery using constant neutral loss scanning liquid chromatography/tandem mass spectrometry.* **Rapid Commun Mass Spectrom** 25(14): 2071-2082.
44. K.S. Lim (2014) Personal communication with B.S. Russell
45. W.A. Cantara, P.F. Crain, J. Rozenski, J.A. Mccloskey, K.A. Harris, X. Zhang, F.A. Vendeix, D. Fabris, P.F. Agris (2011) *The RNA Modification Database, RNAMDB: 2011 update.* **Nucleic Acids Res** 39(Database issue): D195-201.
46. S. Dunin-Horkawicz, A. Czerwoniec, M.J. Gajda, M. Feder, H. Grosjean, J.M. Bujnicki (2006) *MODOMICS: A database of RNA modification pathways.* **Nucleic Acids Res** 34(Database issue): D145-149.
47. D.R. Gough, T.G. Cotter (2011) *Hydrogen peroxide: A Jekyll and Hyde signalling molecule.* **Cell Death Dis** 2: e213.
48. A. Alexandrov, E.J. Grayhack, E.M. Phizicky (2005) *tRNA m^7G methyltransferase Trm8p/Trm82p: evidence linking activity to a growth phenotype and implicating Trm82p in maintaining levels of active Trm8p.* **RNA** 11(5): 821-830.

methylthiotransferase for biosynthesis of 2-methylthio-N^6-threonylcarbamoyladenosine in tRNA. **J Biol Chem** 285(37): 28425-28433.
51. P.F. Agris, F.A. Vendeix, W.D. Graham (2007) *tRNA's wobble decoding of the genome: 40 years of modification.* **J Mol Biol** 366(1): 1-13.
52. P.F. Agris (2008) *Bringing order to translation: The contributions of transfer RNA anticodon-domain modifications.* **EMBO Rep** 9(7): 629-635.
53. E.M. Gustilo, F.A. Vendeix, P.F. Agris (2008) *tRNA's modifications bring order to gene expression.* **Curr Opin Microbiol** 11(2): 134-140.
54. M.Y. Graham, B. Weisblum (1979) *23S ribosomal ribonucleic acid of macrolide-producing streptomycetes contains methylated adenine.* **J Bacteriol** 137(3): 1464-1467.
55. C.T. Chan, Y.H. Chionh, C.H. Ho, K.S. Lim, I.R. Babu, E. Ang, L. Wenwei, S. Alonso, P.C. Dedon (2011) *Identification of N^6,N^6-dimethyladenosine in transfer RNA from Mycobacterium bovis bacille Calmette–Guérin.* **Molecules** 16(6): 5168-5181.
56. N. Chandra, D. Kumar, K. Rao (2011) *Systems biology of tuberculosis.* **Tuberculosis** 91(5): 487-496.
57. J. Mcfadden, D.J.V. Beste, A.M. Kierzek (Eds.) *Systems Biology of Tuberculosis*. 2013, Springer: New York.
58. A. O'garra, P.S. Redford, F.W. Mcnab, C.I. Bloom, R.J. Wilkinson, M.P. Berry (2013) *The immune response in tuberculosis.* **Annu Rev Immunol** 31: 475-527.
59. K.M. Chang, T.L. Hendrickson (2009) *Recognition of $tRNA^{Gln}$ by Helicobacter pylori GluRS2—a $tRNA^{Gln}$-specific glutamyl-tRNA synthetase.* **Nucleic Acids Res** 37(20): 6942-6949.
60. C. Köhrer, D. Mandal, K.W. Gaston, H. Grosjean, P.A. Limbach, U.L. Rajbhandary (2014) *Life without $tRNA^{Ile}$-lysidine synthetase: Translation of the isoleucine codon AUA in Bacillus subtilis lacking the canonical $tRNA_2^{Ile}$.* **Nucleic Acids Res** 42(3): 1904-1915.
61. Y. Ikeuchi, A. Soma, T. Ote, J. Kato, Y. Sekine, T. Suzuki (2005) *Molecular mechanism of lysidine synthesis that determines tRNA identity and codon recognition.* **Mol Cell** 19(2): 235-246.
62. D.A. Israel, S. Salama, C.N. Arnold, S.F. Moss, T. Ando, H.-P. Wirth, K.T. Tham, M. Camorlinga, M.J. Blaser, S. Falkow, R.M. Peek, Jr. (2001) *Helicobacter pylori strain-specific differences in genetic content, identified by microarray, influence host inflammatory responses.* **J Clin Invest** 107(5): 611-620.
63. J.A. Imlay (2013) *The molecular mechanisms and physiological consequences of oxidative stress: Lessons from a model bacterium.* **Nat Rev Microbiol** 11(7): 443-454.
64. J.-P. Yuan, T. Li, X.-D. Shi, B.-Y. Hu, G.-Z. Yang, S.-Q. Tong, X.-K. Guo (2003) *Deletion of Helicobacter pylori vacuolating cytotoxin gene by introduction of directed mutagenesis.* **World J Gastroenterol** 9(10): 2251-2257.
65. D.F. Wyss (2003) *Structure-guided applications in drug discovery.* **Drug Discov Today** 8(20): 924-926.

3. Development of a novel BSL-2 rat model of mycobacterial lung infection and assessment of RNA modifications as urine biomarkers of infection

3.1. Introduction and motivation

Despite decades of research and billions of dollars in funding, tuberculosis (TB) remains a major global health problem [1]. The causative agent, *Mycobacterium tuberculosis* (Mtb), newly infects more than eight million and kills more than one million people each year, making it the second most deadly infectious disease [2]. Worldwide, the total number of people infected with Mtb is estimated to be over two billion, representing one-third of the global population [3]. More than 90% of these people harbor an asymptomatic and often undiagnosed latent infection, which can potentially reactivate and become infectious [4]. Additionally, drug resistance continues to grow rapidly, with new cases of multidrug-resistant (MDR) and extensively drug-resistant (XDR) infection diagnosed each year [5]. While it was traditionally held that acquired drug resistance resulted in impaired fitness and reduced transmissibility, recent evidence indicates that MDR and XDR strains commonly acquire compensatory mutations that allow them to retain full fitness [6]. Taken together, these findings highlight the pressing need for new therapeutics to fight Mtb.

The drug discovery process for Mtb is complex and difficult, as illustrated by the recent approval of the first novel TB therapy in over 40 years [7]. Much of this difficulty owes to the unique, broad set of interactions between Mtb and the host [8], and highlights the need to understand drug targets in the context of the host organism [9, 10]. As such, animal models are invaluable to the study of Mtb and to the development of novel drugs [11]. While a number of animal models of TB have been developed, many of them suffer from shortcomings that limit their utility. The diverse nature of tubercular disease in different animals means that most models fail to recapitulate the full spectrum of human disease. The mouse offers low cost and ease of use, but these animals fail to develop granulomas, which are a major barrier to effective Mtb treatment and are essential to model accurately [12]. Guinea pig and rabbit models both develop severe disease with well organized granulomas, but there is a noted lack of commercial immunological reagents available for these animals [13]. The nonhuman primate provides the

closest approximation to the human disease, but high cost and regulatory difficulties prevent its widespread use [14]. Encouragingly, several recent studies have illustrated the value of the Wistar rat model, which closely recapitulates human pathology, and combines low cost, ease of handling, and a well established role in drug development [15-19]. The comparative features of these various models are summarized in **Table 3-1**.

Model	Granulomas	MNGCs	Necrosis	Cavitation	Hypoxia	Control
Mouse	Not organized	Absent	Rare[a]	Absent	Absent	Absent
Guinea pig	Well organized	Present	Present	Absent	Present	Absent
Rabbit	Well organized	Present	Present	Present[c]	Present	Present[d]
Monkey	Well organized	Present	Present	Present	Present	Present
Wistar rat	*Organized*	*Present*	*Present[b]*	*Absent*	*Present*	*Present[e]*

Table 3-1: Comparison of tuberculosis pathology in animal models. This table summarizes the relevant immunological and pathological features of the major animal models of TB. The Wistar rat model described here is highlighted in the final row. MNGCs: multinucleated giant cells. [a] Only in C3HeB/Fej (lpr1-/-) hyper susceptible mice. [b] Only in higher inoculum infected animals following immune suppression. [c] With some Mtb clinical isolates such as HN878. [d] With some Mtb clinical isolates such as CDC1551. [e] In low inoculum infections. [f] Dose and Mtb strain dependent. Table adapted from [15].

Despite the attractive qualities of the Wistar rat model, its widespread adoption by academic and industrial laboratories is still hampered by the fact that Mtb must be handled in high containment biosafely level 3 (BSL-3) facilities. Such facilities are financially prohibitive to construct and operate [20, 21], and the number of BSL-3 facilities is relatively limited [22]. This problem is exacerbated by the fact that funding for Mtb research and drug development has recently been reduced [3], and by the increasing recognition that Mtb drug discovery, compound screening, and lead optimization needs to be done in animal models [11]. Given that one of the major hurdles to effective treatment is the difficulty of accessing the granuloma and delivering the drug to actively replicating bacteria [23], there is a need for an animal model of granuloma formation that is suitable for work in a BSL-2 facility and is appropriate for drug development studies. Given the ubiquity of the rat in pharmaceutical research and the recent success of the Wistar rat model of TB, we sought to develop a BSL-2 Wistar rat model of tubercular granuloma formation. Galvan *et al.* recently demonstrated the utility of a BSL-2 model using an attenuated strain of BSL-3 pneumonic plague [24], so we used *M. bovis* bacille Calmette-Guérin (BCG) Pasteur—a member of the Mtb complex with over 99.9% sequence identity to Mtb [25, 26]—as a BSL-2 surrogate for Mtb. We evaluated pulmonary infection in the

Wistar rat, tracking the kinetics of bacterial load, immune invasion, cytokine response, and histopathology for eight weeks. We then used this model in a proof-of-concept study to evaluate urine biomarkers of infection. Our results show that pulmonary BCG infection in the Wistar rat is potentially valuable as a model of granuloma formation, and could be useful for future drug and biomarker discovery studies.

3.2. Methods

3.2.1. Animals and husbandry conditions

All animal experiments were performed in facilities approved by the MIT Division of Comparative Medicine (DCM), under the guidance of trained veterinary and husbandry staff, and in accordance with all applicable institutional, state, and federal guidelines. All animals were ~6-week old outbred female Wistar rats (WI:crl, Charles River Laboratories North America). Two cohorts were used: the first contained 34 rats, and the second contained 14 rats. All animals were housed in pairs in ventilator cages, and were fed commercial food and sterile water *ad libitum*, except during fasting (described in more detail in Section **3.2.10**).

3.2.2. Bacterial strains and culture conditions

M. bovis BCG Pasteur was obtained from ATCC (#35734). Glycerol stocks were cultured at 37 °C in 50 ml volumes in 490 cm^2 roller bottles (Corning) in Middlebrook 7H9 media (BD) supplemented with BBL Middlebrook OADC (BD). Cultures were grown to mid-log phase (OD_{600}=0.6) and passaged twice prior to use. To prepare the inoculum, mid-log cultures were pelleted by centrifugation, washed once with PBS (BD), and passed through a 26 g syringe to eliminate clumps. The OD_{600} was measured and adjusted to ~$1x10^8$ bacteria in 1 ml. The inoculum content was confirmed by plating serial dilutions on Difco 7H10 agar (BD) with OADC and counting colony forming units (CFUs) after incubating at 37 °C for 3 weeks.

3.2.3. Endotracheal infection

An endotracheal inhalation infection method was used, as previously described elsewhere [15]. Briefly, rats were anesthetized with isofluorane and suspended by their incisors on a guide

string, which elevated the head and rotated the neck back. Forceps were used to gently pull out the tongue, and a 200 µl sterile pipet tip containing 100 µl of liquid (inoculum or PBS as a sham control) was inserted into the mouth with the tip positioned at the epiglottis. The contents of the pipet tip were dispensed and the rat's nostrils were immediately held to trigger the gasping reflex, which resulted in inhalation of the inoculum. For both cohorts, successful inoculation was confirmed by euthanizing four rats at 1 day post inoculation (as described in **Section 3.2.4.**), aseptically removing the lungs and spleen (as described in **Section 3.2.4.**), and processing them for CFU determination (as described in **Section 3.2.5.**). For the 14-animal cohort, no sham infection was used, and all rats were inoculated with BCG.

3.2.4. Necropsy and tissue collection

For the 34-animal cohort, at predefined time points (1, 2, 3, 4, and 8 weeks post inoculation), four BCG-dosed and two PBS-dosed rats were euthanized by CO_2 asphyxiation. Blood was collected by cardiac puncture and 500 µl aliquots were placed in serum separator tubes (BD), clotted for 10 min, placed on ice, and centrifuged at 8,000 x *g* for 10 min. Serum was then aliquotted and stored at -135 °C until further analysis. Pieces of liver and spleen (~50 mg) were aseptically removed and stored on dry ice. The remaining spleen was placed in sterile PBS and stored on ice until further analysis. The left lung was perfused with 10% PBS-buffered formalin and placed in a histology cassette for parafin embedding and histologic analysis. The right lung was coarsely cut, mixed, and distributed equally between four tubes, as follows: two tubes of sterile PBS on ice and two empty tubes on dry ice, which were then stored at -135 °C until analysis. For the 14-animal cohort, the 10 animals remaining after the day 1 cohort was sacrificed were euthanized at 8 weeks post infection, and the lungs were processed as described above and in **Section 3.2.5**.

3.2.5. CFU determination

Lung and spleen tissue samples were removed from PBS, blotted dry, and weighed. Samples were homogenized in 5 ml fresh sterile PBS using an immersion tissue grinder, then serially diluted and plated on 7H10 agar with OADC. Plates were incubated at 37 °C for 3 weeks and CFUs were counted.

3.2.6. qPCR

DNA was extracted from frozen lung tissue samples as described previously [27]. Samples were homogenized in 5 ml sterile PBS with 0.1% Triton X-100 (Sigma). The homogenate was pelleted by centrifuging at 3,000 x *g* for 10 min, and the bacterial pellet was decanted and resuspended in 1 ml Tris-EDTA. An aliquot of 0.25 ml of 70 °C phenol-chloroform-isoamyl alcohol (Amresco) was added, and the entire volume was transferred to a bead beating tube (MP Biomedicals Lysing Matrix B). Tubes were bead beat for 30 seconds, repeated four times with 30 seconds at 4 °C between each cycle. Cell debris was pelletted by centrifuging at 12,000 x *g* for 10 min, and 50 µl of 5 M NaCl was added to the supernatant. Phenol-chloroform-isoamyl alcohol extraction was repeated on this supernatant, and DNA was precipitated by adding an equal volume of isopropanol. The genomic DNA was ethanol washed, dried, and resuspended in 25 µl of water.

BCG DNA was detected by amplifying a 130 bp fragment from the 85B antigen that is unique to the Mtb complex. We used forward primer 5'-TCAGGGGATGGGGCCTAG-3', reverse primer 5'-GCTTGGGGATCTGCTGCGTA-3', and the dually labeled detector probe 5'-(FAM)-TCGAGTGACCCGGCATGGGAGCGT-3'-(TAMRA) [28], all purchased from IDT. The reaction was performed in a 20 µl volume containing 10 µl of Kapa Probe Fast Universal 2x qPCR Master Mix, 1 µl of primer/probe mix containing 0.5 µM each primer, 0.3 µM probe, 5 µl of DNA, and 4 µl of water. Samples were run on a Roche LC480 instrument using standard settings and 35 amplification cycles. All samples were analyzed in duplicate. A standard curve was constructed from genomic BCG DNA, assuming a genome size of 4.7 Mbp and an average base pair molecular weight of 650 Da (**Figure 3-S2**). The standard curve was used to determine the number of genome copies in each sample, assuming a ploidy value of 2 (**Table 3-S1**).

3.2.7. Flow cytometry

Lung tissue samples were removed from PBS, blotted dry, and cut into small pieces. An amount of tissue equivalent to ~50 µl was transferred to a pre-weighed tube and weighed again. An aliquot of 1 ml of 1 mg/ml collagenase D (Roche) in PBS was added to each tube, and the samples were incubated at 37 °C for 1 h. A single-cell suspension was made by mashing the lung tissue through a 40 µm cell strainer and washing with FACS buffer (PBS supplemented with 5% fetal bovine serum (Seradigm)). The single cell suspension was transferred to a 15 ml

tube and centrifuged at 600 x *g* for 10 min. The supernatant was decanted and the cell pellet was resuspended in 1 ml red blood cell lysis buffer (eBioscience). Tubes were agitated gently by hand for 1 min, and 5 ml of FACS buffer was added to halt the lysis. Tubes were centrifuged at 600 x *g* for 10 min. The supernatant was decanted, and the volume in each tube was measured. Two 50 µl cell aliquots were transferred to new tubes for staining, and two 10 µl aliquots were transferred to new tubes for isotype controls. Fc receptors were blocked by adding a 100 µl aliquot of purified anti-Rat CD32 (BD PharMingen) diluted 1:500 in FACS buffer to each staining tube and incubating the tubes at 4 °C for 30 min.

Two master staining mixes were made as follows. Mix 1 contained 1 µl of each of the following, diluted in FACS buffer to a total volume of 100 µl: PE anti-Rat granulocyte (BD PharMingen), APC anti-Rat CD3 (eBioscience), and PEcy7 anti-Rat CD11b/c (BD PharMingen). Mix 2 contained 1 µl of each of the following, diluted in FACS buffer to a total volume of 100 µl: PE anti-Rat macrophage (eBioscience), APC anti-Rat MHCII (BD PharMingen), and PEcy7 anti-Rat CD11b/c. A 50 µl aliquot of the appropriate master mix was added to each tube. Single color and unstained control tubes contained 50 µl of the appropriate isotype and 0.5 µl of the appropriate dye. Samples were vortexed and incubated at 4 °C for 20 min. After incubation, 1 ml of FACS buffer was added to each tube, and the samples were centrifuged at 600 x *g* for 5 min. The supernatant was removed and 250 µl of FACS buffer with 0.5 µl/ml Sytox Green (Life Technologies) was added to all the tubes, except the unstained and single color controls. The final volume for each tube was measured, and the samples were incubated at room temperature for 10 min prior to analysis. All samples were analyzed on a BD Accuri C6 flow cytometer operated according to the manufacturer's instructions.

3.2.8. Histopathology

Formalin fixed left lungs in histology cassettes were submitted to the MIT DCM staff for paraffin embedding. Sections of 5 µm were sliced and stained with hematoxylin and eosin to prepare slides. Slides were qualitatively analyzed by a veterinary pathologist that was blinded to the infection status of each animal. Complete results are shown in **Table 3-S2.**

3.2.9. Bioplex

Total protein was extracted from frozen lung tissue by homogenizing in tissue lysis buffer supplemented with protease and phosphatase inhibitors according to manufacturer's protocol (Bio-Rad). Protein content was measured with a commercial BCA assay (Thermo). Serum and tissue proteins were then analyzed with the Bio-Plex Pro Rat Cytokine 24-plex Assay Kit according to the manufacturer's instructions (Bio-Rad). Lung cytokines were normalized to total protein content measured by the BCA assay.

3.2.10. Urine collection and processing

For the 14-animal cohort, urine was collected weekly using standard metabolic cages fitted with a 0.2 mm polypropylene mesh screen (Industrial Netting) fitted under the grated floor to catch fecal particulates. Collections were conducted for 10 h with the animals fasting to further reduce contamination by food particulates. The urine collection tubes were suspended in coolers of dry ice and pre-chilled before rats were moved to the cages, which resulted in immediate freezing. Frozen urine samples were stored at -135 °C until further processing.

Upon first thaw, a cocktail of antioxidants and deaminase inhibitors was added to each urine sample, to the following final concentrations: 5 μg/ml coformycin (DTP/NCI Open Chemical Repository), 22 μg/ml butylated hydroxytoluene (Sigma), and 50 μg/ml tetrahydrouridine (EMD) [29]. Samples were then centrifuged at 3,700 x *g* for 10 min to pellet sediment, and the supernatant was aliquoted into new tubes. Given the observation that intact RNA can persist in urine [30, 31], 100 μl aliquots were subjected to nuclease digestion by incubating at 37 °C for 3 h with the following cocktail: 1.0 μl of 1 mg/ml coformycin, 0.5 μl of 100 mM butylated hydroxytoluene, 5.0 μl of 1 mg/ml tetrahydrouridine, 0.2 μl of 50 mM magnesium chloride, 0.5 μl of 1 M pH 7.9 Tris, 4.3 μl of 5 U/μl benzonase (Sigma), 2.1 μl of 0.1 U/μl phosphodiesterase I (Affymetrix), 0.3 μl of 17 U/μl alkaline phosphatase (Sigma). Enzymes were removed by passing through a 10 kDa molecular weight cutoff filter. Creatinine content of the processed urine was measured with a commercial assay kit (R&D Systems), with the results shown in **Table 3-S3**. Processed urine samples were stored at -135 °C until further analysis.

3.2.11. LC-MS/MS

Urine was analyzed using a Thermo Scientific Hypersil GOLD aQ reversed-phase column (150 x 2.1 mm, 3 μm particle size) with a flow rate of 0.3 ml/min at 36 °C. Solvent A was 8 mM ammonium acetate (Sigma) in deionized water (Millipore filtration system) and solvent B was acetonitrile (Sigma). The column was eluted with the following gradient of solvent B: 0–18 min, 0%; 18–23 min, 0–1%; 23–28 min, 1–6%; 28–30 min, 6%; 30–40 min, 6–100%; 40–50 min, 100%; 50–51 min, 100–0%; 51–60 min, 100%. The HPLC column was coupled to an Agilent 6410 Triple Quadrupole mass spectrometer with an electrospray ionization source, which was operated in positive ion mode with the first (Q1) and third (Q3) quadrupoles fixed to unit resolution. Instrument parameters were as follows: gas temperature, 350 °C; gas flow, 12 l/min; nebulizer pressure, 20 psi; capillary voltage, 3500 V. Neutral loss (NL) scanning experiments used a constant fragmentor voltage of 100 V and a constant collision energy of 10 V, and Q3 was set to monitor for ions that lost a mass of 132 or 146 Da. This mass loss corresponds to the characteristic fragmentation of the glycosidic bond to form a neutral sugar moiety (132 Da for ribose, 146 Da for 2'-O-methylribose) and a charged base fragment [32]. Multiple reaction monitoring (MRM) experiments used predetermined, optimized parameters reported by others in our group. The limit of detection (LOD) for the various mass spectral techniques used was determined by injecting 1, 10, and 100 total fmol of a ribonucleoside standard in a urine matrix and comparing the resulting plot to a blank injection to determine the signal to noise ratio. The LOD for NL scanning was >100 fmol and the LOD for MRM was ~1 fmol. Putative ribonucleosides identified in urine were confirmed by comparing retention time and fragmentation pattern to commercial standards (**Figure 3-S6**). To control for difference in instrument response between samples, signal intensities for all species were normalized to the signal intensity for the nucleoside analogue coformycin, which was added to all samples at the same final concentration. To control for differences in urine concentration, signal intensities for all species were normalized by creatinine concentration.

3.2.12. Data analysis

Mass spectrometer data were analyzed with MassHunter Qualitative Analysis (Agilent). Basic graphing was performed with Microsoft Excel. Principal component analysis was performed with Multibase (Numerical Dynamics). Cytokine data were analyzed with Prism (GraphPad).

3.3. Results

3.3.1. Infection is efficient and sustained

We first sought to determine if BCG could successfully infect rat lungs. Twenty-four 6-week old outbred female Wistar rats were dosed endotracheally with a high dose bolus of ~$1x10^8$ CFUs of BCG. An additional 10 rats were dosed with sterile PBS as a sham control. Four rats were sacrificed on day 1 after dosing to confirm infection (**Figure 3-S1**), and the bacterial load was tracked over time. A combination of direct and indirect methods was used to confirm infection: enumeration of CFUs after plating lung homogenate, qPCR of lung DNA extracts with a probe targeted to the 85B antigen unique to the Mtb complex, and presence of elevated pathology in blindly evaluated lung tissue (described in more detail in **Section 3.3.4.**). Recognizing CFU enumeration as the "gold standard", and aiming to guard against false positive qPCR signals and adventitious inflammation unrelated to BCG treatment, we considered rats without detectable CFUs as infected only if both qPCR and pathology results were positive (**Table 3-S1**). A single rat met these criteria, which is consistent with previous reports that the degree of pathology and the CFU burden can be negatively correlated, with greater pathology associated with more robust clearance [33]. A total of 21 of the 24 BCG-dosed rats developed an infection, giving a success rate of 87.5% (**Table 3-2**). We attribute the three failed infections to operator error, as it is possible to trigger the rat's gag reflex and cause ingestion rather than aspiration.

Cohort	Dosed	Infected	Uninfected	Success
Day 1	4	4	0	100%
Week 1	4	3	1	75%
Week 2	4	3	1	75%
Week 3	4	4	0	75%
Week 4	4	4	0	100%
Week 8	4	3	1	75%
Total	**24**	**21**	**3**	**87.5%**

Table 3-2: Summary of infection success rate at each time point. Animals were considered infected if there were CFU counts in the lung or spleen, or if there was both lung inflammation and a positive qPCR signal for the mycobacterial-specific 85B antigen.

Given the observation that qPCR-based bacterial enumeration can diverge rapidly from CFU counts [27], we used only CFUs to track the kinetics of the infection over time. Because severe

Mtb infection is known to lead to bacterial dissemination [14, 34], we also tracked CFU values in the spleen at all time points. At 1 day post infection, the entire inoculum of ~$1x10^8$ CFU was recovered from the lungs of three out of four rats, indicating highly efficient infection. Additionally, two out of four rats had ~$1x10^3$ CFU in the spleen, indicating rapid, early bacterial dissemination (**Figure 3-S1**). After an initial 2-log decrease in the lungs at week 1 (assuming a total lung weight of 1000 mg [35]), the CFU count held relatively stable from weeks 2 through 4, finally dropping another log at the final week 8 time point (**Figure 3-1**). An increase in CFUs, representing bacterial growth, was observed only between weeks 2 and 3. BCG is known to be able to replicate inside rat alveolar macrophages [36], so we attribute the lack of growth at earlier time points to the high burden of infection, which is above what is typically seen at peak infection in animal models [14, 15, 37]. The bacterial load stayed well above the limit of detection during infection, indicating that clearance from the lungs is fairly slow. In contrast, spleen CFUs were detected only infrequently (nine out of 24 rats) and at low levels, indicating that bacteria are rapidly eliminated after initial dissemination. This observation also suggests that the infection is primarily restricted to the lungs, which is supported by the fact that no gross behavioral or morphological changes were seen in any rats at any time points. These data indicate that BCG is capable of establishing a sustained pulmonary infection in the Wistar rat.

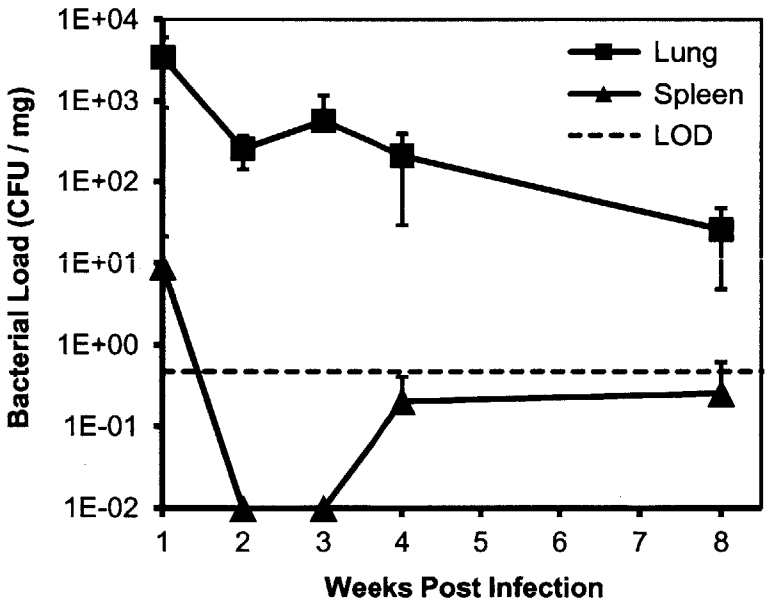

Figure 3-1: Kinetics of bacterial load in lung and spleen. The number of *M. bovis* BCG colony forming units (CFU) was determined at each time point in both lungs and spleen. Values are mean ± SD for four rats at each time point. The mean limit of detection (LOD) was 1 CFU per 2.2 mg of tissue.

3.3.2. Immune infiltration peaks late after infection

The manifestation of TB is the result of a complex interplay between Mtb and the host immune system [38, 39]. To determine the effect of BCG infection on the Wistar rat immune response, we used flow cytometry to measure four cell types that have been implicated in Mtb infection. Granulocytes, which primarily include neutrophils, have been shown to mediate control of BCG lung infection in mice [40]. $CD3^+$ cells are T lymphocytes, which are a major component of human Mtb granulomas [41]. $MHCII^+$ cells are activated professional antigen presenting cells (APCs), including macrophages and dendritic cells, which are responsible for driving the T_H1 immune response to bacterial infection [42, 43]. Finally, $CD11bc^+MHCII^+$ are APCs specifically derived from the lung tissue, as CD11b and CD11c bind integrin proteins and are responsible for immune cell migration from the bloodstream to the tissue [43, 44]. All four cell types were measured at weeks 1 through 4, except for granulocytes, which could not be measured at weeks 1 or 2 due to technical difficulties. Similarly, no measurements were taken at week 8 due to operator error. Despite these limitations, we observed significant increases in all cell types except granulocytes at week 3, and significant increases in all cell types at week 4 (**Figure 3-2**). These results reveal the slow pace of the immune response, which is consistent with observations from Mtb infection, where T cell migration routinely takes more than 2 weeks [44].

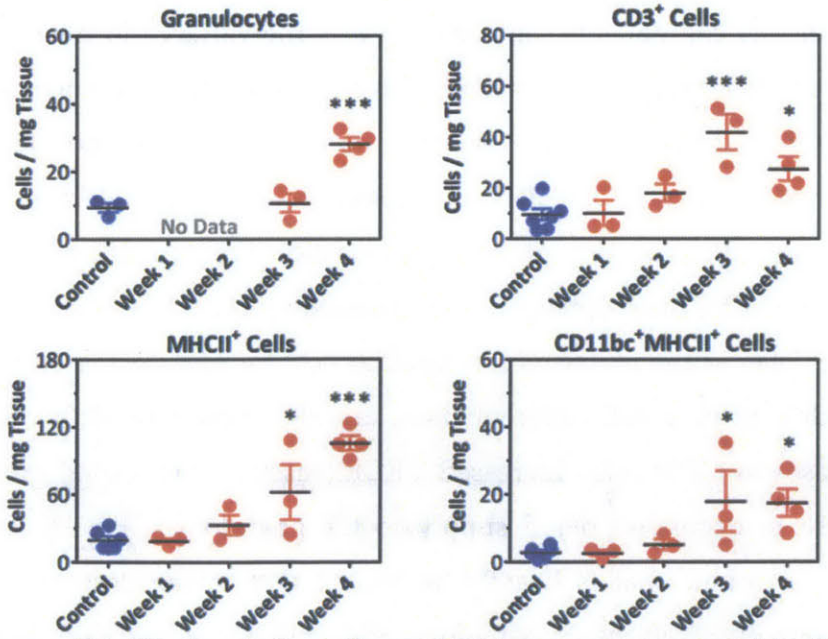

Figure 3-2: Immune cell infiltration in lung tissue. Cell types were measured by flow cytometry of a single-cell suspension from lung. The control group contains uninfected animals from all time points. Granulocytes were not measured at week 1 or 2 due to technical difficulties. * $p<0.05$, *** $p<0.001$.

3.3.3. Cytokine response peaks late after infection

To further elucidate the nature of the immune response in our model, we evaluated a panel of 23 cytokines and chemokines using a commercial multiplexed, bead-based, fluorescent antibody detection kit. We quantified cytokines in both lung tissue and serum samples at all time points. Surprisingly, despite the confined nature of the infection, the profiles for all cytokines were qualitatively similar for the serum and tissue samples (**Figures 3-S3** and **3-S4**, respectively). We attribute this finding to the highly vascular nature of the lungs, which can be 20% blood by weight even after complete exsanguination [35, 45, 46]. Principal component analysis (PCA)—a multivariate statistical method that can reveal hidden correlations between multiple interactions—was applied to the cytokine data in an attempt to highlight important pathways, but this was uninformative (**Figure 3-S5**). We then looked to the literature, which consistently described a significant delay (>2 weeks) in the onset of significant cytokine response during Mtb infection [38, 44, 47]. This observation was consistent with our own results showing that immune infiltration into the lungs was not significantly elevated until week 3 after infection. Reasoning that the cytokine response would similarly peak late, we applied PCA to the cytokine measurements at weeks 4 and 8 post-infection, which revealed good separation by infection status in the serum cytokines (though not in the tissue cytokines) (**Figure 3-3**).

The first two principal components captured ~84% of the variance in the samples, indicating that a relatively small subset of the cytokines drives most of the difference. By examining the loadings plot, we can identify cytokines strongly associated with the infected and uninfected rats. Doing so reveals several associations consistent with our understanding of the Mtb immune response and the process of granuloma formation. For example, infected animals show increased levels of M-CSF (macrophage colony stimulating factor), consistent with the key role that macrophages play as the preferred intracellular host for Mtb. Increased levels of RANTES and IL-2, both drivers of T cell differentiation, are also consistent with our observation of significant increases in $CD3^+$ cells. Increased VEGF (vascular endothelial growth factor) may reflect a response to decreased blood supply to the granulomas. Finally, IL-17 is a potent proimflammatory cytokine that is heavily associated with tissue destruction [48], which is consistent with our observations of pathology and epithelial disruption (described in more detail in **Section 3.3.4.**). In contrast, uninfected animals show decreased levels of IFN-γ,

consistent with the key role that it plays in mediating the response to Mtb [44]. Reduced levels of G-CSF (granulocyte colony stimulating factor) may reflect the ability of granulocytes to act as facilitative hosts for Mtb infection [44], while reduced levels of proinflammatory IL-1α and IL-18 are consistent with the generalized lung pathology we see. Finally, reduced levels of IL-4, which stimulates APCs, likely reflect the significant increase in MHCII$^+$ cells in the lungs. Taken together, these data are consistent with our current understanding of the immune response to Mtb infection [38, 44], and indicate that the BCG model accurately recapitulates the delayed immune response and inflammatory environment seen in TB.

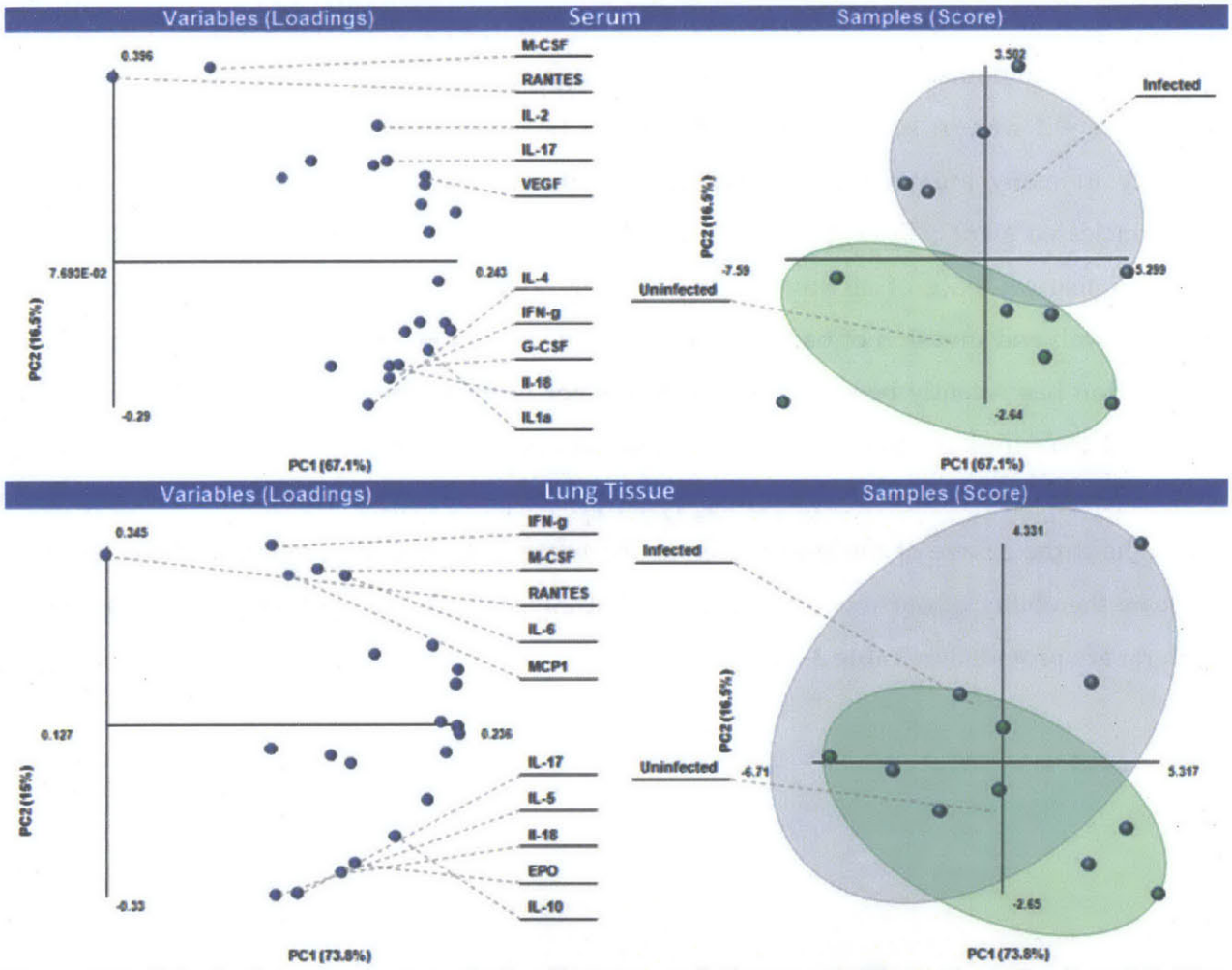

Figure 3-3: Principal component analysis of serum and tissue cytokines at weeks 4 and 8. The loadings plot shows the 10 cytokines with the highest contribution to the variance seen in the score plot, showing specific associations with both uninfected and infected rats. Data were mean-centered and SD normalized prior to calculation, and the one rat that was dosed but not infected was excluded.

3.3.4. Pathology is prominent throughout infection

One of the hallmarks of Mtb infection, as well as one of the most significant barriers to effective treatment, is the development of highly organized granulomas [11, 12, 23, 39, 49]. Previous work with the Wistar rat infected with virulent Mtb revealed the formation of well organized granulomas that were structurally similar to those seen in human disease [15, 18]. To determine if BCG infection produced similar features, we subjected formalin-fixed slices of the whole left lung for histopathological evaluation by a blinded veterinary pathologist. The results showed that BCG rapidly induces widespread, prominent pathology, with several features that are characteristic of human TB (**Figure 3-4**). Of particular importance is the rapid formation of coalescing granulomas, which show the beginnings of structure as early as week 1. Many of these are >0.1 mm in size (**Figure 3-4A**), which has been used as an empirical indicator of severity in many animal models [44]. Granulomas frequently contained large numbers of multinucleated giant cells (**Figure 3-4B**), which are a classic marker of Mtb infection [8, 12, 38]. There is also evidence of airway impingement by granulomas, as well as destruction of the alveolar wall and invasion of bacteria into the air space of the lungs (**Figure 3-4C**). Such tissue destruction has recently been implicated as a major factor in Mtb virulence and pathogenesis [50], and may indicate that our model is also amenable to transmission studies. Qualitative evaluation of all rats also revealed that the degree of pathology is maintained at a high level throughout the course of the study, even as the bacterial burden drops (**Figure 3-5**). This may indicate the ability of our model to form a latent infection. The full pathology descriptions for each rat are provided in **Table 3-S2**.

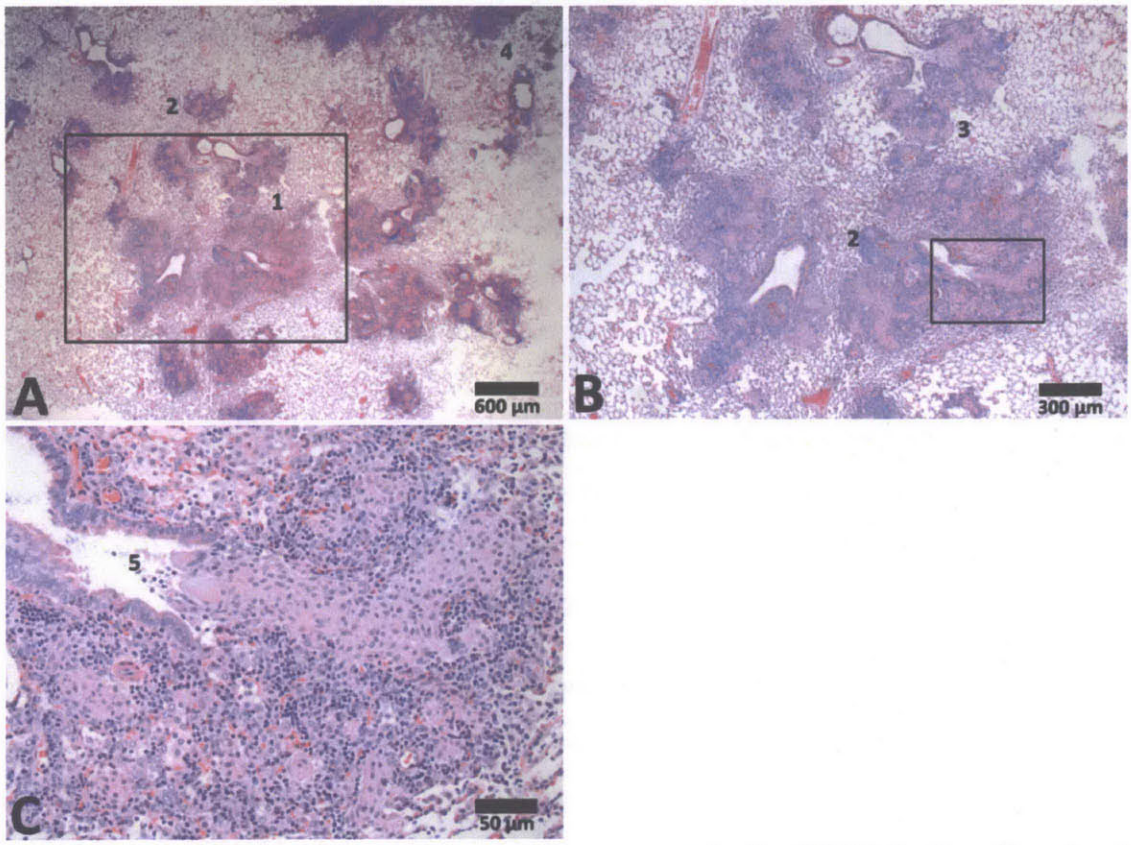

Figure 3-4: Histopathologic micrographs of rat lung one week after BCG infection. Hematoxylin and eosin stained sections of the left lung from a single animal. **A:** 2x magnification. **B:** 4x magnification of the region outlined in A. **C:** 20x magnification of the region highlighted in B. Key pathological features are labeled as follows: 1) large regions of inflammation with increased cellularity; 2) coalescing granulomas of lymphocytes, macrophages, and mutlinucleated giant cells; 3) peribronchiolar localization of granulomas; 4) scattered smaller granulomas throughout the parenchyma; 5) attenuation of bronchiolar epithelium by impinging granulomas.

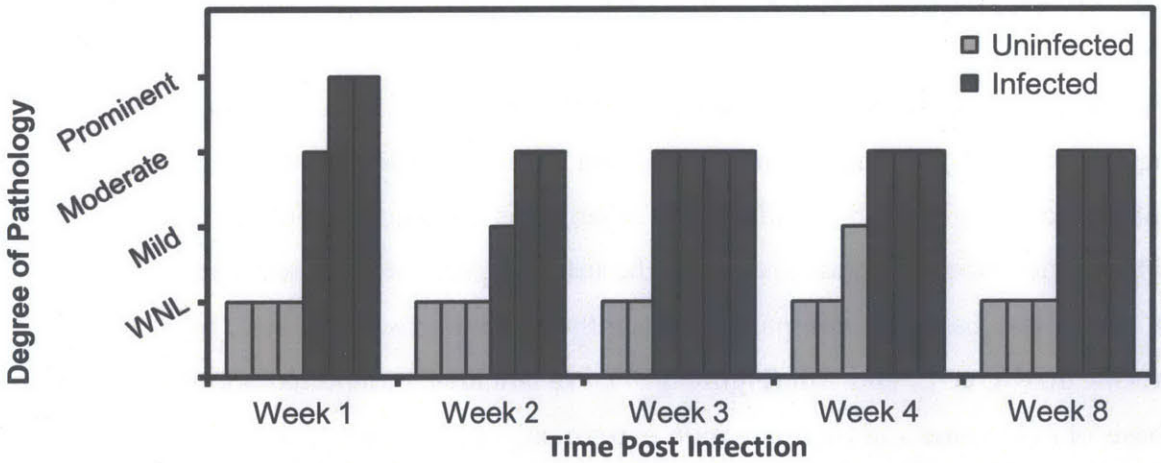

Figure 3-5: Summary of lung pathology by time. The overall degree of lung pathology for each animal was qualitatively evaluated by a blinded pathologist after examining hematoxylin and eosin stained sections of the whole left lung. Each bar represents one animal.

3.3.5. Urine ribonucleoside profile does not correlate with infection

Having established the BCG-infected rat model as an accurate reflection of granuloma formation and Mtb-related inflammation and lung pathology, we next sought to use the model in a proof-of-concept biomarker study. Worldwide efforts aimed at TB control are still hampered by the lack of effective, sensitive, rapid diagnostics for Mtb infection [3, 4, 6, 51]. Given the longstanding knowledge that modified ribonucleosides are excreted in urine rather than recycled by nucleoside salvage pathways [32, 52, 53], as well as the observation that members of the Mtb complex harbor RNA modifications not found in other organisms [54], we hypothesized that BCG-specific ribonucleosides in the urine of infected rats could be detected and quantified by liquid chromatography-coupled tandem mass spectrometry (LC-MS/MS) [29, 55-57], and that such modifications could be used as biomarkers of infection.

For this study, 14 6-week old outbred female Wistar rats were dosed endotracheally with ~$1x10^8$ CFUs of BCG. Urine was collected from all rats before dosing and was used as the uninfected control. After sacrificing four rats on day 1 and plating lung homogenates to confirm infection, urine was collected from the remaining 10 rats at weeks 1, 3, 5, and 7. All rats were then sacrificed and lung homogenates were plated to confirm infection, which revealed six of the 10 rats had BCG CFUs in the lungs (**Figure 3-S6**). Because only half the rats had detectable CFUs at day 1, we assumed that the rats without detectable CFUs at the end were not infected. We then limited our analysis to the six rats with confirmed infections and detectable CFUs, with pre-infection urine from each corresponding animal as the negative control.

We began with a semi-targeted approach to identify putative ribonucleosides in the urine by using neutral loss (NL) scanning, which identified ribonucleosides based on the characteristic fragmentation of the glycosidic bond [32, 55]. Using this approach, we identified a total of 32 potential modified ribonucleoside species in the urine (**Figure 3-6**). We were able to positively identify 11 of these based on comparison to synthetic standards: m^5C, m^3C, m^1A, m^2A, m^7G, m^2G, $m^2{}_2G$, Cm, t^6A, ac^4C, and Am (**Figure 3-S7**). We tentatively identified another two species on the basis of m/z value and fragmentation pattern only: $m^{2,2,7}G$ and $m^6{}_2Am$. The remaining 20 species did not correspond to any known ribonucleosides [58-60]. However, none of the 32 species detected were unique to either uninfected or infected urine, ruling them out as potential pathogen-specific biomarkers. Given the relative insensitivity and high limit of detection of the

neutral loss method, we then employed a targeted approach using multiple reaction monitoring to detect modified ribonucleosides known to exist in BCG but not in the rat (19 species in total, based on our own previous and unpublished data). This method also failed to identify any BCG-specific ribonucleosides in the urine of any rats.

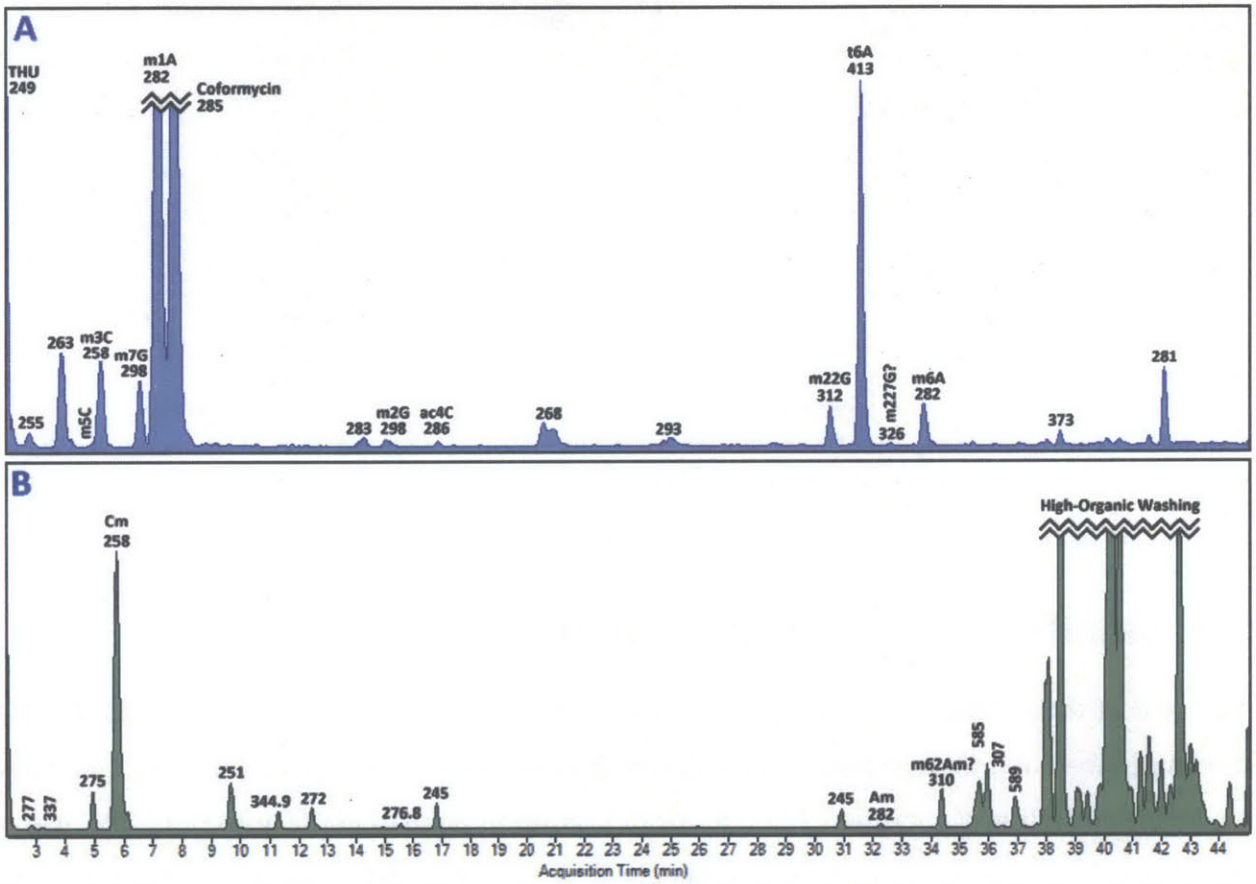

Figure 3-6: Representative neutral loss chromatograms for infected rat urine. Numbers indicate the m/z value for the parent ion. Identities were confirmed by comparison to synthetic standards, unless noted with a question mark, in which case identities are putative based only on m/z value and fragmentation pattern. Species without an identity do not match any known modifications. A total of 32 putative species were discovered, with 11 confirmed and two tentatively identified. The y-axis in both plots is arbitrary and relatively scaled to the same maximum. High intensity peaks are truncated for better visibility. **A**: Loss of 132 Da corresponding to ribose. **B**: Loss of 146 corresponding to 2'-O-methylribose.

As a final test of the urine biomarker hypothesis, we quantified the levels of eight of the 11 confirmed species (m^5C, m^3C, m^1A, m^2A, m^7G, m^2G, $m^2{}_2G$, Cm) in both pre- and post-infection urine. We excluded three species (t^6A, ac^4C, Am) because they were frequently absent from the urine, though without any pattern to their absence. To account for differences in urine concentration, we used the Jaffe method to measure creatinine concentration (**Table 3-S3**) and normalized ribonucleoside abundances accordingly (**Table 3-S4**). We used PCA to determine if

any species correlated with infection status, which revealed no separation (**Figure 3-7**). Overall, our results do not support the utility of modified ribonucleosides as biomarkers of infection.

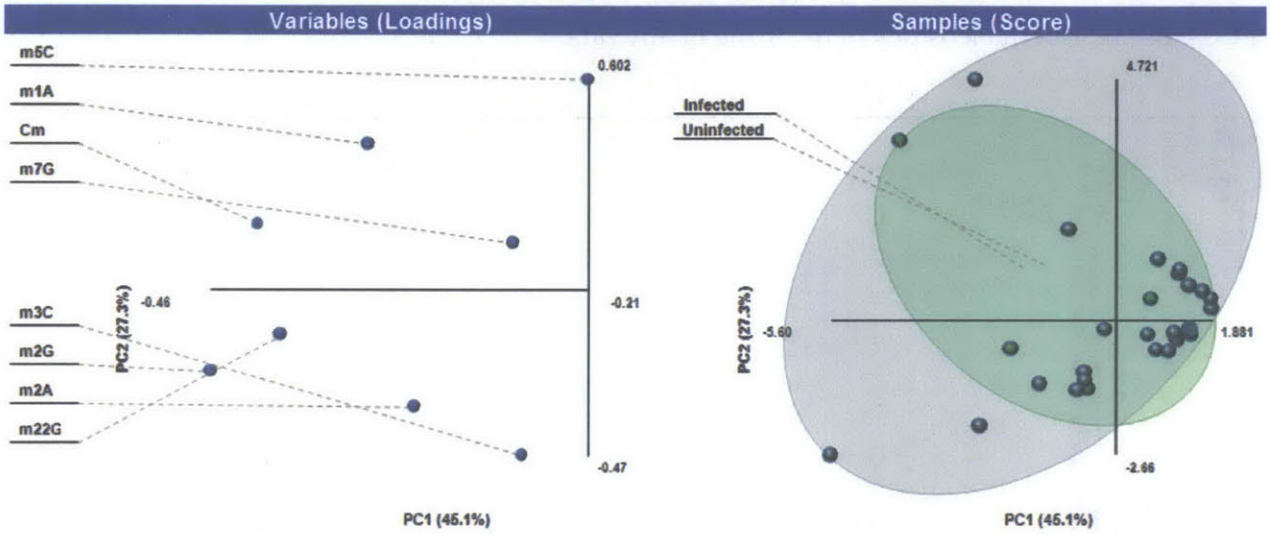

Figure 3-7: Principal component analysis of confirmed ribonucleosides. Normalized abundances for eight ribonucleosides that were confirmed and found in all samples were analyzed at 1, 3, 5, and 7 weeks post-infection. Pre-infection urine was the negative control. No correlation between infection status and modification pattern was seen. Data were mean-centered and normalized prior to calculation.

3.4. Significance and future directions

The goal of these studies was two-fold: to evalute BCG infection in the Wistar rat as a BSL-2 model of tubercular disease that is amenable to drug delivery studies, and to use that model to evaluate the utility of modified ribonucleosides as urine biomarkers of infection. The use of BSL-2 members of the Mtb complex as models for TB is well established in the literature, and previous studies have demonstrated development of disease and formation of granulomas in mice [40, 61-63], rats [43, 64], zebrafish [41, 65], and pigs [66]. However, all of these models have significant shortcomings when compared to our study, as described below.

Most mouse models of tuberculosis, including those using BCG, fail to form organized granulomas (excluding humanized mice and the recently developed C3HeB/Fej strain). One possible explanation for this deficiency is that mice lack matrix metalloproteinase 1 (MMP-1), which has recently been implicated in tissue destruction and granuloma formation in human TB [50, 67, 68]. In contrast, Wistar rats are known to express MMP-1 [69], which may explain our observation of organized granulomas and alveolar wall destruction (**Figure 3-4C**). Previous rat models of BCG infection have relied on systemic infection and granuloma formation in several

organs, and do not recapitulate the key features of lung pathology. Zebrafish develop severe disease and well organized, caseous granulomas after exposure to *M. marinum*, but their immunologic response appears to differ significantly from that in mammals. In particular, the zebrafish model lacks widespread infiltration of lymphocytes, which are a key feature of human TB [44]. In contrast, our rat model shows a significant increase in lymphocytes at both weeks 3 and 4 (as determined by flow cytometry), as well as granulomas containing large numbers of lymphocytes (as determined by histological examination). Additionally, comparative genomics reveals that *M. marinum* differs significantly from Mtb, sharing only 85% sequence identity and lacking orthologues of many genes required for mammalian lung colonization and transmission. Finally, Bolin *et al.* demonstrated many years ago that BCG infection in swine provides an excellent model for both pulmonary and disseminated tuberculosis, but these animals' large size and difficult handling requirements preclude their widespread use in standard laboratories. Here we describe pulmonary BCG infection in the Wistar rat, and note that it combines easy handling with sustained lung infection and defined granuloma formation.

Our findings shed more light on the complicated process of granuloma formation. In particular, it is interesting to note that BCG induces granuloma formation despite lacking ESAT-6 (6-kDa early secretory antigenic target) [70], which has been implicated in disease progression and granuloma formation [49, 71]. As noted above, mice fail to develop granulomas even in the presence of ESAT-6, indicating the importance of interplay between pathogen and host factors. Our data suggest that ESAT-6 is not essential for organized granuloma formation, and further support the importance of MMP-1.

In a proof-of-concept study, we were unable to establish any modified ribonucleosides as urine biomarkers of infection. We attribute our inability to detect modifications unique to infected urine to insufficient sensitivity. For example, if there were a BCG-specific modification that occurred at only one location on only one tRNA isoacceptor (such as is the case for the bacterial modification lysidine [72]), that modification would be present in our urine samples at a concentration of roughly 300 aM (based on a 3,000 CFU reduction per week as seen between weeks 1 and 2, and assuming there are 375,000 tRNAs per bacterial cell [73]). This is several orders of magnitude below the limit of detection for our LC-MS/MS methods, but as analytical techniques become more sophisticated, this concentration may fall within the bounds of reality,

so the method can be revisited as necessary. For example, recent advances combining nanoflow chromatography with high resolution ion trap mass spectrometers has enabled neutral loss scanning of nucleosides with single-digit-femtomolar sensitivity [74]. We attribute our inability to correlate patterns of excreted modifications with infection status to the overwhelming influence of variability between individual animals, which has long been observed as a significant hurdle to the development of effective urine biomarkers [32, 52, 75, 76].

As with any study, particularly when developing a new animal model, there are some limitations that must be addressed. While our model maintained a high burden of infection throughout our study, we did not extend our studies past the 8 week time point, so we do not know how long the infection would be sustained. One of the key features of the Wistar rat Mtb model was that it maintained detectable CFUs past 38 weeks, making it a potential model for latency. We also evaluated only a single high dose inoculum, and several studies in the rat have revealed divergent pathologies based on the size of the inoculum. Finally, we did not evaluate the oxygen tension or hypoxic status of the granulomas, which was another key feature of the Wistar model. Overall, these limitations do not detract from the utility of our model, but instead provide guidance for further studies.

Moving forward, we intend to complete characterization of the model using a variety of parameters. We have undertaken immunohistochemistry to visualize CD3, MPO, and iNOS, which will reveal T cells, neutrophils, and macrophages, respectively. These results will allow us to determine the detailed structure of the granulomas, which will reveal the degree to which they recapitulate human disease, and strengthen the model as a drug development platform. We are also exploring collagen staining as a way to highlight tissue destruction and support our proposed involvement of MMP-1. Finally, we have undertaken acid-fast staining and the use of morphometric software to evaluate the extent of granuloma formation and the partitioning of the bacterial burden between granulomas and more diffuse inflammation [77]. These studies will provide a robust description of pulmonary BCG infection in the Wistar rat, which we believe will be a valuable model for future tuberculosis research.

3.5. Supplementary material

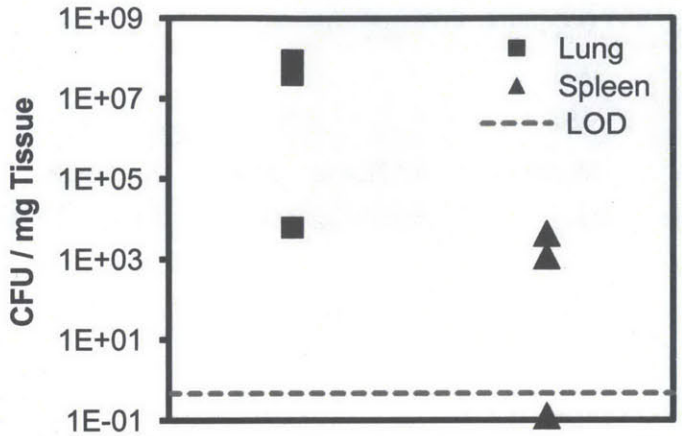

Figure 3-S1: Day 1 necropsy CFU counts. Four dosed rats were sacrificed 1 day after infection to confirm successful dosing. Homogenates of both lung and spleen were plated. Nearly the full inoculum (~1x10^8 CFU) was recovered from three of four lungs, while two of four rats had dissemination to spleen.

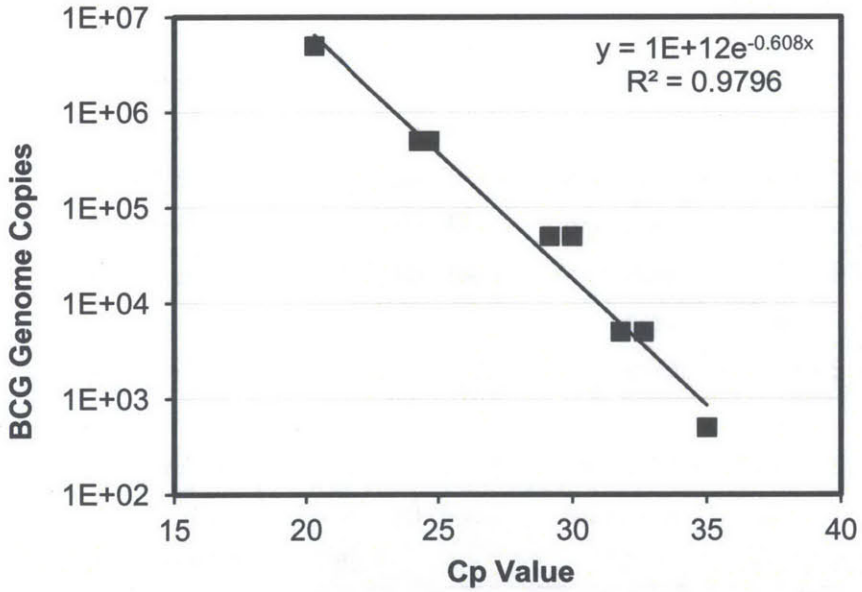

Figure 3-S2: qPCR calibration curve. BCG genomic DNA corresponding to 5x10^6, 5x10^5, 5x10^4, 5x10^3, and 5x10^2 genome copies was analyzed in duplicate using a probe for the mycobacterial 85B antigen.

Animal	Cohort	Dosed	Pathology	CFU/mg	Cp	CEQ/mg	Notes	Status
A.0	Week 1	No	WNL					Uninfected
A.1	Week 1	No	WNL					Uninfected
1.0	Week 1	Yes	WNL		35	4.64E+01	Max Cp	Uninfected
1.1	Week 1	Yes	Prominent	3.15E+02				Infected

Animal	Cohort	Dosed	Pathology	CFU/mg	Cp	CEQ/mg	Notes	Status
2.0	Week 1	Yes	Prominent	6.65E+03				Infected
2.1	Week 1	Yes	Moderate	3.28E+03	29.6	1.79E+03		Infected
B.0	Week 2	No	WNL					Uninfected
B.1	Week 2	No	WNL					Uninfected
3.0	Week 2	Yes	Moderate	4.12E+02	31.475	3.40E+02		Infected
3.1	Week 2	Yes	Mild	1.74E+02	35	2.03E+02	Max Cp	Infected
4.0	Week 2	Yes	WNL		35	2.25E+01	Max Cp	Uninfected
4.1	Week 2	Yes	Moderate	1.73E+02	34.46	1.15E+02		Infected
C.0	Week 3	No	WNL					Uninfected
C.1	Week 3	No	WNL		35	4.10E+01	Max Cp	Uninfected
5.0	Week 3	Yes	Moderate	1.42E+03	21.665	2.23E+05		Infected
5.1	Week 3	Yes	Moderate	9.60E+01	30.51	1.13E+03		Infected
6.0	Week 3	Yes	Moderate		35	6.48E+01	Max Cp	Infected
6.1	Week 3	Yes	Moderate	1.66E+02	33.055	2.78E+02		Infected
D.0	Week 4	No	WNL					Uninfected
D.1	Week 4	No	WNL		33.825	1.98E+02		Uninfected
7.0	Week 4	Yes	Mild	2.10E+01	35	5.12E+01	Max Cp	Infected
7.1	Week 4	Yes	Moderate	2.49E+02	29.645	5.31E+03		Infected
8.0	Week 4	Yes	Moderate	4.84E+02	27.925	2.32E+03		Infected
8.1	Week 4	Yes	Moderate	8.04E+01	35	1.19E+02	Max Cp	Infected
E.0	Week 8	No	WNL					Uninfected
E.1	Week 8	No	WNL					Uninfected
9.0	Week 8	Yes	Moderate	5.57E+01				Infected
9.1	Week 8	Yes	Moderate	8.33E+00	23.565	1.69E+04		Infected
10.0	Week 8	Yes	Moderate	1.38E+01	27.535	2.10E+03		Infected
10.1	Week 8	Yes	WNL		35	1.76E+01	Max Cp	Uninfected

Table 3-S1: Summary of qPCR and CFU results. Dosing status, pathology, CFU counts, qPCR results, and final status (infected or uninfected) are shown for each animal. WNL: within normal limits. CEQ: chromosomal equivalent units, assuming a ploidy value of 2 [27]. Max Cp indicates uncertainty in the qPCR result, as the value returned was at or below the concentration of the lowest standard.

Animal	Cohort	Status	Pathology	Description
A.0	Week 1	Uninfected	WNL	Small number of small perivascular accumulations of lymphocytes; normal for rat
A.1	Week 1	Uninfected	WNL	Small number of small perivascular accumulations of lymphocytes; normal for rat
1.0	Week 1	Uninfected	WNL	Moderate number of peribronchiolar aggregates of

Animal	Cohort	Status	Pathology	Description
				predominantly lymphocytes with occasional macrophages – these are not granulomas though
1.1	Week 1	Infected	Prominent	Marked increase in cellularity due to inflammation that comprises coalescing granulomas (consisting of a mixture of epthelioid macrophages and lymphocytes – and often with a peribronchiolar location) that produce a large region of inflammation, with scattered smaller granuloma elsewhere throughout the parenchyma
2.0	Week 1	Infected	Prominent	Marked increase in cellularity due to inflammation that comprises coalescing granulomas (consisting of a mixture of epthelioid macrophages and lymphocytes – and often with a peribronchiolar location) that produce multiple larger regions of inflammation, with scattered smaller granulomas elsewhere throughout the parenchyma; mild attenuation of bronchiolar epithelium in regions where granulomas impinge on them; also there are very large peribronchiolar lymphocyte aggregates that distort the airways – much larger than what would be considered WNL for a rat.
2.1	Week 1	Infected	Moderate	Moderate increase in cellularity due to inflammation that comprises coalescing granulomas (consisting of a mixture of epthelioid macrophages and lymphocytes – and often with a peribronchiolar location) that produce scattered small to moderately sized granulomas throughout the parenchyma
B.0	Week 2	Uninfected	WNL	Small number of small perivascular accumulations of lymphocytes; normal for rat
B.1	Week 2	Uninfected	WNL	Small number of small perivascular accumulations of lymphocytes; normal for rat
3.0	Week 2	Infected	Moderate	Moderate increase in cellularity due to inflammation that comprises coalescing granulomas (consisting of a mixture of epthelioid macrophages and lymphocytes – and often with a peribronchiolar location) that produce scattered small to moderately sized granulomas throughout the parenchyma; mild attenuation of bronchiolar epithelium in regions where granulomas impinge on them
3.1	Week 2	Infected	Mild	Mild increase in cellularity due to inflammation that comprises coalescing granulomas (consisting of a mixture of epthelioid macrophages and lymphocytes – and often with a peribronchiolar location) that produce scattered small granulomas throughout the parenchyma; mild attenuation of bronchiolar epithelium in regions where granulomas impinge on them
4.0	Week 2	Uninfected	WNL	WNL
4.1	Week 2	Infected	Moderate	Moderate increase in cellularity due to inflammation that comprises coalescing granulomas (consisting of a mixture of epthelioid macrophages and lymphocytes and multinucleated giant cells – and often with a peribronchiolar location) that produce

Animal	Cohort	Status	Pathology	Description
				scattered small to moderately sized granulomas throughout the parenchyma; mild attenuation of bronchiolar epithelium in regions where granulomas impinge on them
C.0	Week 3	Uninfected	WNL	Small number of small perivascular accumulations of lymphocytes; normal for rat
C.1	Week 3	Uninfected	WNL	Small number of small perivascular accumulations of lymphocytes; normal for rat
5.0	Week 3	Infected	Moderate	Moderate increase in cellularity due to inflammation that comprises coalescing granulomas (consisting of a mixture of epthelioid macrophages and lymphocytes and multinucleated giant cells – and often with a peribronchiolar location) that produce scattered small to moderately sized granulomas throughout the parenchyma; mild attenuation of bronchiolar epithelium in regions where granulomas impinge on them; also a couple of peribronchiolar lymphocyte aggregates that are much larger than what is WNL
5.1	Week 3	Infected	Moderate	Moderate increase in cellularity due to inflammation that comprises coalescing granulomas (consisting of a mixture of epthelioid macrophages and lymphocytes – and often with a peribronchiolar location) that produce scattered small to moderately sized granulomas throughout the parenchyma; mild attenuation of bronchiolar epithelium in regions where granulomas impinge on them; larger than normal peribronchiolar lymphocyte aggregates
6.0	Week 3	Infected	Moderate	Moderate increase in cellularity due to inflammation that comprises coalescing granulomas (consisting of a mixture of epthelioid macrophages and lymphocytes and multinucleated giant cells – and often with a peribronchiolar location) that produce scattered small to moderately sized granulomas throughout the parenchyma; mild attenuation of bronchiolar epithelium in regions where granulomas impinge on them; larger than normal peribronchiolar lymphocyte aggregates
6.1	Week 3	Infected	Moderate	Moderate increase in cellularity due to inflammation that comprises coalescing granulomas (consisting of a mixture of epthelioid macrophages and lymphocytes and multinucleated giant cells – and often with a peribronchiolar location) that produce scattered small to moderately sized granulomas throughout the parenchyma; mild attenuation of bronchiolar epithelium in regions where granulomas impinge on them; larger than normal peribronchiolar lymphocyte aggregates
D.0	Week 4	Uninfected	WNL	Small number of small perivascular accumulations of lymphocytes; normal for rat
D.1	Week 4	Uninfected	WNL	Small number of small perivascular accumulations of lymphocytes; normal for rat

Animal	Cohort	Status	Pathology	Description
7.0	Week 4	Infected	Mild	Mild increase in cellularity due to inflammation that comprises coalescing granulomas (consisting of a mixture of epthelioid macrophages and lymphocytes and multinucleated giant cells – and often with a peribronchiolar location) that produce scattered small to moderately sized granulomas throughout the parenchyma; mild attenuation of bronchiolar epithelium in regions where granulomas impinge on them;
7.1	Week 4	Infected	Moderate	Moderate increase in cellularity due to inflammation that comprises coalescing granulomas (consisting of a mixture of epthelioid macrophages and lymphocytes and multinucleated giant cells – and often with a peribronchiolar location) that produce scattered small to moderately sized granulomas throughout the parenchyma; mild attenuation of bronchiolar epithelium in regions where granulomas impinge on them; mild increase in size of peribronchiolar lymphocyte aggregates
8.0	Week 4	Infected	Moderate	Moderate increase in cellularity due to inflammation that comprises coalescing granulomas (consisting of a mixture of epthelioid macrophages and lymphocytes and multinucleated giant cells – and often with a peribronchiolar location) that produce scattered small to moderately sized granulomas throughout the parenchyma; mild attenuation of bronchiolar epithelium in regions where granulomas impinge on them; mild increase in size of peribronchiolar lymphocyte aggregates
8.1	Week 4	Infected	Moderate	Moderate increase in cellularity due to inflammation that comprises coalescing granulomas (consisting of a mixture of epthelioid macrophages and lymphocytes – and often with a peribronchiolar location) that produce scattered small to moderately sized granulomas throughout the parenchyma; mild attenuation of bronchiolar epithelium in regions where granulomas impinge on them; mild increase in size of peribronchiolar lymphocyte aggregates
E.0	Week 8	Uninfected	WNL	Moderate number of peribronchiolar aggregates of predominantly lymphocytes with occasional macrophages – these are not granulomas though; normal for rat
E.1	Week 8	Uninfected	WNL	Small number of small perivascular accumulations of lymphocytes; normal for rat
9.0	Week 8	Infected	Moderate	Moderate increase in cellularity due to inflammation that comprises coalescing granulomas (consisting of a mixture of epthelioid macrophages and lymphocytes and multinucleated giant cells – and often with a peribronchiolar location) that produce scattered small to moderately sized granulomas throughout the parenchyma; mild attenuation of bronchiolar epithelium in regions where granulomas impinge on them

Animal	Cohort	Status	Pathology	Description
9.1	Week 8	Infected	Moderate	Moderate increase in cellularity due to inflammation that comprises coalescing granulomas (consisting of a mixture of epthelioid macrophages and lymphocytes and multinucleated giant cells and foci of mineralization – and often with a peribronchiolar location) that produce scattered small to moderately sized granulomas throughout the parenchyma; mild attenuation of bronchiolar epithelium in regions where granulomas impinge on them
10.0	Week 8	Infected	Moderate	Moderate increase in cellularity due to inflammation that comprises coalescing granulomas (consisting of a mixture of epthelioid macrophages and lymphocytes and multinucleated giant cells and foci of mineralization – and often with a peribronchiolar location) that produce scattered small to moderately sized granulomas throughout the parenchyma; mild attenuation of bronchiolar epithelium in regions where granulomas impinge on them
10.1	Week 8	Uninfected	WNL	Some medium-sized perivascular accumulations of lymphocytes; normal for rat

Table 3-S2: Complete pathology descriptions for each animal. A blinded veterinary pathologist qualitatively evaluated the overall degree of pathology and the key pathological features in hematoxylin and eosin stained sections of the left lung. WNL: within normal limits.

Figure 3-S3: Serum cytokine panel results. A total of 23 cytokines were measured in serum from all animals. The uninfected group contains the sham-infected animals from each time point, and excludes the animals that were dosed but not infected. For each cytokine, abundance at weeks 1, 2, 3, 4, and 8 post-infection are shown.

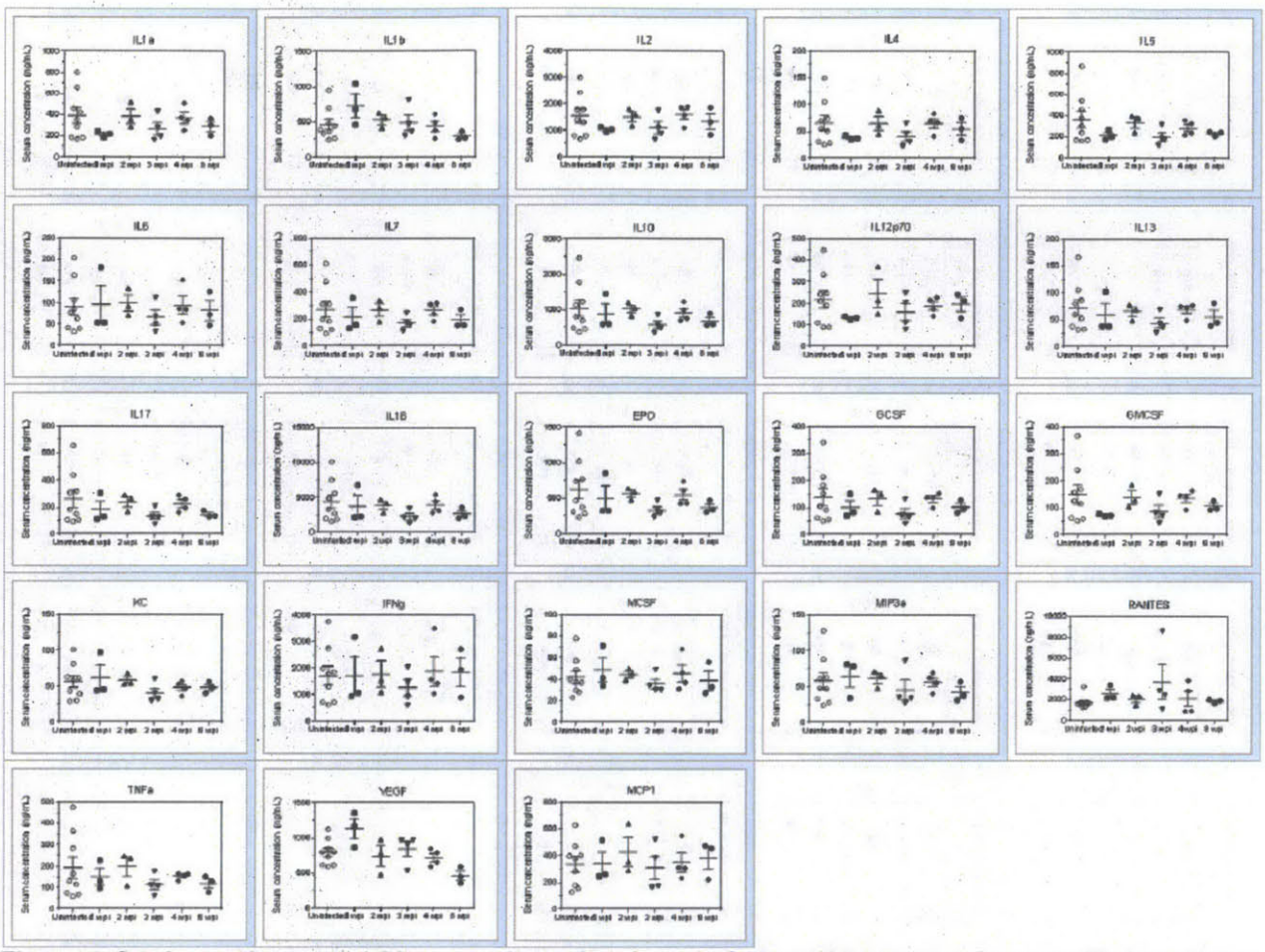

Figure 3-S4: Lung tissue cytokine panel results. A total of 23 cytokines were measured in lung tissue from all animals. The uninfected group contains the sham-infected animals from each time point, and excludes the animals that were dosed but not infected. For each cytokine, abundance at weeks 1, 2, 3, 4, and 8 post-infection are shown.

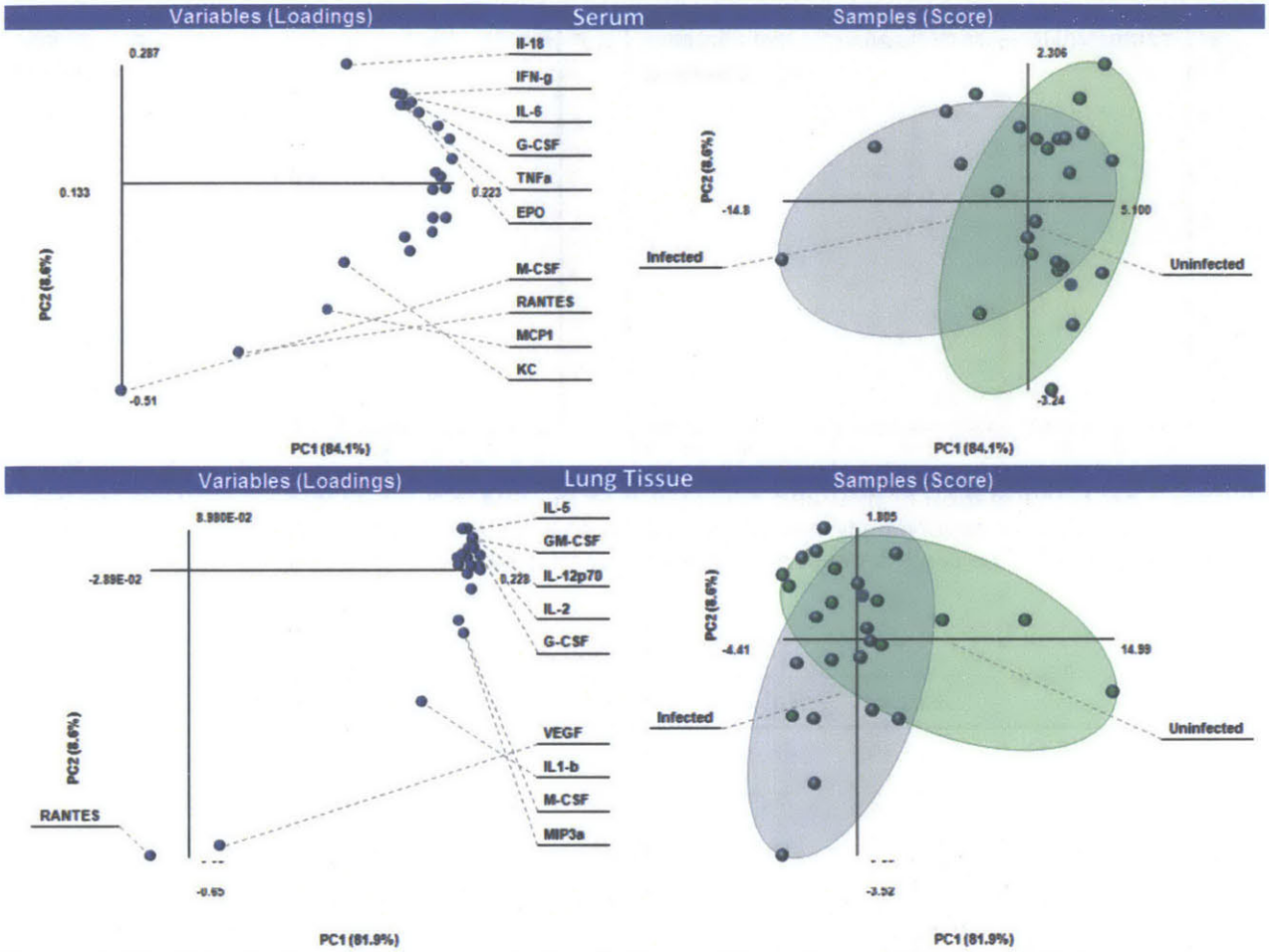

Figure 3-S5: Principal component analysis of 23 cytokines from all animals. Data were mean-centered and SD normalized prior to calculation, and data from the three rats that were dosed but not infected were excluded.

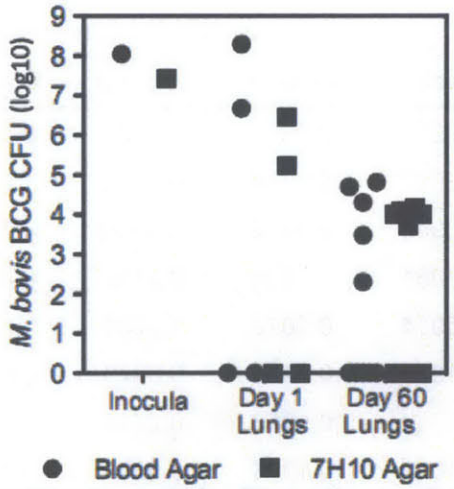

Figure 3-S6: CFU counts for the 10 rats used for biomarker analysis. Of the14 rats dose on day 0, two had confirmed infection at day 1, and six had confirmed infection at day 60. Only rats with confirmed infection were analyzed in subsequent experiments. Experiments were performed by Megan McBee.

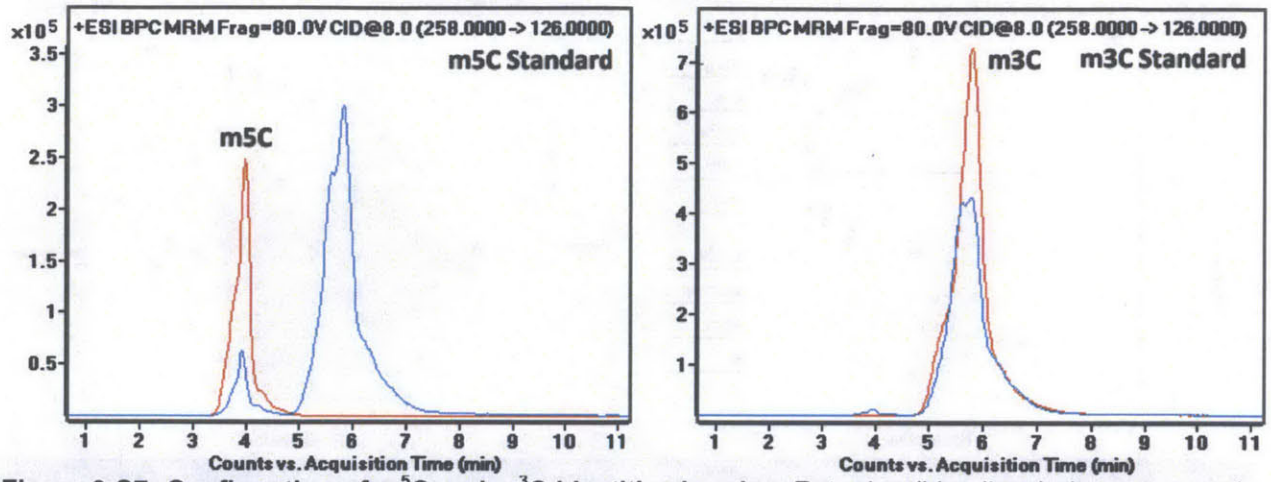

Figure 3-S7: Confirmation of m^5C and m^3C identities in urine. Rat urine (blue lines) shows two peaks with m/z transition corresponding to methylcytidine. Comparison to synthetic standards (red lines) reveals the identity of each. The same process was repeated for all eight ribonucleoside species confirmed.

Time	Creatinine Concentration (mg/dL)					
	Rat 4.0	Rat 5.0	Rat 5.1	Rat 6.0	Rat 6.1	Rat 7.0
Week 0	43.49	48.14	20.79	37.87	31.37	65.47
Week 1	45.02	75.99	22.64	32.46	52.41	48.96
Week 3	17.48	18.88	60.69	47.82	46.29	86.57
Week 5	8.43	21.69	34.30	17.22	31.18	46.67
Week 7	9.77	5.94	40.30	29.27	38.70	107.98

Table 3-S3: Creatinine concentration for rats with confirmed infections. To normalize ribonucleoside abundances according to urine concentration, creatinine values were measured by the Jaffe method in each animal and at each time point.

#	rN	Normalized Abundance				
		Week 0	Week 1	Week 3	Week 5	Week 7
Rat 4.0	m^5C	0.0265	0.6817	2.1655	0.0000	0.2455
	m^3C	0.2967	0.0084	0.0000	1.0391	0.0532
	m^1A	1.3945	2.0494	17.0752	4.7976	1.4200
	m^2A	0.2051	0.1334	0.2142	0.4660	0.2406
	m^7G	1.5914	0.1070	1.0286	0.2050	0.2394
	m^2G	0.1394	0.0165	0.0470	0.0798	0.1399
	$m^2{}_2G$	0.8742	0.1053	0.2717	0.2586	0.3244
	Cm	0.1852	0.1331	0.6558	0.3207	0.3915
Rat 5.0	m^5C	0.0119	0.1899	0.0000	0.0000	0.1489
	m^3C	0.1646	0.0026	0.5144	0.5341	0.3164

#	rN	Normalized Abundance				
		Week 0	Week 1	Week 3	Week 5	Week 7
5.0	m^1A	0.7756	1.0216	2.9582	5.1226	2.4629
	m^2A	0.4759	0.0838	0.1247	0.0970	0.8437
	m^7G	0.0657	0.0780	0.2375	0.2183	0.0170
	m^2G	0.1136	0.0162	0.0180	0.0546	0.0701
	m^2_2G	0.7928	0.0551	0.0833	0.1561	0.4316
	Cm	0.0468	0.0051	0.0114	0.0310	0.2786
5.1	m^5C	1.6833	0.6571	0.4160	0.0098	0.2244
	m^3C	0.0000	0.0071	0.0000	0.5794	0.0000
	m^1A	13.3951	4.1676	2.2708	3.4354	1.8422
	m^2A	0.0159	0.2057	0.1111	0.4348	0.0254
	m^7G	0.0966	0.3546	0.1309	0.1466	0.1502
	m^2G	0.1882	0.0127	0.0144	0.1157	0.0076
	m^2_2G	0.6923	0.0635	0.0817	0.2874	0.0507
	Cm	1.7865	0.1696	0.1030	0.4007	0.1366
6.0	m^5C	0.2353	0.0413	0.2142	0.9796	0.5402
	m^3C	0.0000	1.3927	0.0000	0.0000	0.0091
	m^1A	2.4615	4.9094	1.5486	8.8557	2.4514
	m^2A	0.0167	0.3306	0.0220	0.1575	0.0283
	m^7G	0.0995	0.3144	0.0424	0.3904	0.2164
	m^2G	0.0640	0.2387	0.0154	0.1060	0.0070
	m^2_2G	0.3041	0.5215	0.0566	0.3567	0.1328
	Cm	0.3079	0.5315	0.0590	0.2506	0.1687
6.1	m^5C	0.0074	0.0228	0.0000	0.0317	0.0058
	m^3C	0.2659	0.3634	0.2402	0.9323	0.3169
	m^1A	1.9352	1.3919	2.1738	5.6524	1.9932
	m^2A	0.0746	0.2504	0.1211	0.2034	0.0153
	m^7G	0.0404	0.0365	0.1752	0.0079	0.0160
	m^2G	0.0286	0.0394	0.0143	0.1707	0.0269
	m^2_2G	0.1485	0.1366	0.1074	0.5242	0.1359
	Cm	0.0180	0.1600	0.0411	0.4205	0.1092
7.0	m^5C	0.0140	0.0264	0.0382	0.1823	0.0243
	m^3C	0.2704	0.4115	0.3454	1.3048	0.3300
	m^1A	1.6403	2.0467	2.2959	7.2815	1.8395

#	rN	Normalized Abundance				
		Week 0	Week 1	Week 3	Week 5	Week 7
7.0	m^2A	0.0569	0.0623	0.0633	1.3761	0.0241
	m^7G	0.0020	0.0046	0.0207	0.5988	0.0316
	m^2G	0.0451	0.0994	0.0321	0.3067	0.0145
	$m^2{}_2G$	0.2003	0.1534	0.1752	0.6311	0.1121
	Cm	0.1577	0.1482	0.1759	1.0553	0.1609

Table 3-S4: Normalized abundances of urinary ribonucleosides. The eight confirmed species that were present in all animals were measured at weeks 0 (uninfected), 1, 3, 5, and 7 post-infection. Abundances were normalized by urine creatinine concentration.

3.6. References

1. C.J. Murray, A.D. Lopez (2013) *Measuring the global burden of disease.* **N Engl J Med** 369(5): 448-457.
2. World Health Organization (2011) *The top 10 causes of death.* WHO Fact Sheet N°310. Last updated July 2013. Accessed on 8 April 2014. Available from: http://www.who.int/mediacentre/factsheets/fs310/en/.
3. S. Keshavjee, P.E. Farmer (2012) *Tuberculosis, drug resistance, and the history of modern medicine.* **N Engl J Med** 367(10): 931-936.
4. A. Zumla, M. Raviglione, R. Hafner, C.F. Von Reyn (2013) *Tuberculosis.* **N Engl J Med** 368(8): 745-755.
5. G.B. Migliori, A. Matteelli, D. Cirillo, M. Pai (2008) *Diagnosis of multidrug-resistant tuberculosis and extensively drug-resistant tuberculosis: Current standards and challenges.* **Can J Infect Dis Med Microbiol** 19(2): 169-172.
6. N. Casali, V. Nikolayevskyy, Y. Balabanova, S.R. Harris, O. Ignatyeva, I. Kontsevaya, J. Corander, J. Bryant, J. Parkhill, S. Nejentsev, R.D. Horstmann, T. Brown, F. Drobniewski (2014) *Evolution and transmission of drug-resistant tuberculosis in a Russian population.* **Nat Genet** 46(3): 279-286.
7. R. Osborne (2013) *First novel anti-tuberculosis drug in 40 years.* **Nat Biotechnol** 31(2): 89-91.
8. J. Mcfadden, D.J.V. Beste, A.M. Kierzek (Eds.) *Systems Biology of Tuberculosis*. 2013, Springer: New York.
9. H. Tomioka (2013) *New approaches to tuberculosis – novel drugs based on drug targets related to toll-like receptors in macrophages.* **Curr Pharm Des**.
10. N. Chandra, D. Kumar, K. Rao (2011) *Systems biology of tuberculosis.* **Tuberculosis** 91(5): 487-496.
11. V. Dartois, C.E. Barry, 3rd (2013) *A medicinal chemists' guide to the unique difficulties of lead optimization for tuberculosis.* **Bioorg Med Chem Lett** 23(17): 4741-4750.
12. E. Guirado, L.S. Schlesinger (2013) *Modeling the Mycobacterium tuberculosis granuloma – the critical battlefield in host immunity and disease.* **Front Immunol** 4(98).
13. U.D. Gupta, V.M. Katoch (2005) *Animal models of tuberculosis.* **Tuberculosis** 85(5-6): 277-293.

14. V.E. Calderon, G. Valbuena, Y. Goez, B.M. Judy, M.B. Huante, P. Sutjita, R.K. Johnston, D.M. Estes, R.L. Hunter, J.K. Actor, J.D. Cirillo, J.J. Endsley (2013) *A humanized mouse model of tuberculosis.* **PLoS One** 8(5): e63331.
15. A. Singhal, M. Aliouat El, M. Herve, V. Mathys, M. Kiass, C. Creusy, B. Delaire, L. Tsenova, L. Fleurisse, J. Bertout, L. Camacho, D. Foo, H.C. Tay, J.Y. Siew, W. Boukhouchi, M. Romano, B. Mathema, V. Dartois, G. Kaplan, P. Bifani (2011) *Experimental tuberculosis in the Wistar rat: A model for protective immunity and control of infection.* **PLoS One** 6(4): e18632.
16. Y. Heng, P.G. Seah, J.Y. Siew, H.C. Tay, A. Singhal, V. Mathys, M. Kiass, P. Bifani, V. Dartois, M. Herve (2011) *Mycobacterium tuberculosis infection induces hypoxic lung lesions in the rat.* **Tuberculosis** 91(4): 339-341.
17. N. Kumar, K.G. Vishwas, M. Kumar, J. Reddy, M. Parab, C.L. Manikanth, B.S. Pavithra, R.K. Shandil (2014) *Pharmacokinetics and dose response of anti-TB drugs in rat infection model of tuberculosis.* **Tuberculosis.**
18. A. Singhal, V. Mathys, M. Kiass, C. Creusy, B. Delaire, M. Aliouat El, V. Dartois, G. Kaplan, P. Bifani (2011) *BCG induces protection against Mycobacterium tuberculosis infection in the Wistar rat model.* **PLoS One** 6(12): e28082.
19. S. Gaonkar, S. Bharath, N. Kumar, V. Balasubramanian, R.K. Shandil (2010) *Aerosol infection model of tuberculosis in Wistar rats.* **Int J Microbiol** 2010: 426035.
20. J. Baum (2008) *Biohazard containment facilities: Planning and design considerations.* Last updated Accessed on 19 December 2013. Available from: http://www.ghdonline.org/uploads/LabBiosafetyPlanning071208-Part1.pdf.
21. K.M. Berger. *The broader effects of biosecurity regulations*, in *The CIP Report.* 2009, George Mason University.
22. K. Rhodes. *High-containment biosafety laboratories: Preliminary observations on the oversight of the proliferation of BSL-3 and BSL-4 laboratories in the United States*, G.A. Office. Editor. 2007.
23. V. Dartois (2014) *The path of anti-tuberculosis drugs: From blood to lesions to mycobacterial cells.* **Nat Rev Microbiol** 12(3): 159-167.
24. E.M. Galvan, M.K. Nair, H. Chen, F. Del Piero, D.M. Schifferli (2010) *Biosafety level 2 model of pneumonic plague and protection studies with F1 and Psa.* **Infect Immun** 78(8): 3443-3453.
25. W.J. Philipp, S. Nair, G. Guglielmi, M. Lagranderie, B. Gicquel, S.T. Cole (1996) *Physical mapping of Mycobacterium bovis BCG Pasteur reveals differences from the genome map of Mycobacterium tuberculosis H37Rv and from M. bovis.* **Microbiology** 142: 3135-3145.
26. M.A. Behr, P.M. Small (1998) *A historical and molecular phylogeny of BCG strains.* **Vaccine** 17: 915-922.
27. E.J. Muñoz-Elías, J. Timm, T. Botha, W.T. Chan, J.E. Gomez, J.D. Mckinney (2005) *Replication dynamics of Mycobacterium tuberculosis in chronically infected mice.* **Infect Immun** 73(1): 546-551.
28. A. Lewin, B. Freytag, B. Meister, S. Sharbati-Tehrani, H. Schafer, B. Appel (2003) *Use of a quantitative TaqMan-PCR for the fast quantification of mycobacteria in broth culture, eukaryotic cell culture and tissue.* **J Vet Med B Infect Dis Vet Public Health** 50(10): 505-509.

29. K. Taghizadeh, J.L. Mcfaline, B. Pang, M. Sullivan, M. Dong, E. Plummer, P.C. Dedon (2008) *Quantification of DNA damage products resulting from deamination, oxidation and reaction with products of lipid peroxidation by liquid chromatography isotope dilution tandem mass spectrometry.* **Nat Protoc** 3(8): 1287-1298.
30. S.I. Quek, M.E. Ho, M.A. Loprieno, W.J. Ellis, N. Elliott, A.Y. Liu (2012) *A multiplex assay to measure RNA transcripts of prostate cancer in urine.* **PLoS One** 7(9): e45656.
31. T. Muthukumar, D. Dadhania, R. Ding, C. Snopkowski, R. Naqvi, J.B. Lee, C. Hartono, B. Li, V.K. Sharma, S.V. Seshan, S. Kapur, W.W. Hancock, J.E. Schwartz, M. Suthanthiran (2005) *Messenger RNA for FOXP3 in the urine of renal-allograft recipients.* **N Engl J Med** 353(22): 2342-2351.
32. F. Teichert, S. Winkler, H.C. Keun, W.P. Steward, A.J. Gescher, P.B. Farmer, R. Singh (2011) *Evaluation of urinary ribonucleoside profiling for clinical biomarker discovery using constant neutral loss scanning liquid chromatography/tandem mass spectrometry.* **Rapid Commun Mass Spectrom** 25(14): 2071-2082.
33. J. Dormans, M. Burger, D. Aguilar, R. Hernandez-Pando, K. Kremer, P. Roholl, S.M. Arend, D. Van Soolingen (2004) *Correlation of virulence, lung pathology, bacterial load and delayed type hypersensitivity responses after infection with different Mycobacterium tuberculosis genotypes in a BALB/c mouse model.* **Clin Exp Immunol** 137(3): 460-468.
34. A. Menin, R. Fleith, C. Reck, M. Marlow, P. Fernandes, C. Pilati, A. Bafica (2013) *Asymptomatic cattle naturally infected with Mycobacterium bovis present exacerbated tissue pathology and bacterial dissemination.* **PLoS One** 8(1): e53884.
35. National Bioresource Project *Rat Strains (Organ Weight)*. Rat Phenome Database. Last updated 7 April 2014. Accessed on 15 April 2014. Available from: http://www.anim.med.kyoto-u.ac.jp/NBR/strainsx/OW_list.aspx.
36. G. Jorgens, F.C. Bange, P.F. Muhlradt, R. Pabst, U.A. Maus, T. Tschernig (2009) *Synthetic lipopeptide MALP-2 inhibits intracellular growth of Mycobacterium bovis BCG in alveolar macrophages—preliminary data.* **Inflammation** 32(4): 247-251.
37. R.L. Elwood, S. Wilson, J.C. Blanco, K. Yim, L. Pletneva, B. Nikonenko, R. Samala, S. Joshi, V.G. Hemming, M. Trucksis (2007) *The American cotton rat: A novel model for pulmonary tuberculosis.* **Tuberculosis** 87(2): 145-154.
38. N.W. Schluger, W.N. Rom (1998) *The host immune response to tuberculosis.* **Am J Respir Crit Care Med** 157: 679-691.
39. B.M. Saunders, W.J. Britton (2007) *Life and death in the granuloma: Immunopathology of tuberculosis.* **Immunol Cell Biol** 85(2): 103-111.
40. S.A. Fulton, S.M. Reba, T.D. Martin, W.H. Boom (2002) *Neutrophil-mediated mycobacteriocidal immunity in the lung during Mycobacterium bovis BCG infection in C57BL/6 mice.* **Infect Immun** 70(9): 5322-5327.
41. L.E. Swaim, L.E. Connolly, H.E. Volkman, O. Humbert, D.E. Born, L. Ramakrishnan (2006) *Mycobacterium marinum infection of adult zebrafish causes caseating granulomatous tuberculosis and is moderated by adaptive immunity.* **Infect Immun** 74(11): 6108-6117.
42. X. Bai, S.E. Wilson, K. Chmura, N.E. Feldman, E.D. Chan (2004) *Morphometric analysis of Th_1 and Th_2 cytokine expression in human pulmonary tuberculosis.* **Tuberculosis** 84(6): 375-385.

43. T. Tsuchiya, K. Chida, T. Suda, E.E. Schneeberger, H. Nakamura (2002) *Dendritic cell involvement in pulmonary granuloma formation elicited by bacillus Calmette–Guérin in rats.* **Am J Respir Crit Care Med** 165(12): 1640-1646.
44. A. O'garra, P.S. Redford, F.W. Mcnab, C.I. Bloom, R.J. Wilkinson, M.P. Berry (2013) *The immune response in tuberculosis.* **Annu Rev Immunol** 31: 475-527.
45. R.J. Trudnowski, R.C. Rico (1974) *Specific gravity of blood and plasma at 4 and 37 °C.* **Clin Chem** 20(5): 615-616.
46. C.M. Doerschuk, H.S. Sekhon (1990) *Pulmonary blood volume and edema in postpneumonectomy lung growth in rats.* **J Appl Physiol** 69(3): 1178-1182.
47. J. Wakeham, J. Wang, J. Magram, K. Croitoru, R. Harkness, P. Dunn, A. Zganiacz, Z. Xing (1998) *Lack of both types 1 and 2 cytokines, tissue inflammatory responses, and immune protection during pulmonary infection by Mycobacterium bovis Bacille Calmette–Guérin in IL-12-deficient mice.* **J Immunol** 160: 6101-6111.
48. S.L. Gaffen (2008) *An overview of IL-17 function and signaling.* **Cytokine** 43(3): 402-407.
49. H.E. Volkman, T.C. Pozos, J. Zheng, J.M. Davis, J.F. Rawls, L. Ramakrishnan (2010) *Tuberculous granuloma induction via interaction of a bacterial secreted protein with host epithelium.* **Science** 327(5964): 466-469.
50. P.T. Elkington, J.M. D'armiento, J.S. Friedland (2011) *Tuberculosis immunopathology: The neglected role of extracellular matrix destruction.* **Sci Transl Med** 3(71): 71ps76.
51. World Health Organization. *Global Tuberculosis Report.* 2013.
52. E. Dudley, F. Lemiere, W. Van Dongen, E. Esmans, A.M. El-Sharkawi, D.E. Games, A.G. Brenton, R.P. Newton (2003) *Urinary modified nucleosides as tumor markers.* **Nucleosides Nucleotides Nucleic Acids** 22(5-8): 987-989.
53. C.W. Gehrke, K.C. Kuo, T.P. Waalkes, E. Borek (1979) *Patterns of urinary excretion of modified nucleosides.* **Cancer Res** 39(4): 1150-1153.
54. C.T. Chan, Y.H. Chionh, C.H. Ho, K.S. Lim, I.R. Babu, E. Ang, L. Wenwei, S. Alonso, P.C. Dedon (2011) *Identification of N^6,N^6-dimethyladenosine in transfer RNA from Mycobacterium bovis bacille Calmette–Guérin.* **Molecules** 16(6): 5168-5181.
55. E.L. Esmans, D. Broes, I. Hoes, F. Lemiere, K. Vanhoutte (1998) *Liquid chromatography–mass spectrometry in nucleoside, nucleotide and modified nucleotide characterization.* **J Chromatogr A** 794: 109-127.
56. Z. Meng, P.A. Limbach (2006) *Mass spectrometry of RNA: Linking the genome to the proteome.* **Brief Funct Genomic Proteomic** 5(1): 87-95.
57. D. Su, C.T. Chan, C. Gu, K.S. Lim, Y.H. Chionh, M.E. Mcbee, B.S. Russell, I.R. Babu, T.J. Begley, P.C. Dedon (2014) *Quantitative analysis of ribonucleoside modifications in tRNA by HPLC-coupled mass spectrometry.* **Nat Protoc** 9(4): 828-841.
58. W.A. Cantara, P.F. Crain, J. Rozenski, J.A. Mccloskey, K.A. Harris, X. Zhang, F.A. Vendeix, D. Fabris, P.F. Agris (2011) *The RNA Modification Database, RNAMDB: 2011 update.* **Nucleic Acids Res** 39(Database issue): D195-201.
59. S. Dunin-Horkawicz, A. Czerwoniec, M.J. Gajda, M. Feder, H. Grosjean, J.M. Bujnicki (2006) *MODOMICS: A database of RNA modification pathways.* **Nucleic Acids Res** 34(Database issue): D145-149.
60. J. Rozenski, P.F. Crain, J.A. Mccloskey (1999) *The RNA Modification Database: 1999 update.* **Nucleic Acids Res** 27(1): 196-197.

61. I.M. Orme, F.M. Collins (1986) *Aerogenic vaccination of mice with Mycobacterium bovis BCG.* **Tubercle** 67: 133-140.
62. V. Kindler, A.-P. Sappino, G.E. Grau, P.-F. Piguet, P. Vassalli (1989) *The inducing role of tumor necrosis factor in the development bactericidal granulomas during BCG infection.* **Cell** 56: 731-740.
63. A.M. Minassian, E.O. Ronan, H. Poyntz, A.V. Hill, H. Mcshane (2011) *Preclinical development of an in vivo BCG challenge model for testing candidate TB vaccine efficacy.* **PLoS One** 6(5): e19840.
64. M. Shirai, A. Sato, K. Chida (1995) *The influence of ovarian hormones on the granulomatous inflammatory process in the rat lung.* **Eur Respir J** 8(2): 272-277.
65. D.M. Tobin, L. Ramakrishnan (2008) *Comparative pathogenesis of Mycobacterium marinum and Mycobacterium tuberculosis.* **Cell Microbiol** 10(5): 1027-1039.
66. C.A. Bolin, D.L. Whipple, K.V. Khanna, J.M. Risdahl, P.K. Peterson, T.W. Molitor (1997) *Infection of swine with Mycobacterium bovis as a model of human tuberculosis.* **J Infect Dis** 176: 1559-1566.
67. P.T. Elkington, T. Shiomi, R. Breen, R.K. Nuttall, C.A. Ugarte-Gil, N.F. Walker, L. Saraiva, B. Pedersen, F. Mauri, M. Lipman, D.R. Edwards, B.D. Robertson, J. D'armiento, J.S. Friedland (2011) *MMP-1 drives immunopathology in human tuberculosis and transgenic mice.* **J Clin Invest** 121(5): 1827-1833.
68. P. Salgame (2011) *MMPs in tuberculosis: granuloma creators and tissue destroyers.* **J Clin Invest** 121(5): 1686-1688.
69. T.B. Grivas, E.S. Vasiliadis, A. Kaspiris, L. Khaldi, D. Kletsas (2011) *Expression of matrix metalloproteinase-1 (MMP-1) in Wistar rat's intervertebral disc after experimentally induced scoliotic deformity.* **Scoliosis** 6(1): 9.
70. M. Harboe, T. Oettinger, H.G. Wiker, I. Rosenkrands, P. Andersen (1996) *Evidence for occurrence of the ESAT-6 protein in Mycobacterium tuberculosis and virulent M. bovis and for its absence in Mycobacterium bovis BCG.* **Infect Immun** 64(1): 16-22.
71. D.G. Foo, H.C. Tay, J.Y. Siew, A. Singhal, L. Camacho, P. Bifani, V. Dartois, M. Herve (2011) *T cell monitoring of chemotherapy in experimental rat tuberculosis.* **Antimicrob Agents Chemother** 55(8): 3677-3683.
72. Y. Ikeuchi, A. Soma, T. Ote, J. Kato, Y. Sekine, T. Suzuki (2005) *Molecular mechanism of lysidine synthesis that determines tRNA identity and codon recognition.* **Mol Cell** 19(2): 235-246.
73. H. Dong, L. Nilsson, C.G. Kurland (1996) *Co-variation of tRNA abundance and codon usage in Escherichia coli at different growth rates.* **J Mol Biol** 260(5): 649-663.
74. S. Balbo, S.S. Hecht, P. Upadhyaya, P.W. Villalta (2014) *Application of a high-resolution mass-spectrometry-based DNA adductomics approach for identification of DNA adducts in complex mixtures.* **Anal Chem** 86(3): 1744-1752.
75. C.W. Gehrke, K.C. Kuo, T.P. Waalkes, E. Borek (1979) *Patterns of urinary excretion of modified nucleosides.* **Cancer Res** 39: 1150-1153.
76. P.C. Dedon, M.S. Demott, C.E. Elmquist, E.G. Prestwich, J.L. Mcfaline, B. Pang (2007) *Challenges in developing DNA and RNA biomarkers of inflammation.* **Biomark Med** 1(2): 293-312.
77. M.V. Palmer, W.R. Waters, T.C. Thacker (2007) *Lesion development and immunohistochemical changes in granulomas from cattle experimentally infected with Mycobacterium bovis.* **Vet Pathol** 44(6): 863-874.

4. Bacterial DNA phosphorothioation in resistance to oxidative and antibiotic stresses

4.1. Introduction and motivation

Phosphorothioation is a unique DNA modification in which one of the nonbridging phosphate oxygens is replaced by a sulfur [1]. Phosphorothioates (PTs) were originally developed and described as synthetic modifications to stabilize oligonucleotides against degradation [2-4], but they are now known to occur endogenously in a large, diverse number of bacteria and archaea [5-7]. PT is the only known endogenous DNA modification containing sulfur, as well as the only known backbone modification [8]. Endogenous PT modifications are inserted at consensus sequences (which vary between organisms) in a site- and stereo-specific manner [9]. The machinery needed to create the PT modification is contained in a five- or eight-gene cluster known as *dnd*, which is carried on mobile genetic elements [10]. Despite years of research, the exact function of PT modifications remains unclear.

The *dnd* gene cluster can be divided into two functional groupings. The first five genes, *dndA-E*, are involved in inserting the PT modification into DNA: *dndC-E* are absolutely required; *dndB* is not required but appears to control the specificity of insertion; and *dndA* is often absent, but functionally complemented by a native host protein [11-16]. The other three genes, *dndF-H*, were recently demonstrated to restrict the incorporation of non-PT DNA into a PT-containing host [17]. In this way, PT seems to function as a novel restriction-modification (R-M) system, similar to a methylation-based R-M system. Supporting this possibility is the observation that PT shares the sequence specificity and discretely quantified, consensus-based levels of incorporation that are hallmarks of methylation R-M systems [18]. Similarly, PT may also function as a type of bacterial defense mechanism or "immunity" similar to a CRISPR-Cas system [19]. Surprisingly, many organisms harboring *dndA-E* lack the associated *dndF-H* genes needed for restriction, pointing to another, as-yet uncharacterized function of PT [20].

Xie *et al.* recently demonstrated that bacteria harboring PT modification are more resistant to oxidative stress in the form of hydrogen peroxide (H_2O_2) [21], which may provide a possible explanation for the widespread distribution of PT without the associated restriction system. Given the observation that many human pathogens harbor PT modifications [22], we wondered

to what extent PT might be clinically relevant. In particular, we were inspired by recent (though controversial [23]) reports that antibiotics achieve their bactericidal effect through reactive oxygen species (ROS) stress [24, 25]. This potential link to antibiotic resistance is especially relevant given the pressing need for new ways to combat the spread of resistance [26-28]. To that end, we sought to determine the extent of protection conferred by PT by examining the oxidative and antibiotic resistance profiles of three bacterial species harboring PT modifications. Our results reveal that the protective effects of PT are both toxicant- and organism-dependent.

4.2. Methods

4.2.1. Bacterial strains, plasmids, and culture conditions

Citrobacter rodentium DBS100 was obtained as a frozen glycerol stock from Dr. Alexander Sheh (MIT Division of Comparative Medicine). Derivative DBS805 was constructed by Dr. Lianrong Wang by transforming DBS100 with plasmid pJTU1980, which was a derivative of plasmid pACYC184Cm^RTet^R in which the Tet^R gene was disrupted by insertion of the genes *dndB-E* from *Salmonella enterica* Cerro 87. DBS803 was constructed by Dr. Michael DeMott by transforming DBS100 with a derivative of plasmid pACYC184 Cm^RTet^R in which the Tet^R gene was disrupted by insertion of a random 20-mer oligonucleotide. *S. enterica* Cerro 87 and the derivative strain XTG103 in which the entire *dndB-H* cluster was removed by in-frame deletion were obtained from the laboratory of Dr. Zixin Deng. *Streptomyces lividans* 1326 and an unnamed derivate strain in which the *dndC* gene was removed by in-frame deletion were obtained from Dr. Lianrong Wang. Plate cultures of *C. rodentium* were grown at 37 °C on LB agar (BD) supplemented with 50 μg/ml chloramphenicol (Sigma) for plasmid maintenance. Liquid cultures were grown at 37 °C with shaking in LB broth (BD) supplemented with 30 μg/ml chloramphenicol. Plate cultures of *S. enterica* were grown at 37 °C on LB agar, and liquid cultures were grown at 37 °C with shaking in LB broth. Plate cultures of *S. lividans* were grown on tryptic soy agar (BD) at 30 °C, and liquid cultures were grown 30 °C in trypic soy broth (BD) supplemented with 1% agar as a dispersant. All plate cultures were stored at 4 °C for a maximum of 2 weeks before being rederived from frozen stocks. Primary overnight liquid cultures from single colonies were used for all experiments.

4.2.2. Growth curves

H_2O_2, streptomycin, kanamycin, and ampicillin were all purchased from Sigma. Saturated overnight cultures (OD_{600}>1.0) were normalized to a turbidity of 0.1 using the appropriate growth media before all exposures. H_2O_2 stock concentration was checked before each exposure by measuring the absorbance at 240 nm and using the molar absorptivity of 43.6 $M^{-1}cm^{-1}$ [29], and the dose was adjusted accordingly. Antibiotic working stocks were made fresh from dry chemicals before each exposure. Exposures were conducted in a 96-well plate format in a final volume of 200 µl. Plates were loaded into a Bio-Tek ELx808 plate reader fitted with a heated shaker, and were grown with shaking at optimal temperature (37 °C for *C. rodentium* and *S. enterica*, 30 °C for *S. lividans*) and time (overnight for *C. rodentium* and *S. enterica*, 48 h for *S. lividans*). Turbidity was measured every 10 min for overnight exposures and every 30 min for 48 h exposures. Given our previous observation of evaporation from the peripheral plate wells, the outer perimeter was filled with plain media and used as the sterility control and blank.

4.2.3. Spot plate assay

Exposure plates were prepared as described above for growth curves, but were then incubated with shaking at the appropriate temperature for either 30 min (H_2O_2) or 2 h (antibiotics). After incubation and mixing by repetitive pipetting, a multichannel pipet was used to remove 4 µl aliquots, which were then spotted directly onto large LB agar plates. Plates were grown overnight at 37 °C and imaged with a FluorChem CCD camera.

4.3. Results

4.3.1. Diverse PT genotypes do not alter the growth phenotype

The first step in our studies was to establish specific backgrounds in which to examine the effects of PT. Because multiple potential functions have been proposed, and because the set of *dnd* genes varies significantly even between PT-containing organisms, we chose to examine three different PT systems. One system relied on artificial introduction of PT modifications (but not restriction) into a naturally PT-negative organism. Another system relied on a naturally PT-positive organism that also contained the associated restriction genes. The final system relied on

a naturally PT-positive organism that lacked the associated restriction genes. In this way we were able to examine the effect of both the source of PT (artificial vs. naturally acquired) as well as the effect of the associated restriction genes. This set of organisms would also give us insight into the mechanism of PT-associated resistance: if the protection were purely chemical and mediated by the PT modification itself, it should be recapitulated in the artificial system. If instead the protection relied on a more complicated PT function (such as gene regulation), then that should be absent from the artificial system.

The artificial system was based on the mouse pathogen *C. rodentium* DBS100 [30], which others in our laboratory had confirmed naturally lacked PT through previous experiments. We used two plasmid-containing derivatives of DBS100 that were previously developed by other members of our laboratory. *C. rodentium* DBS803Cm^R carried the low copy vector plasmid pACYC184Cm^RTet^R, and *C. rodentium* DBS805Cm^R carried same plasmid with the addition of the four-gene *dndB-E* cluster from *S. enterica* Cerro 87 [18]. The restriction-positive native system was based on the same strain used by Xie *et al.*, *S. enterica* Cerro 87, which harbors *dndB-H*. The PT-negative component of this system was termed *S. enterica* XTG103, a derivative of Cerro 87 with an in-frame deletion of the entire *dnd* cluster. This strain was obtained from collaborators. The restriction-negative native system was based on *Streptomyces lividans* 1326, which harbors a *dndA-E* cluster that is genetically distinct from that found in *S. enterica* [18]. The PT-negative component of this system was an in-frame deletion of *dndC*, previously constructed by other members of our laboratory. For all strains, the appropriate *dnd* sequence was confirmed by GeneWiz sequencing, and the appropriate PT status was confirmed by a previously established liquid chromatography-coupled tandem mass spectrometry (LC-MS/MS) method [18].

Having established our test organisms, we next sought to determine the effect of PT on growth under normal conditions. As shown in **Figure 4-1**, the presence or absence of PT had no effect on the growth of any of the organisms. This finding ensured that our test organisms were well controlled and that any treatment-induced differences between strains could be attributed solely to the presence of the stress. We next determined the oxidative and antibiotic stress resistance profiles for each strain.

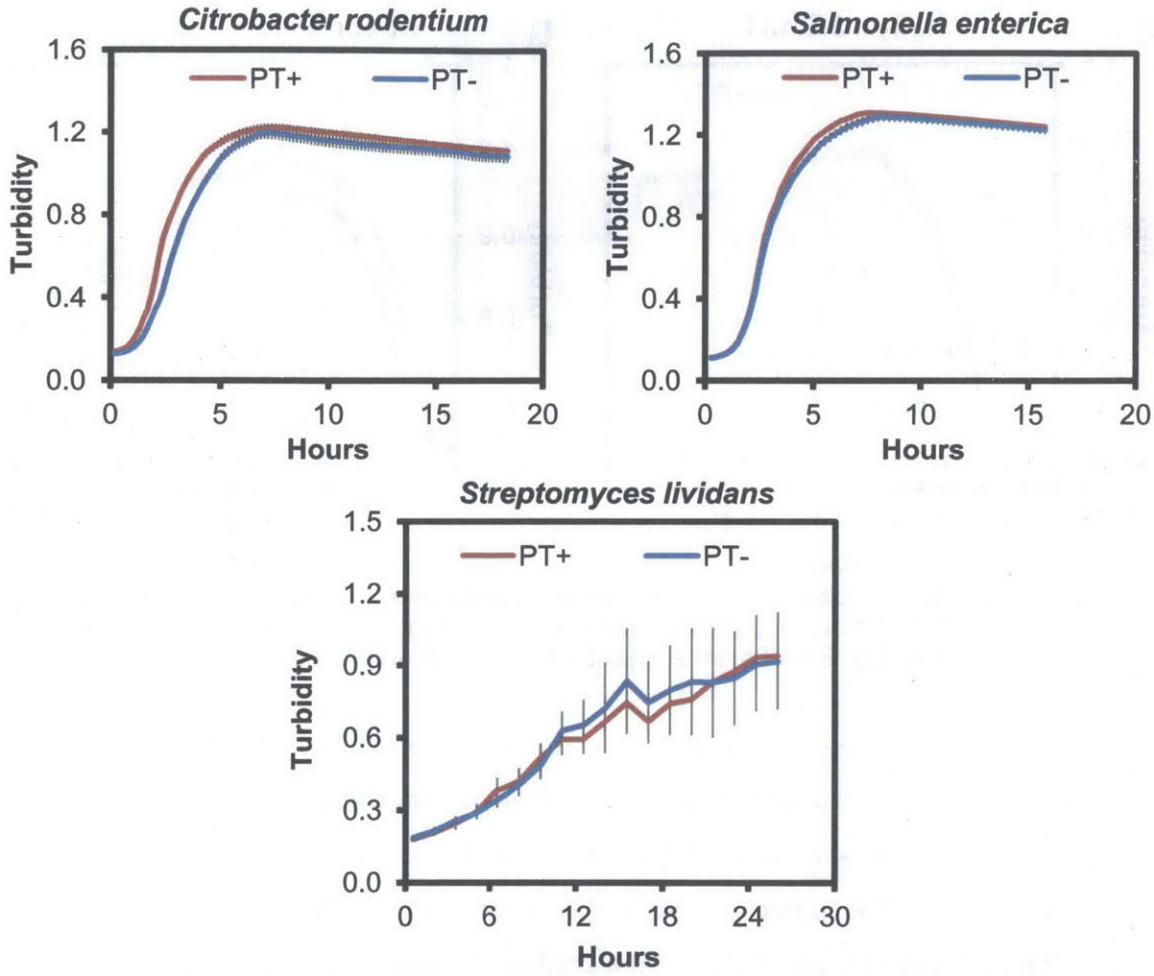

Figure 4-1: Control growth of bacteria ± PT modifications. All strains were normalized to the same starting turbidity and grown under optimal conditions in untreated growth media. Error bars are ± SD for four biological replicates.

4.3.2. Artificial PT confers resistance only to antibiotic stress

We first sought to recapitulate the H_2O_2 resistance reported by Xie *et al.* in our artificial PT system, in order to test the hypothesis that resistance is mediated by the chemical properties of the PT bond. Surprisingly, our data showed that PT-containing *C. rodentium* was much more susceptible to H_2O_2 exposure. A dose-dependent effect of H_2O_2 was seen for both strains, with a single illustrative dose is shown in **Figure 4-2A**. We then examined the antibiotic resistance profiles of the two strains, using the aminoglycoside streptomycin (chosen because *C. rodentium* is resistant to β-lactams [31], and fluoroquinolones pose significant solubility problems [32]). In contrast to the H_2O_2 results, PT-containing *C. rodentium* was more resistant to streptomycin. Again, a dose-dependent effect was seen, and a single illustrative dose is shown (**Figure 4-2B**).

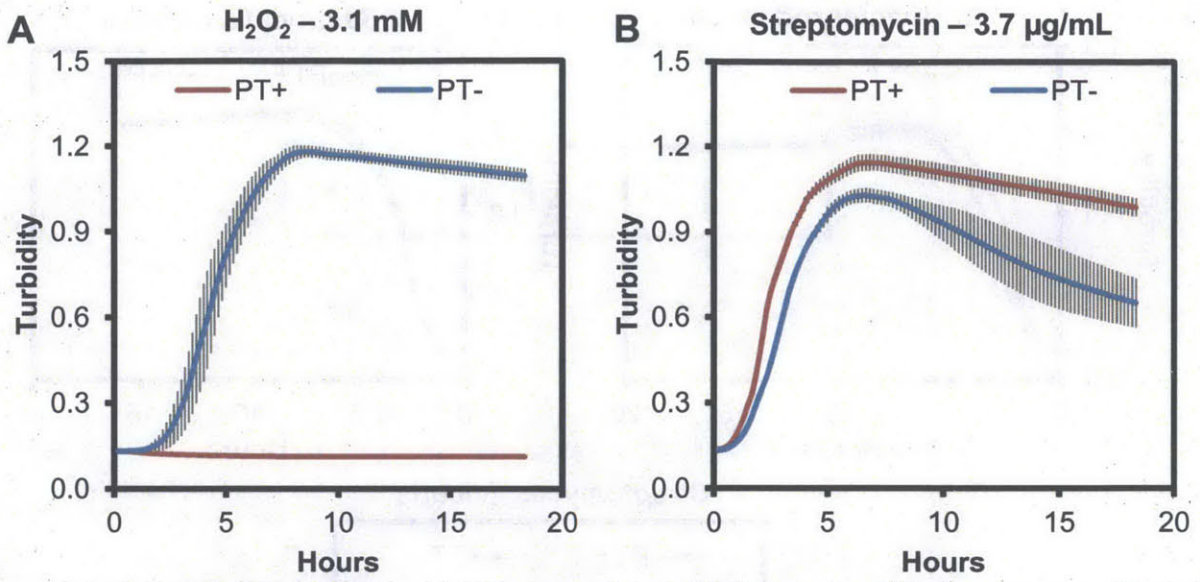

Figure 4-2: Growth of *C. rodentium* ± PT exposed to oxidative and antibiotic stresses. All strains were normalized to the same starting turbidity and exposed to hydrogen peroxide (A) or streptomycin (B) for 18 h at 37 °C with shaking. Error bars are ± SD for four biological replicates.

To determine if these effects were mediated by growth inhibition or by killing (i.e. bacteriostatic vs. bactericidal activity), we used a technique developed in-house to quickly visualize cell death following treatment. As shown in **Figure 4-3**, the bactericidal effects of both H_2O_2 and streptomycin reflected the patterns seen in the growth curves. We interpreted these data to mean that the protective effects of PT are not mediated solely by its chemical properties, so we next examined the effect of PT in a native context.

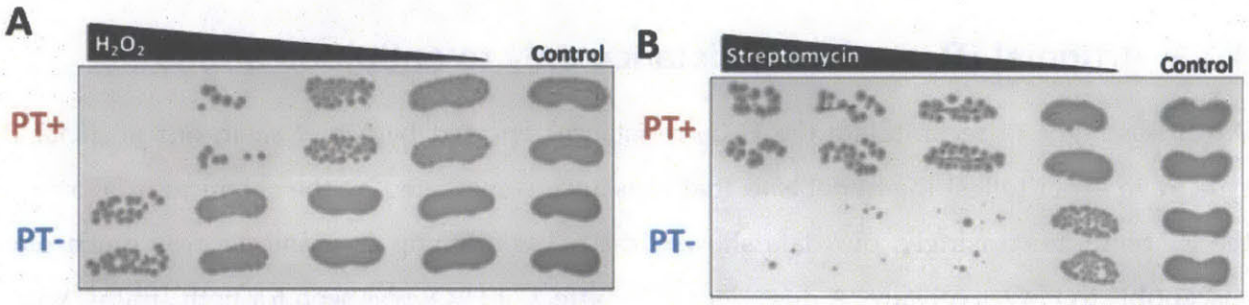

Figure 4-3: Bactericidal effects of oxidative and antibiotic stresses in *C. rodentium* ± PT. Strains were normalized to the same starting turbidity and exposed to hydrogen peroxide for 30 min (A) or to streptomycin for 2 h (B) at 37 °C with shaking, after which 4 µl aliquots were removed and spotted directly onto nonselective media that was grown overnight. The far right column is an untreated control, and the two rows in each category (± PT) are technical duplicates.

4.3.3. Native PT plus restriction confers resistance only to oxidative stress

Again, we first sought to recapitulate the H_2O_2 resistance phenotype reported by Xie *et al.* in our naturally restriction-positive, PT-positive *S. enterica* system. This experiment was an important control, as this strain was the same one originally used to demonstrated H_2O_2 resistance. As expected, we saw a dose-dependent effect under H_2O_2 stress, with better growth in the PT-positive strain than in the PT-negative strain (**Figure 4-4A**). Surprisingly, however, we found no difference between the two strains after exposure to kanamycin (**Figure 4-4B**), another aminoglycoside chosen because our *S. enterica* strains displayed resistance to streptomycin.

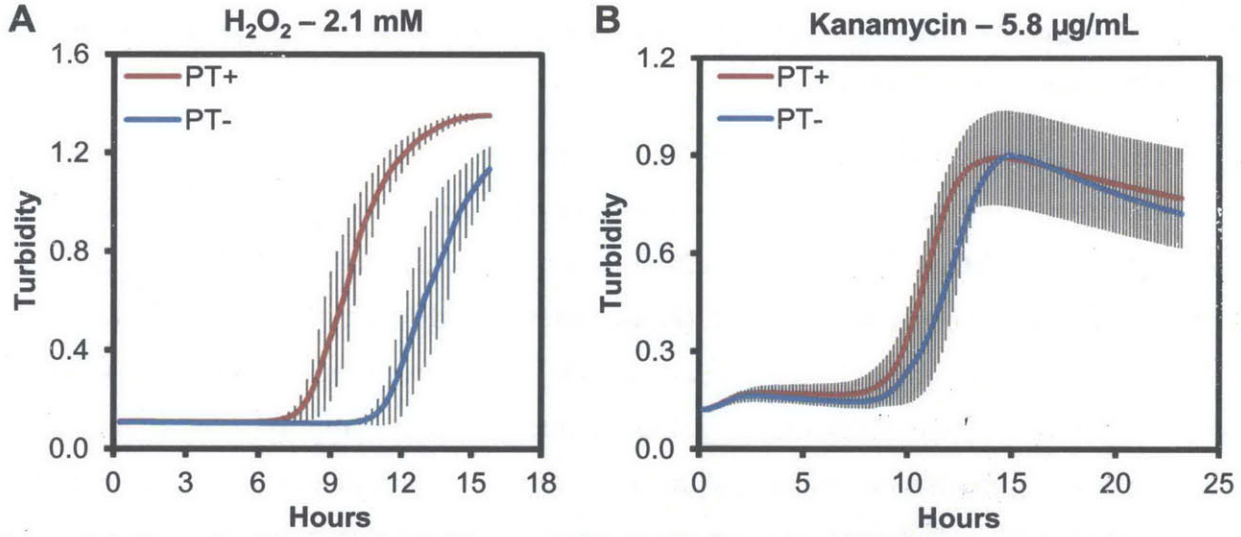

Figure 4-4: Growth of *S. enterica* ± PT exposed to oxidative and antibiotic stresses. All strains were normalized to the same starting density and exposed to H_2O_2 (A) or kanamycin (B) for 18 h at 37 °C with shaking. Error bars are ± SD for four biological replicates.

Because of the growth delay seen during kanamycin treatment (which was not observed for streptomycin), we questioned whether there was bactericidal activity, so we again used our in-house assay to visualize cell death. As seen in **Figure 4-5**, there was an identical dose-dependent bactericidal effect of kanamycin in both strains. Given that we did not see synergistic toxicity as with H_2O_2 in *C. rodentium*, we reasoned that the simplest explanation for this result was a lack of ROS generated by the kanamycin treatment [23]. We also could not rule out the possibility that exposure altered the levels of PT and resulted in deleterious effects from the *dndF-H* proteins, which our collaborators have shown are toxic on their own. Thus, we finally sought to determine the effect of PT without the confounding effect of the restriction system.

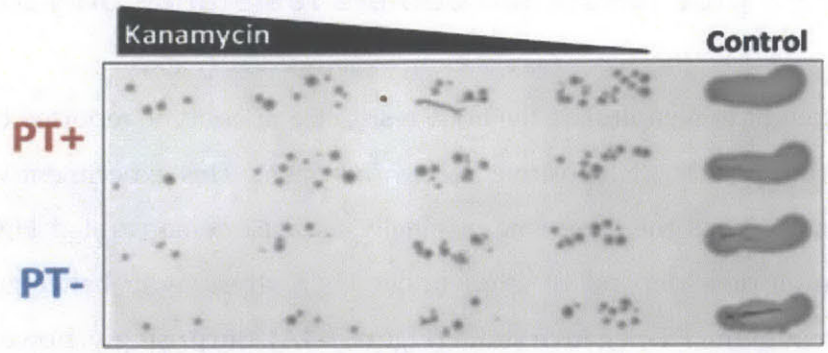

Figure 4-5: Bactericidal effect of antibiotic stress in *S. enterica* ± PT. Strains were normalized to the same starting turbidity and exposed to kanamycin for 2 h at 37 °C with shaking, after which 4 µl aliquots were removed and spotted directly onto nonselective media that was grown overnight. The far right column is an untreated control, and the two rows in each category (± PT) are technical duplicates.

4.3.4. Native PT minus restriction confers resistance to both oxidative and antibiotic stresses

As before, we began by attempting to recapitulate the H_2O_2 resistance previously reported. As with *S. enterica*, we were able to observe a significant survival advantage in the PT-positive strain of *S. lividans* (**Figure 4-6A**). Intriguingly, we observed an even more striking resistance phenotype under exposure to ampicillin (**Figure 4-6B**), which is a β-lactam we chose because our strains displayed aminoglycoside resistance [33]. The spore-forming nature of *S. lividans* prevented the use of our cell death assay, but we interpreted the drop in turbidity and nearly complete lack of growth seen with ampicillin as evidence of a bactericidal effect. Our data show that the effect of PT is dependent on both the genotype of the *dnd* cluster as well as the toxicant.

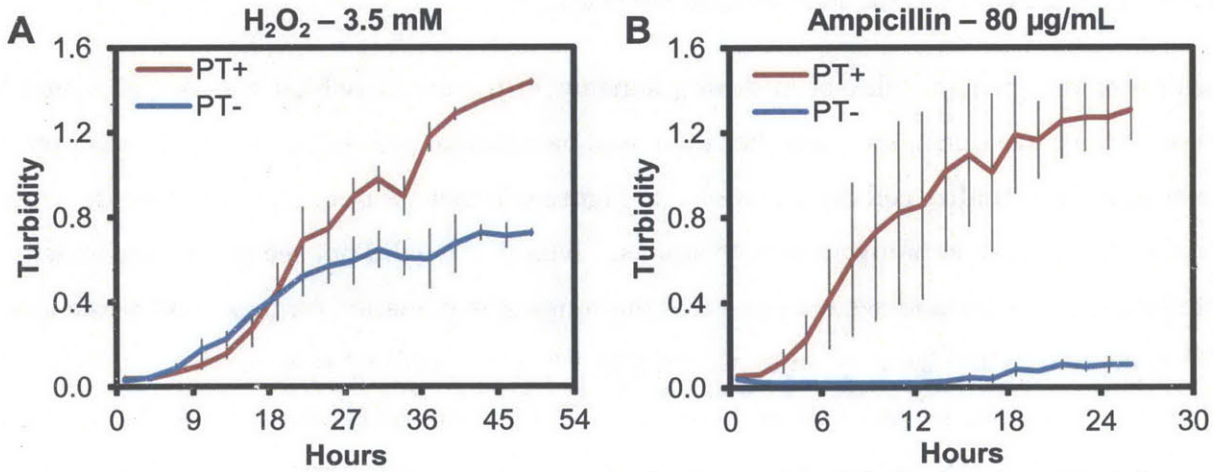

Figure 4-6: Growth of *S. lividans* ± PT exposed to oxidative and antibiotic stresses. All strains were normalized to the same starting turbidity and exposed to hydrogen peroxide (A) or ampicllin (B) for 48 h or 26 h (respectively) at 30 °C with shaking. Error bars are ± SD for four biological replicates.

4.4. Significance and future directions

The goal of these studies was to determine the impact of PT modifications on oxidative and antibiotic resistance in a variety of organisms and genetic backgrounds. Here we report a systemic analysis of the impact of multiple PT genotypes on both oxidative and antibiotic stress resistance in multiple bacterial species. Our data show that the protective effects of PT are not generalized, and depend on both the toxicant and organism.

Our data indicate that PT does not always protect against either H_2O_2 or antibiotics. However, it is important to recognize that this does not necessarily preclude the possibility that PT always functions as an antioxidant and/or ROS scavenger because neither H_2O_2 nor antibiotics have definitively been shown to always produce ROS. There have now been several studies showing that antibiotics do not require ROS and do not always generate ROS while exerting their bactericidal effects [34, 35]. Additionally, others have pointed to a synergistic interaction between 4Fe-4S clusters (such as DndC) and aminoglycosides [23], which may complicate the interpretation of our results. Finally, while H_2O_2 is often used as a positive control for ROS, there is clear evidence that its presence is not always toxic [36, 37], and experiments in our laboratory have shown that H_2O_2 exposure does not always produce ROS (**Figure 4-S1**) [38].

Our findings also raise more questions about the exact mechanism(s) by which PT confers protection. In particular, our data do not support the hypothesis (originally offered by Xie *et al.*) that the mechanism is purely physicochemical, and mediated by preferential ROS reaction with PT DNA. If that were the case, we should not observe drastic differences in protection across bacterial species and *dnd* genotypes. Additionally, our preliminary experiments with *S. enterica* exposed to nitric oxide indicate that PT has no impact on survival, which suggests that the mechanism is neither universal nor solely chemically mediated. Finally, unlike Xie *et al.*, we did not see any evidence of PT consumption following H_2O_2 treatment, as determined by a previously established LC-MS/MS method [18] (**Figure 4-S2**). Given that our quantification method is several orders of magnitude more sensitive, and that the H_2O_2 doses we examined were more physiologically relevant (50 mM maximum in our studies vs. 800 mM maximum in Xie *at al.*), we conclude that protection does not depend on consumption of PT modifications.

One possible explanation for the diverse phenotypes observed is that PT may be "pleotropic" in nature, and its function may depend on both its genomic context and the available host cellular machinery. This could explain the differences seen between native and artificial PT, as well as between organisms possessing or lacking the associated restriction components. For example, rather than simply marking host DNA, PT could play a role in the regulation of gene expression. This possibility is supported by recent observations of DNA modification-dependent enzymes (Type IV R-M systems) [39], as well as by reports that some Type IV enzymes specifically interact with PT DNA [40]. This explanation is further supported by our observations on the distribution of PT modifications across the genome. While earlier data from our laboratory indicated that only ~10% of the PT consensus sequences in an organism were actually modified [18], recent next generation sequencing data revealed that all possible sites are modified, but that only a fraction are modified in any given genome [41]. This raises the possibility that PT modifications are dynamic, and that their locations change over type as a function of outside factors. In this way, PT might contribute to enhanced stress response through a transcriptional mechanism, but only in organisms with the appropriate machinery.

Given that PT always conferred some type of stress resistance, its potential clinical impact and relevance to human health must still be considered. This is especially true given that PT has been found in numerous human pathogens [20], as well as in several clinical isolates [22, 42]. PT modifications have long been known to be immunostimulatory [43-45], though the exact motif responsible is still unknown [46]. This may indicate that PT is linked to or is an enhancer of virulence when found in pathogenic species. In support of this possibility, others have reported on shared resistance determinants between environmental and pathogenic bacteria [47].

Another potential link between PT and human health involves the microbiome. We recently discovered that many PT modifications are present in the feces of healthy mice (**Figure 4-S3**), but not in mouse genomic DNA. This result indicates that there are PT-containing microbes in the gut. In addition, given that several different dinucleotide sequences have been observed, it is reasonable to expect that multiple PT-containing species are present. If these species have enhanced stress response, then they may be overrepresented in the gut following antibiotic treatment or infection and inflammation. In this way, PT-containing microbes could guide the "blooming" of the gut and dysbiosis that is seen after disruption of the normal microbiome [48].

In summary, our studies demonstrate that PT modifications play an important role in bacterial stress response, and highlight the fact that our understanding of their function remains limited. Moving forward, we will address many of the questions raised by these initial findings. We will complement our existing data by expanding the range of stresses examined, and use flow cytometry to determine the ROS burden following treatment. Our recent technical achievements with next generation sequencing and PT mapping will also allow us to examine the PT landscape before and after various treatments, which will permit testing the possibility that there is dynamic PT restructuring. Finally, we have undertaken a study using a mouse model of colitis [49] to determine the role of PT in microbiome dynamics. These studies will enhance our understanding of PT biology, and may provide us with new tools to combat antibiotic resistance and enhance human health.

4.5 Supplementary material

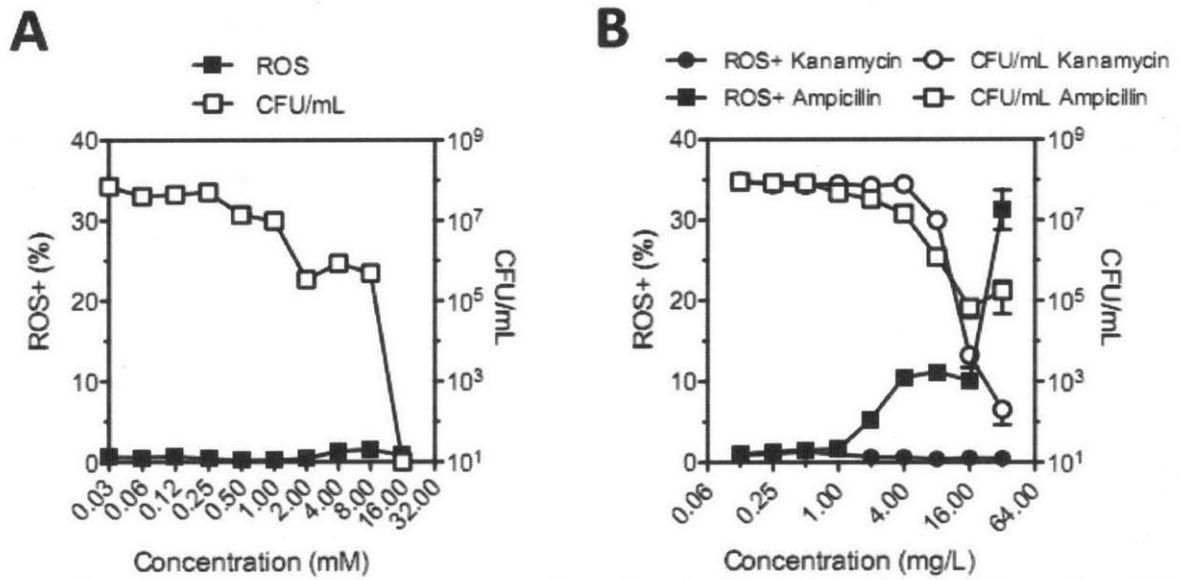

Figure 4-S1: Lack of reactive oxygen species after toxic hydrogen peroxide and antibiotic exposure. *Escherichia coli* DH5α was exposed to either H_2O_2 (A) or antibiotics (B) for 30 min and the proportion of cells producing reactive oxygen species (ROS) was quantified by flow cytometry. Neither H_2O_2 nor kanamycin induce ROS formation, even at highly toxic doses, whereas ampicillin leads to significant ROS production. Experiments were performed by Mariam Sharaf and Megan McBee.

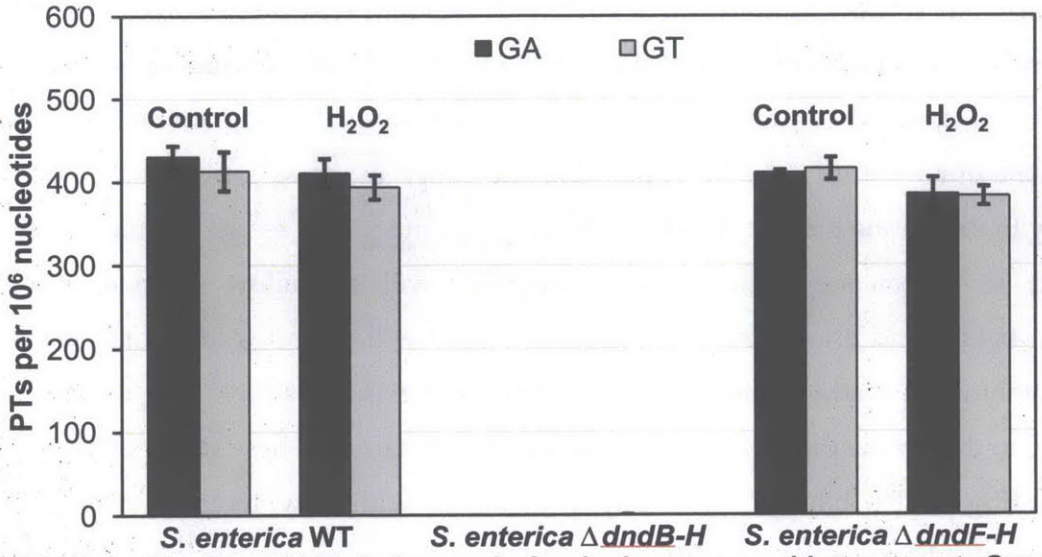

Figure 4-S2: Quantification of PTs before and after hydrogen peroxide treatment. Genomic DNA was extracted after exposure using phenol-chloroform, and PT dinucleotides were quantified by LC-MS/MS. Results are mean ± SD for n = 4 (technical duplicates of biological duplicates). Experiments were performed by Michael DeMott and Stefanie Kellner.

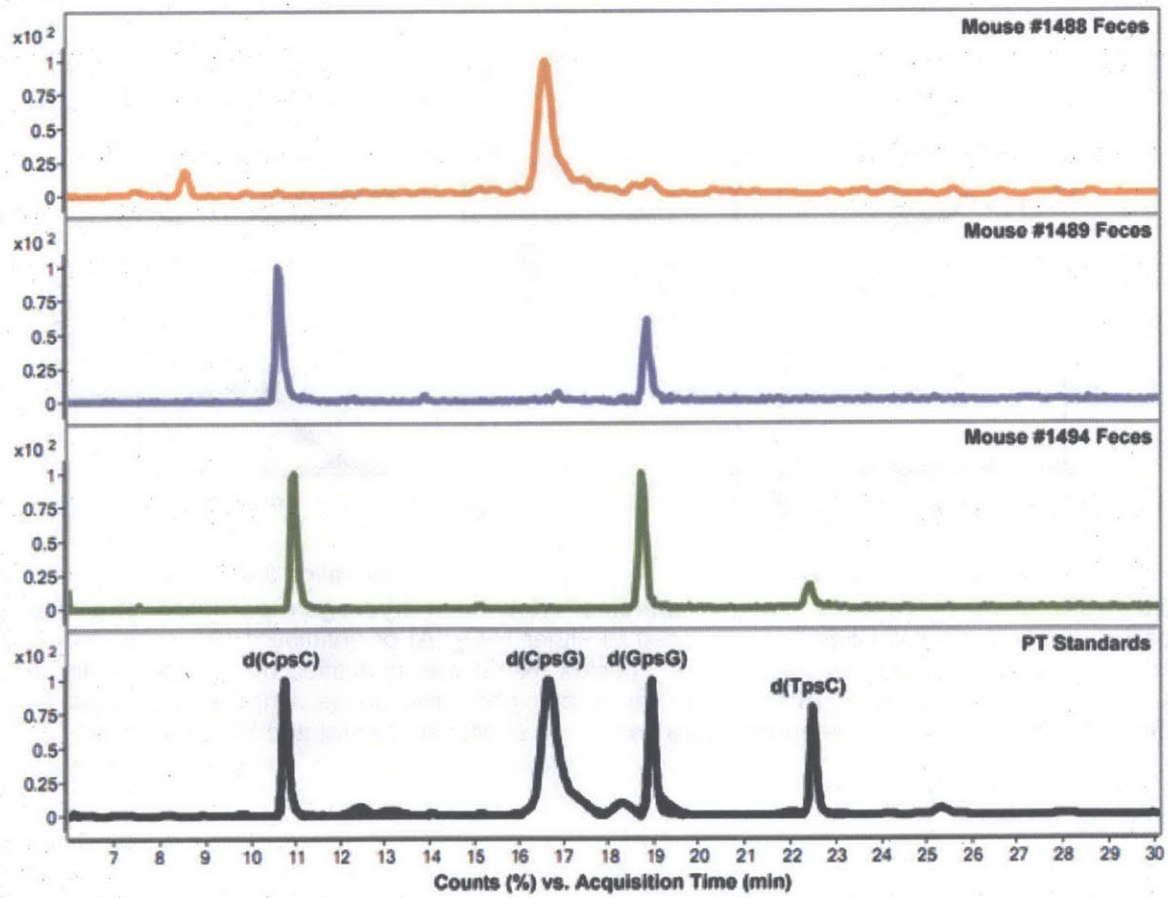

Figure 4-S3: LC-MS/MS analysis of PT content in mouse feces. DNA was extracted from single fecal pellets using phenol-chloroform and bead beating, and PT dinucleotides were prepurified by HPLC and quantified by LC-MS/MS. Experiments were performed by Bo Cao.

4.6. References

1. F. Eckstein (1970) *Nucleoside phosphorothioates.* **J Am Chem Soc** 92(15): 4718-4723.
2. F. Eckstein, H. Sternbach (1967) *Nucleoside 5'-O-phosphorothioates as inhibitors for phosphatases.* **Biochim Biophys Acta** 146(2): 618-619.
3. S.D. Putney, S.J. Benkovic, P.R. Schimmel (1981) *A DNA fragment with an α-phosphorothioate nucleotide at one end is asymmetrically blocked from digestion by exonuclease III and can be replicated in vivo.* **Proc Natl Acad Sci USA** 78(12): 7350-7354.
4. B.V. Potter, F. Eckstein (1984) *Cleavage of phosphorothioate-substituted DNA by restriction endonucleases.* **J Biol Chem** 259(22): 14243-14248.
5. P. Dyson, M. Evans (1998) *Novel post-replicative DNA modification in Streptomyces: Analysis of the preferred modification site of plasmid pIJ101.* **Nucleic Acids Res** 26(5): 1248-1253.
6. X. Zhou, X. He, J. Liang, A. Li, T. Xu, T. Kieser, J.D. Helmann, Z. Deng (2005) *A novel DNA modification by sulphur.* **Mol Microbiol** 57(5): 1428-1438.
7. L. Wang, S. Chen, T. Xu, K. Taghizadeh, J.S. Wishnok, X. Zhou, D. You, Z. Deng, P.C. Dedon (2007) *Phosphorothioation of DNA in bacteria by dnd genes.* **Nat Chem Biol** 3(11): 709-710.
8. S. Chen, L. Wang, Z. Deng (2010) *Twenty years hunting for sulfur in DNA.* **Protein & Cell** 1(1): 14-21.
9. J. Liang, Z. Wang, X. He, J. Li, X. Zhou, Z. Deng (2007) *DNA modification by sulfur: Analysis of the sequence recognition specificity surrounding the modification sites.* **Nucleic Acids Res** 35(9): 2944-2954.
10. T. Xu, J. Liang, S. Chen, L. Wang, X. He, D. You, Z. Wang, A. Li, Z. Xu, X. Zhou, Z. Deng (2009) *DNA phosphorothioation in Streptomyces lividans: Mutational analysis of the dnd locus.* **BMC Microbiol** 9: 41.
11. D. You, L. Wang, F. Yao, X. Zhou, Z. Deng (2007) *A novel DNA modification by sulfur: DndA is a NifS-like cysteine desulfurase capable of assembling DndC as an iron−sulfur cluster protein in Streptomyces lividans.* **Biochemistry** 46(20): 6126-6133.
12. F. Yao, T. Xu, X. Zhou, Z. Deng, D. You (2009) *Functional analysis of spfD gene involved in DNA phosphorothioation in Pseudomonas fluorescens Pf0-1.* **FEBS Lett** 583(4): 729-733.
13. F. Chen, K. Lin, Z. Zhang, L. Chen, X. Shi, C. Cao, Z. Wang, J. Liang, Z. Deng, G. Wu (2011) *Purification, crystallization and preliminary X-ray analysis of the DndE protein from Salmonella enterica serovar Cerro 87, which is involved in DNA phosphorothioation.* **Acta Crystallogr Sect F Struct Biol Cryst Commun** 67(Pt 11): 1440-1442.
14. X. An, W. Xiong, Y. Yang, F. Li, X. Zhou, Z. Wang, Z. Deng, J. Liang (2012) *A novel target of IscS in Escherichia coli: Participating in DNA phosphorothioation.* **PLoS One** 7(12): e51265.
15. F. Chen, Z. Zhang, K. Lin, T. Qian, Y. Zhang, D. You, X. He, Z. Wang, J. Liang, Z. Deng, G. Wu (2012) *Crystal structure of the cysteine desulfurase DndA from Streptomyces lividans which is involved in DNA phosphorothioation.* **PLoS One** 7(5): e36635.

16. W. Hu, C. Wang, J. Liang, T. Zhang, Z. Hu, Z. Wang, W. Lan, F. Li, H. Wu, J. Ding, G. Wu, Z. Deng, C. Cao (2012) *Structural insights into DndE from Escherichia coli B7A involved in DNA phosphorothioation modification.* **Cell Res** 22(7): 1203-1206.
17. T. Xu, F. Yao, X. Zhou, Z. Deng, D. You (2010) *A novel host-specific restriction system associated with DNA backbone S-modification in Salmonella.* **Nucleic Acids Res** 38(20): 7133-7141.
18. L. Wang, S. Chen, K.L. Vergin, S.J. Giovannoni, S.W. Chan, M.S. Demott, K. Taghizadeh, O.X. Cordero, M. Cutler, S. Timberlake, E.J. Alm, M.F. Polz, J. Pinhassi, Z. Deng, P.C. Dedon (2011) *DNA phosphorothioation is widespread and quantized in bacterial genomes.* **Proc Natl Acad Sci USA** 108(7): 2963-2968.
19. K.S. Makarova, Y.I. Wolf, E.V. Koonin (2013) *Comparative genomics of defense systems in archaea and bacteria.* **Nucleic Acids Res** 41(8): 4360-4377.
20. H.Y. Ou, X. He, Y. Shao, C. Tai, K. Rajakumar, Z. Deng (2009) *dndDB: A database focused on phosphorothioation of the DNA backbone.* **PLoS One** 4(4): e5132.
21. X. Xie, J. Liang, T. Pu, F. Xu, F. Yao, Y. Yang, Y.L. Zhao, D. You, X. Zhou, Z. Deng, Z. Wang (2012) *Phosphorothioate DNA as an antioxidant in bacteria.* **Nucleic Acids Res** 40(18): 9115-9124.
22. S.T. Howard, K.L. Newman, S. Mcnulty, B.A. Brown-Elliott, R. Vasireddy, L. Bridge, R.J. Wallace, Jr. (2013) *Insertion site and distribution of a genomic island conferring DNA phosphorothioation in the Mycobacterium abscessus complex.* **Microbiology** 159(Pt 11): 2323-2332.
23. B. Ezraty, A. Vergnes, M. Banzhaf, Y. Duverger, A. Huguenot, A.R. Brochado, S.Y. Su, L. Espinosa, L. Loiseau, B. Py, A. Typas, F. Barras (2013) *Fe-S cluster biosynthesis controls uptake of aminoglycosides in a ROS-less death pathway.* **Science** 340(6140): 1583-1587.
24. M.A. Kohanski, D.J. Dwyer, B. Hayete, C.A. Lawrence, J.J. Collins (2007) *A common mechanism of cellular death induced by bactericidal antibiotics.* **Cell** 130(5): 797-810.
25. J.J. Foti, B. Devadoss, J.A. Winkler, J.J. Collins, G.C. Walker (2012) *Oxidation of the guanine nucleotide pool underlies cell death by bactericidal antibiotics.* **Science** 336(6079): 315-319.
26. G.L. French (2010) *The continuing crisis in antibiotic resistance.* **Int J Antimicrob Agents** 36(Suppl 3): S3-7.
27. I.M. Gould (2010) *Coping with antibiotic resistance: The impending crisis.* **Int J Antimicrob Agents** 36(Suppl 3): S1-2.
28. J.H. Rex (2014) *ND4BB: Addressing the antimicrobial resistance crisis.* **Nat Rev Microbiol** 12(4): 231-232.
29. A.G. Hildebraunt, I. Roots (1975) *Reduced nicotinamide adenine dinucleotide phosphate (NADPH)-dependent formation and breakdown of hydrogen peroxide during mixed function oxidation reactions in liver microsomes.* **Arch Biochem Biophys** 171(2): 385-397.
30. D.B. Schauer, B.A. Zabel, I.F. Pedraza, C.M. O'hara, A.G. Steigerwalt, D.J. Brenner (1995) *Genetic and biochemical characterization of Citrobacter rodentium sp. nov.* **J Clin Microbiol** 33(8): 2064-2068.
31. S.A. Luperchio, D.B. Schauer (2001) *Molecular pathogenesis of Citrobacter rodentium and transmissible murine colonic hyperplasia.* **Microbes Infect** 3(4): 333-340.

32. C. Stratton (1992) *Fluoroquinolone antibiotics: Properties of the class and individual agents.* **Clin Ther** 14(3): 348-375; discussion 347.
33. G. Jenkins, E. Cundliffe (1991) *Cloning and characterization of two genes from Streptomyces lividans that confer inducible resistance to lincomycin and macrolide antibiotics.* **Gene** 108: 55-62.
34. I. Keren, Y. Wu, J. Inocencio, L.R. Mulcahy, K. Lewis (2013) *Killing by bactericidal antibiotics does not depend on reactive oxygen species.* **Science** 339(6124): 1213-1216.
35. Y. Liu, J.A. Imlay (2013) *Cell death from antibiotics without the involvement of reactive oxygen species.* **Science** 339(6124): 1210-1213.
36. D.R. Gough, T.G. Cotter (2011) *Hydrogen peroxide: A Jekyll and Hyde signalling molecule.* **Cell Death Dis** 2: e213.
37. J.A. Imlay (2013) *The molecular mechanisms and physiological consequences of oxidative stress: Lessons from a model bacterium.* **Nat Rev Microbiol** 11(7): 443-454.
38. M.E. Mcbee (2014) Personal communication with B.S. Russell
39. W.A. Loenen, E.A. Raleigh (2014) *The other face of restriction: Modification-dependent enzymes.* **Nucleic Acids Res** 42(1): 56-69.
40. G. Liu, H.Y. Ou, T. Wang, L. Li, H. Tan, X. Zhou, K. Rajakumar, Z. Deng, X. He (2010) *Cleavage of phosphorothioated DNA and methylated DNA by the Type IV restriction endonuclease ScoMcrA.* **PLoS Genet** 6(12): e1001253.
41. B. Cao, Q. Cheng, T.A. Clark, X. Xiong, X. Zheng, V. Butty, S.S. Levine, G. Yuan, M. Boitano, K. Luong, Y. Song, X. Zhou, Z. Deng, S.W. Turner, J. Korlach, D. You, L. Wang, S. Chen, P.C. Dedon (2014) *Genomic mapping of phosphorothioates reveals partial modification of short consensus sequences.* **Nat Protoc** (Accepted).
42. Y. Zhang, M.A. Yakrus, E.A. Graviss, N. Williams-Bouyer, C. Turenne, A. Kabani, R.J. Wallace, Jr. (2004) *Pulsed-field gel electrophoresis study of Mycobacterium abscessus isolates previously affected by DNA degradation.* **J Clin Microbiol** 42(12): 5582-5587.
43. S.A. Halperin, B.J. Ward, M. Dionne, J.M. Langley, S.A. Mcneil, B. Smith, D. Mackinnon-Cameron, W.L. Heyward, J.T. Martin (2013) *Immunogenicity of an investigational hepatitis B vaccine (hepatitis B surface antigen co-administered with an immunostimulatory phosphorothioate oligodeoxyribonucleotide) in nonresponders to licensed hepatitis B vaccine.* **Hum Vaccin Immunother** 9(7): 1438-1444.
44. S.A. Halperin, G. Van Nest, B. Smith, S. Abtahi, H. Whiley, J.J. Eiden (2003) *A phase I study of the safety and immunogenicity of recombinant hepatitis B surface antigen co-administered with an immunostimulatory phosphorothioate oligonucleotide adjuvant.* **Vaccine** 21(19-20): 2461-2467.
45. Q. Zhao, D. Yu, S. Agrawal (1999) *Site of chemical modifications in CpG containing phosphorothioate oligodeoxynucleotide modulates its immunostimulatory activity.* **Bioorg Med Chem Lett** 9(24): 3453-3458.
46. F. Brugnolo, F. Annunziato, S. Sampognaro, C. Manuelli, L. Cosmi, S. Romagnani, E. Maggi, P. Parronchi (2001) *Phosphorothioate oligonucleotides: Looking for the motif(s) possessing immunostimulatory activities in humans.* **Adv Exp Med Biol** 495: 261-264.
47. K.J. Forsberg, A. Reyes, B. Wang, E.M. Selleck, M.O. Sommer, G. Dantas (2012) *The shared antibiotic resistome of soil bacteria and human pathogens.* **Science** 337(6098): 1107-1111.
48. B. Stecher, L. Maier, W.D. Hardt (2013) *'Blooming' in the gut: How dysbiosis might contribute to pathogen evolution.* **Nat Rev Microbiol** 11(4): 277-284.

49. A. Mangerich, C.G. Knutson, N.M. Parry, S. Muthupalani, W. Ye, E. Prestwich, L. Cui, J.L. Mcfaline, M. Mobley, Z. Ge, K. Taghizadeh, J.S. Wishnok, G.N. Wogan, J.G. Fox, S.R. Tannenbaum, P.C. Dedon (2012) *Infection-induced colitis in mice causes dynamic and tissue-specific changes in stress response and DNA damage leading to colon cancer.* **Proc Natl Acad Sci USA** 109(27): E1820-1829.

5. Summary of contributions

The goal of this thesis was to investigate the functions of nucleic acid modifications in pathogenic bacteria, and to determine if these modifications play a role in the disease process. To that end, we undertook a series of studies designed to assess the function and utility of nucleic acid modifications in bacterial pathogenesis, diagnosis, and therapy. Our results contain several novel observations that provide significant insight into the disease process of important human pathogens, and we report several discoveries that could guide the development of novel preventative, diagnostic, and therapeutic interventions. Here we briefly review these contributions, with an emphasis on the potential impacts to human health.

Our initial study was designed to test a broad hypothesis about the role of nucleic acid modifications in bacteria, and examined the role of modified ribonucleosides in tRNA in the pathogenesis of *Helicobacter pylori* infection, the world's most common infectious disease [1]. This study was guided by two observations. The first was the recent discovery (by members of our laboratory and collaborators) of a novel translational control mechanism in which tRNA modifications bias the translation of specific mRNA transcripts [2, 3]. The second was the report that *H. pylori* relies primarily on post-transcriptional regulators to control virulence [4]. We used our recently developed platform [5] to quantitatively profile tRNA modifications in response to two key early barriers to *H. pylori* colonization, hydrochloric acid and hydrogen peroxide. We first determined the spectrum of modified ribonucleosides in *H. pylori* tRNA, which is the first such report to our knowledge. We then demonstrated that these modifications change in specific and significant ways in response to toxicants, and that the patterns of modifications can serve as biomarkers of exposure. We also identified several modifications that are highly correlated with stress response, including at least one specific to bacterial tRNA. Our data suggest that tRNA modifications may play a role in *H. pylori* pathogenesis. In addition, others in our laboratory have previously demonstrated that blocking the formation of modifications that are correlated with stress can induce sensitivity to that stress [6]. Our work may thus lead to the identification of new potential targets for the development of *H. pylori* therapies designed to prevent infection. Given the high prevalence of *H. pylori* [7], its strong association with gastric cancer [8-10], and the increasing cases of antibiotic resistance [11-15], our results may one day have a significant impact on human health.

Having established that nucleic acid modifications are potentially important in bacterial infections, we then sought to expand our studies beyond cell culture systems to more clinically relevant animal models of disease. To do so, we first developed a novel rat model of *Mycobacterium tuberculosis* (Mtb)-type lung disease that can be handled in standard biosafety level 2 (BSL-2) laboratories. By working in the rat, we created a BSL-2 model of mycobacterial disease that is amenable to pharmacokinetic and drug development studies. The potential utility of this model lies in the high costs and relatively small number of high containment laboratories capable of performing studies in Mtb animal models [16-18]. We demonstrated that pulmonary infection of rats with *M. bovis* bacille Calmette-Guérin Pasteur induces a sustained infection, strong immune response, and robust pathology that recapitulates the granulomatous nature of human tuberculosis. We then demonstrated the potential utility of this animal model in screening for potential biomarkers of infection. The need for new diagnostic and therapeutic approaches to Mtb is well known [19-21], and given the recent recognition that Mtb drug discovery needs to be performed in animal models that accurately reflect human granulomas [22-25], our results could accelerate the pace of Mtb drug and diagnostic discovery.

We finally sought to expand our studies to have human health impact by examining the role of a nucleic acid modification known to frequently occur in clinical bacterial isolates [26]. To that end we examined the role of DNA phosphorothioation in resistance to oxidative and antibiotic stresses, using both a variety of phosphorothioation systems and a variety of pathogenic bacteria. We built on previous reports by our collaborators to create a systematic profile of the impact of DNA phosphorothioation on bacterial stress response. We demonstrated that, contrary to recent literature reports [27], the protective effects of phosphorothioation are not generalized, but are dependent on both the type of stress and the host genetics. We also showed that phosphorothioation has the capacity to confer resistance to both the bacteriostatic and bactericidal effects of some common antibiotics. While still in the early stages, this observation may one day lead to new targets for the development of a new class of antibiotics or antibiotic adjuvants [28]. Given the widespread nature of phosphorothioation [29-31], its capacity for horizontal gene transfer [32], and the looming crisis in antibiotic resistance [33-36], our results may become an important part of the clinical management of bacterial infections.

Taken together, these studies provide evidence that nucleic acid modifications play important roles in bacterial pathogens, and that they may have the potential to impact all stages of the disease process. We believe that our work will provide guidance for the future development of new tools to fight infectious diseases.

5.1. References

1. R.A. Feldman, A.J.P. Eccersley, J.M. Hardie (1998) *Epidemiology of Helicobacter pylori: Acquisition, transmission, population prevalence and disease-to-infection ratio.* **Br Med Bull** 54(1): 39-53.
2. P.C. Dedon, T.J. Begley (2014) *A system of RNA modifications and biased codon use controls cellular stress response at the level of translation.* **Chem Res Toxicol** 27(3): 330-337.
3. C.T. Chan, Y.L. Pang, W. Deng, I.R. Babu, M. Dyavaiah, T.J. Begley, P.C. Dedon (2012) *Reprogramming of tRNA modifications controls the oxidative stress response by codon-biased translation of proteins.* **Nat Commun** 3: 937.
4. F.M. Barnard, M.F. Loughlin, H.P. Fainberg, M.P. Messenger, D.W. Ussery, P. Williams, P.J. Jenks (2003) *Global regulation of virulence and the stress response by CsrA in the highly adapted human gastric pathogen Helicobacter pylori.* **Mol Microbiol** 51(1): 15-32.
5. D. Su, C.T. Chan, C. Gu, K.S. Lim, Y.H. Chionh, M.E. Mcbee, B.S. Russell, I.R. Babu, T.J. Begley, P.C. Dedon (2014) *Quantitative analysis of ribonucleoside modifications in tRNA by HPLC-coupled mass spectrometry.* **Nat Protoc** 9(4): 828-841.
6. C.T. Chan, M. Dyavaiah, M.S. Demott, K. Taghizadeh, P.C. Dedon, T.J. Begley (2010) *A quantitative systems approach reveals dynamic control of tRNA modifications during cellular stress.* **PLoS Genet** 6(12): e1001247.
7. B. Bauer, T.F. Meyer (2011) *The human gastric pathogen Helicobacter pylori and its association with gastric cancer and ulcer disease.* **Ulcers** 2011: 1-23.
8. P. Malfertheiner, P. Sipponen, M. Naumann, P. Moayyedi, F. Megraud, S.D. Xiao, K. Sugano, O. Nyren (2005) *Helicobacter pylori eradication has the potential to prevent gastric cancer: A state-of-the-art critique.* **Am J Gastroenterol** 100(9): 2100-2115.
9. D.B. Polk, R.M. Peek, Jr. (2010) *Helicobacter pylori: Gastric cancer and beyond.* **Nat Rev Cancer** 10(6): 403-414.
10. L.E. Wroblewski, R.M. Peek, Jr. (2013) *Helicobacter pylori in gastric carcinogenesis: Mechanisms.* **Gastroenterol Clin North Am** 42(2): 285-298.
11. F. Megraud (2004) *H. pylori antibiotic resistance: Prevalence, importance, and advances in testing.* **Gut** 53(9): 1374-1384.
12. L. Fischbach, E.L. Evans (2007) *Meta-analysis: The effect of antibiotic resistance status on the efficacy of triple and quadruple first-line therapies for Helicobacter pylori.* **Aliment Pharmacol Ther** 26(3): 343-357.
13. A. Khan, A. Farooqui, H. Manzoor, S.S. Akhtar, M.S. Quraishy, S.U. Kazmi (2012) *Antibiotic resistance and cagA gene correlation: A looming crisis of Helicobacter pylori.* **World J Gastroenterol** 18(18): 2245-2252.

14. W. Wu, Y. Yang, G. Sun (2012) *Recent insights into antibiotic resistance in Helicobacter pylori eradication.* **Gastroenterol Res Pract** 2012: 723183.
15. M.C. Camargo, A. Garcia, A. Riquelme, W. Otero, C.A. Camargo, T. Hernandez-Garcia, R. Candia, M.G. Bruce, C.S. Rabkin (2014) *The Problem of Helicobacter pylori resistance to antibiotics: A systematic review in Latin America.* **Am J Gastroenterol** 109(4): 485-495.
16. K. Rhodes. *High-containment biosafety laboratories: Preliminary observations on the oversight of the proliferation of BSL-3 and BSL-4 laboratories in the United States*, G.A. Office. Editor. 2007.
17. J. Baum (2008) *Biohazard containment facilities: Planning and design considerations.* Last updated Accessed on 19 December 2013. Available from: http://www.ghdonline.org/uploads/LabBiosafetyPlanning071208-Part1.pdf.
18. K.M. Berger. *The broader effects of biosecurity regulations*, in *The CIP Report.* 2009, George Mason University.
19. N. Casali, V. Nikolayevskyy, Y. Balabanova, S.R. Harris, O. Ignatyeva, I. Kontsevaya, J. Corander, J. Bryant, J. Parkhill, S. Nejentsev, R.D. Horstmann, T. Brown, F. Drobniewski (2014) *Evolution and transmission of drug-resistant tuberculosis in a Russian population.* **Nat Genet** 46(3): 279-286.
20. World Health Organization. *Global Tuberculosis Report.* 2013.
21. R. Osborne (2013) *First novel anti-tuberculosis drug in 40 years.* **Nat Biotechnol** 31(2): 89-91.
22. N. Kumar, K.G. Vishwas, M. Kumar, J. Reddy, M. Parab, C.L. Manikanth, B.S. Pavithra, R.K. Shandil (2014) *Pharmacokinetics and dose response of anti-TB drugs in rat infection model of tuberculosis.* **Tuberculosis**.
23. V. Dartois (2014) *The path of anti-tuberculosis drugs: From blood to lesions to mycobacterial cells.* **Nat Rev Microbiol** 12(3): 159-167.
24. E. Guirado, L.S. Schlesinger (2013) *Modeling the Mycobacterium tuberculosis granuloma – the critical battlefield in host immunity and disease.* **Front Immunol** 4(98).
25. V. Dartois, C.E. Barry, 3rd (2013) *A medicinal chemists' guide to the unique difficulties of lead optimization for tuberculosis.* **Bioorg Med Chem Lett** 23(17): 4741-4750.
26. S.T. Howard, K.L. Newman, S. Mcnulty, B.A. Brown-Elliott, R. Vasireddy, L. Bridge, R.J. Wallace, Jr. (2013) *Insertion site and distribution of a genomic island conferring DNA phosphorothioation in the Mycobacterium abscessus complex.* **Microbiology** 159(Pt 11): 2323-2332.
27. X. Xie, J. Liang, T. Pu, F. Xu, F. Yao, Y. Yang, Y.L. Zhao, D. You, X. Zhou, Z. Deng, Z. Wang (2012) *Phosphorothioate DNA as an antioxidant in bacteria.* **Nucleic Acids Res** 40(18): 9115-9124.
28. L.R. Marks, E.A. Clementi, A.P. Hakansson (2012) *The human milk protein-lipid complex HAMLET sensitizes bacterial pathogens to traditional antimicrobial agents.* **PLoS One** 7(8): e43514.
29. B. Cao, Q. Cheng, T.A. Clark, X. Xiong, X. Zheng, V. Butty, S.S. Levine, G. Yuan, M. Boitano, K. Luong, Y. Song, X. Zhou, Z. Deng, S.W. Turner, J. Korlach, D. You, L. Wang, S. Chen, P.C. Dedon (2014) *Genomic mapping of phosphorothioates reveals partial modification of short consensus sequences.* **Nat Protoc** (Accepted).

30. Y. Zhang, M.A. Yakrus, E.A. Graviss, N. Williams-Bouyer, C. Turenne, A. Kabani, R.J. Wallace, Jr. (2004) *Pulsed-field gel electrophoresis study of Mycobacterium abscessus isolates previously affected by DNA degradation.* **J Clin Microbiol** 42(12): 5582-5587.
31. U. Romling, B. Tummler (2000) *Achieving 100% typeability of Pseudomonas aeruginosa by pulsed-field gel electrophoresis.* **J Clin Microbiol** 38(1): 464-465.
32. H.Y. Ou, X. He, Y. Shao, C. Tai, K. Rajakumar, Z. Deng (2009) *dndDB: A database focused on phosphorothioation of the DNA backbone.* **PLoS One** 4(4): e5132.
33. G.L. French (2010) *The continuing crisis in antibiotic resistance.* **Int J Antimicrob Agents** 36(Suppl 3): S3-7.
34. I.M. Gould (2010) *Coping with antibiotic resistance: The impending crisis.* **Int J Antimicrob Agents** 36(Suppl 3): S1-2.
35. S.T. Shulman (2013) *The antibiotic crisis.* **Pediatr Ann** 42(7): 260-261.
36. J.H. Rex (2014) *ND4BB: Addressing the antimicrobial resistance crisis.* **Nat Rev Microbiol** 12(4): 231-232.